Chem Soc Rev

TUTORIAL REVIEW

Published on 17 September 2026

Cite this: DOI: 10.1039/d4cs00811a

Carbon–carbon bond cleavage for lignin and plastics deconstruction

Davide Rigo,[ad] Brandon L. Frey,[ae] Alison Sy-min Chang,[a] Marcos G. Farpón,[b] Erik T. Ouellette,[a] Yuriy Román-Leshkov,*[b] Gregg T. Beckham*[ade] and Joseph M. Samec*[cf]

Received 19th March 2026

DOI: 10.1039/d4cs00811a

rsc.li/chem-soc-rev

The cleavage of C–O bonds has enabled significant progress in both lignin valorization and recycling of polyester plastics. However, for the more recalcitrant fraction(s) of these feedstocks – namely, C–C linkages found in lignin and polymer backbones – the selective cleavage of C–C bonds remains a critical challenge. Selective cleavage of these bonds is essential to enhance both the carbon efficiency and economic viability of biorefining and plastics deconstruction to value-added products. This review provides an overview of the available methodologies for C–C bond cleavage useful for lignin and plastics deconstruction, with particular focus on accessible reaction mechanisms. Methods for C–C bond cleavage from other areas of chemistry are considered alongside approaches specifically applied to lignin and plastics. We provide perspective on promising C–C bond cleavage methods, substrate classes, engineering considerations, and guidelines for reporting C–C bond cleavage yields.

Key learning points

(1) How the structures and reactivities of C–C linkages in lignin and plastics govern their susceptibility to catalytic cleavage.
(2) The principal mechanisms used to cleave C–C bonds in lignin, including metal-mediated, radical, oxidative, and organo-mediated pathways.
(3) The major strategies for cleaving polymer backbones in plastics, including hydrogenolysis, hydrocracking, metathesis, oxidation, and radical fragmentation.
(4) Opportunities to transfer catalytic and mechanistic concepts between lignin valorization and plastics deconstruction.
(5) Priorities for advancing the fields, including improved mechanistic understanding, realistic feedstocks, standardized yield reporting, catalyst and reactor design, and integrated upgrading processes.

1. Introduction

Since the inception of organic chemistry, the formation of carbon–carbon (C–C) bonds has been a central objective in the field, as exemplified by numerous transformations: the Grignard (1912)[1] and Diels Alder (1950) reactions,[2] Ziegler–Natta polymerization (1963),[3] Wittig olefination (1979),[4] [2+2] cycloaddition,[5] olefin metathesis (2005),[6] Negishi/Suzuki/Heck cross-couplings (2010),[7] photocatalysis, and asymmetric catalysis (2021).[8] Historically, this goal has relied almost solely on the coupling of petroleum-derived feedstocks, but a growing emphasis on planetary stewardship has spurred a global transition towards sustainable chemistry that relies on biogenic feedstocks and emphasizes circularity in carbon flows.[9,10] Despite significant progress towards the production of bio-derived chemicals and designed polymers for carbon circularity *via* C–X bond cleavage,[11,12] there remains a significant amount of underutilized carbon trapped in C–C linkages occurring in both bio-feedstocks and in synthetic plastics. The design of strategies to utilize these C–C-linked species is critical for the success of a sustainable chemical industry.[13,14]

Lignin and synthetic plastics are among the most abundant carbon-rich residual streams annually produced. Lignin, a complex aromatic polymer found in plant cell walls, accounts for approximately 10–30 wt% of plant biomass.[13] The global annual generation of biomass waste is estimated at $\sim 10^3$ Gt year^{-1}, comprising industrial crops, forestry residues, and agricultural/food waste, among others.[15,16] Complete recovery and

[a] Renewable Resources and Enabling Sciences Center, National Laboratory of the Rockies, Golden, CO, USA
[b] Department of Chemical Engineering, Massachusetts Institute of Technology, Cambridge, MA, USA. E-mail: yroman@mit.edu
[c] Department of Chemistry, Stockholm University, Stockholm, 114 18, Sweden. E-mail: joseph.samec@su.se
[d] Center for Bioenergy Innovation, Oak Ridge National Laboratory, Oak Ridge, TN, USA
[e] BOTTLE Consortium, Golden, CO, USA. E-mail: gregg.beckham@nrel.gov
[f] Wallenberg Initiative Materials Science for Sustainability, Department of Chemistry, Stockholm University, Stockholm, 114 18, Sweden

fractionation of this waste biomass would yield $\sim 10^2$ Gt year^{-1} of lignin, the largest bio-available source of aromatic compounds.[13,17–19] Kraft pulping alone, the dominant industrial method for wood processing, generates roughly 70 million metric tons (MMt) of isolated Kraft lignin annually.[20] In parallel, the total annual production of plastics was estimated at $\sim$391 MMt in 2021,[21,22] with polyethylene (PE, including low, linear-low, and high-density polyethylene; LDPE, LLDPE, and HDPE) and polypropylene (PP) accounting for approximately 41% of the plastics market.[23]

Despite their abundance, only small portions of lignin and plastics are currently converted to value-added chemicals and products, underscoring the urgent need for innovative methods to valorize them. Specifically, lignin is predominantly burned to generate energy for process heat,[20] while only a small percentage of plastics is currently recycled with most of it being landfilled or incinerated.[23,24] Incineration merely recovers a percentage of the energy content while producing CO_x and other products, but not the material itself, making it a suboptimal valorization method for these residual streams. Thus, chemical depolymerization *via* C–C bond cleavage represents an alternative strategy with immense potential. To date, many deconstruction strategies have been tested with lignin and plastics and increasing research focus has grown in recent decades.[24] However, compared to C–C bond formation reactions, selective and efficient C–C bond cleavage remains significantly underexplored.[24–26]

Acknowledging numerous reviews describing cleavage of specific types of C–C bonds,[27–36] and the cleavage of C–C bonds in lignin[37] and in plastics,[14] the aim of the current review is to unify and critically discuss strategies for C–C bond cleavage relevant to the depolymerization of both lignin and petroleum-derived polymers with a focus on the corresponding reaction mechanisms. First, we describe relevant bonds in both lignin and plastic feedstocks. Second, we present a general overview of

Davide Rigo

Davide Rigo worked at the National Renewable Energy Laboratory (NREL; Golden, CO) studying catalytic methods for lignin and plastics depolymerization. Previously, he had a postdoctoral appointment at Aalto University and he received his cotutelle PhD degree (2022) from the Università Ca' Foscari di Venezia (Italy) and the University of Sydney (Australia). He currently is a Marie Skłodowska-Curie Postdoc fellow at ICIQ in Tarragona. His interests are in the catalytic valorization of biomass and biobased chemical platforms, lignin, and in sustainable plastics.

Brandon L. Frey

Brandon L. Frey received his PhD in Chemistry from Texas A&M University in 2023, where his research focused on organo-electrocatalytic transformations and mechanistic investigations. He is currently a Postdoctoral Research Fellow at the National Laboratory of the Rockies, where his research centers on plastics valorization through autoxidation, with an emphasis on developing sustainable strategies for polymer upcycling and elucidating oxidation mechanisms.

Alison Sy-min Chang

Alison Chang received her PhD in Chemistry from the University of Oregon in 2024, where her research focused on nickel-catalyzed alkene transformations and mechanistic studies of transition-metal-catalyzed reactions. She subsequently completed postdoctoral research at the National Laboratory of the Rockies (NLR), developing metal-catalyzed oxidation strategies for lignin valorization. She is currently an R&D Scientist II at Honeywell UOP in Des Plaines, Illinois, where she develops and scales catalytic materials and process technologies for refining and petrochemical applications.

Marcos G. Farpón

Marcos G. Farpón is currently working as a Postdoctoral Researcher at MIT in the group led by Prof. Yuriy Román-Leshkov, supported by a Ramón Areces fellowship. He received his PhD in 2024 at the Institute for Chemical Technology (ITQ CSIC-UPV, Valencia, Spain) under the supervision of Dr Gonzalo Prieto, working on the design of novel tandem catalytic processes for the conversion of ethylene and syngas into C3 high-added value chemicals integrating concepts such as single atom catalysis (SACs) or electrification strategies. His current work at MIT focuses on the deconstruction of plastics and lignin into sustainable fuels and chemicals.

relevant C–C bond cleavage methods and their reaction mechanisms. Lastly, we illustrate how these mechanistic principles have been used in lignin and plastic deconstruction, excluding systems dominated by C–O bond scission (*e.g.*, β–O–4 interunits in lignin or ester bonds in plastics), which have been extensively reviewed.[24,25,38–42] Overall, this work aims to highlight opportunities in lignin and plastics deconstruction *via* C–C bond cleavage. Given the fundamental and technical significance of this topic, we envision that this research will continue to grow in importance.

2. C–C bonds in lignin and plastics

2.1. Lignin

The complex structure of lignin is dependent on the original biomass source and the conditions used for lignin isolation. In its "native" form, lignin exhibits both C–O and C–C bonds, including β–O–4, 5–O–4, β–5, β–β, β–1, and 5–5 linkages (Fig. 1A).[43–51] A challenge inherent to lignin is that most known biomass processing strategies modify the native lignin structure. In many cases, additional C–C linkages form due to condensation reactions that occur during high-temperature processing (above ~100 °C).[52–63] Procedures for biomass fractionation fall into two methods: (i) "conventional" pulping processes and (ii) "lignin-first" strategies.

Pulping methods generate 'technical lignins,' which typically exhibit a higher number of C–C bonds relative to native lignin. During conventional pulping (*e.g.*, Kraft), labile C–O bonds are cleaved while other lignin fragments undergo repolymerization *via* condensation reactions, yielding technical lignins with new C–C bonds.[37,48,65–68] The severe fractionation conditions result in the formation of α–5, 5–CH_2–5 (methylene), and vinyl–alkyl/–aryl structures, among others (Fig. 1C). In the case of organosolv

Erik T. Ouellette

Erik T. Ouellette worked as a Postdoctoral Researcher at the National Laboratory of the Rockies (formerly NREL), where his studies focused on homogeneous catalysis for lignin valorization and plastics deconstruction. He received his PhD in Inorganic Chemistry from the University of California, Berkeley in 2023 and is currently the Head of Catalysis at Radical Dot, GmbH.

Yuriy Román-Leshkov

Yuriy Román-Leshkov is the Robert T. Haslam (1911) Professor of Chemical Engineering at MIT, where he directs a research group working at the intersection of heterogeneous catalysis, materials science, and sustainable chemical processes. His group develops catalytic technologies for converting biomass and waste feedstocks into fuels and chemicals, with emphasis on sustainable aviation fuels, molecular engineering of catalysts, and chemical recycling waste plastics. Originally from Mexico City, Prof. Román earned his BS from the University of Pennsylvania and his PhD from the University of Wisconsin-Madison, followed by postdoctoral work at Caltech. He has been on the MIT faculty since 2010.

Gregg T. Beckham

Gregg T. Beckham is a Senior Research Fellow and Group Leader at the National Laboratory of the Rockies (NLR). He currently leads and works with an interdisciplinary team at NREL in biomass conversion and plastics recycling and redesign. He received his PhD in Chemical Engineering at MIT in 2007.

Joseph M. Samec

Joseph Samec received his PhD from the University of Stockholm, Sweden, in 2005 with Prof. Bäckvall as supervisor. After a postdoctoral stay with Prof. Grubbs at CalTech, USA, during 2006–2007, he was appointed as Assistant Professor at University of Uppsala in Sweden. In 2015 he moved to Stockholm University where he is currently professor. His research interests focus on green chemistry in organic synthesis and biomass processing and applications. 2012 he founded RenFuel, a start-up company that is producing biofuels from lignin; and then 2015 RenCom (now Lignin Industries) and 2018 LigniCore that produce materials from lignin.

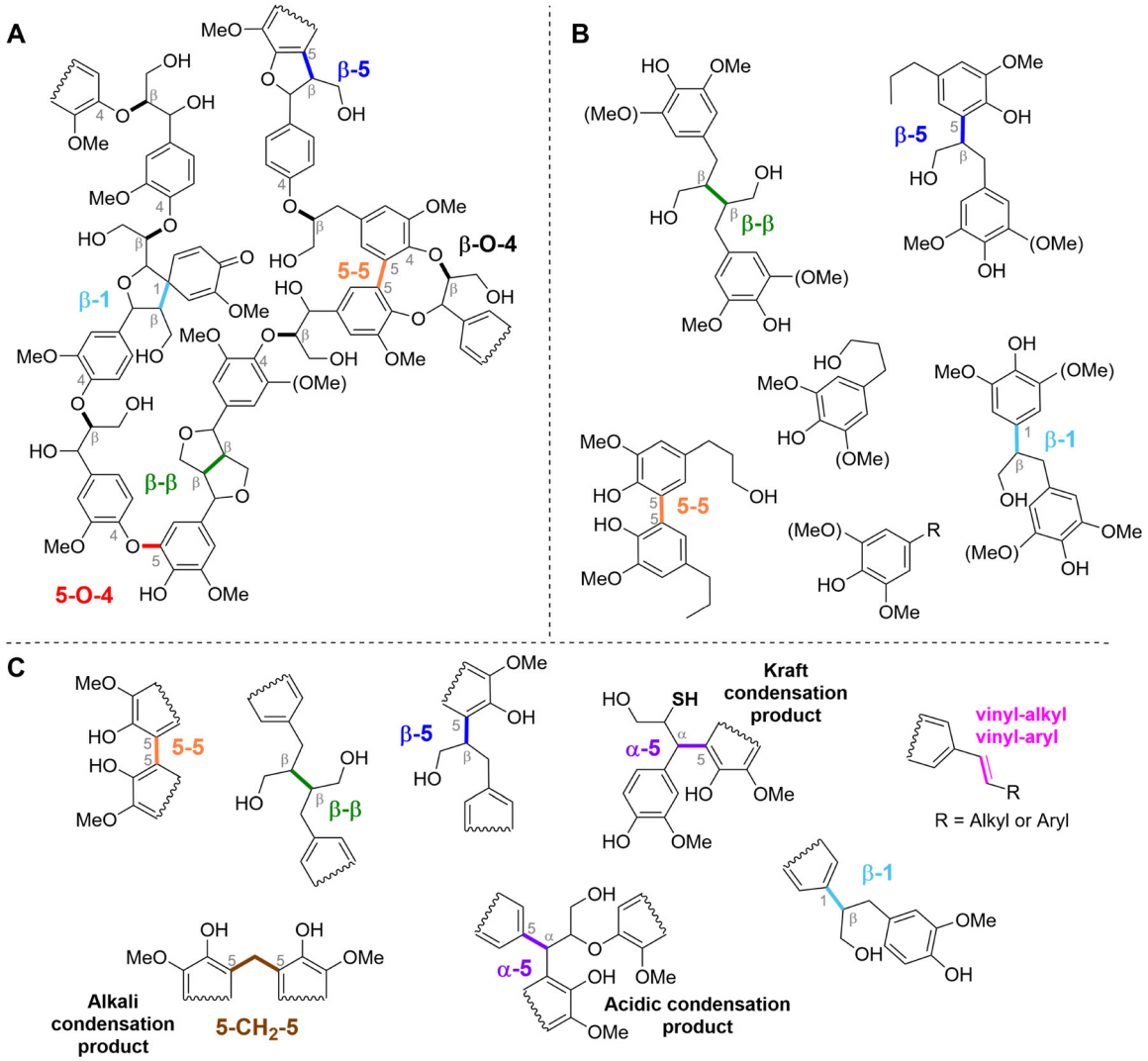

Fig. 1 (A) Representative structure and linkages of native lignin. (B) Monomers and dimers generally produced after lignin-first approaches.[64] (C) Condensed lignin structures formed after conventional fractionation processes, such as Kraft, sulfite, alkali or acid treatments. Different types of linkages between aromatic units are highlighted in different colors.

(acid- or base-catalyzed) and sulfite pulping methods, functional groups (*e.g.*, ethoxy) or heteroatoms (*e.g.*, sulfur) are introduced within the lignin backbone.

In contrast, lignin-first processing utilizes stabilization strategies during fractionation (*e.g.*, reductive catalytic fractionation (RCF), aldehyde assisted, diol assisted, oxidations, *etc.*)[69–72] to minimize condensation (C–C bond formation) during lignin extraction.[69,73–76] The main products of lignin-first catalytic depolymerization, such as RCF, are lignin oils that are generally soluble in organic solvents. They contain aromatic monomers/dimers and oligomers rich in β–5, β–β, 5–5 and β–1 C–C bonds (Fig. 1B).[64,77,78] Lignin-first strategies reported to date only target the deconstruction of labile C–O bonds and lack methods to cleave the C–C bonds present in native lignin. Notably, through selective C–O bond cleavage of β–O–4 linkages – the most abundant lignin motif – theoretical monomer yields are ~10–15 wt% and ~35 wt% from softwoods and hardwoods, respectively.[72,79] The yields have been estimated following the commonly used formula (eqn (1)):

$$\text{theoretical monomer yield} = x^2 \quad (1)$$

in which x is the percentage of β–O–4 bonds present in the lignin substrate. This highlights the importance of C–C bond cleavage to achieve high monomer yields from lignin substrates, since overall monomer yields are inherently limited when only considering cleavage of C–O bonds.

The relative abundance of common lignin C–C linkages and the degree of condensation,[80] related to the amount of C–C and C–O linkages of the aromatic ring, depend on the biomass type and its processing strategy. In general, β–5 are the most abundant C–C bonds in lignin, followed by β–β and β–1 units.[46,49,67,81–86] Several C=C linkages are also present, especially in lignins derived from mildly acidic fractionation methods.[47,87,88] or *via* supercritical water treatment.[89] Consistently, β–5 bonds are the most abundant

C–C linkages in RCF oils, constituting 35–45% of the overall C–C bonds.[64,77,90] Additionally, RCF oil is also characterized by 20–23% of 5–5 bonds. The remaining 5–20% of C–C bonds are typically β–β and β–1 units.

Based on available computational data calculated on model compounds computed using density functional theory and benchmarked against CBS-QB3 complete basis set calculations,[91] 5–5 bonds exhibit the highest bond dissociation energy (BDE) and enthalpy (BDH), followed by β–5 and β–1 units (112–118, 101–108, and 65–69 kcal mol^{-1}, respectively). These values represent the energy/enthalpy contained in each specific bond and are, thus, useful to consider in homolytic bond cleavage processes, such as cracking and pyrolysis. In general, while BDE/BDH values reflect bond strength and the thermodynamics of homolytic cleavage, kinetic factors such as stereochemistry, steric hindrance, and catalyst binding affinity also influence C–C bond cleavage. For instance, the presence of functionality (*e.g.*, hydroxy groups) that can coordinate readily to metal centers, enables more kinetically favorable C–C cleavage pathways in organometallic catalysis, even for C–C bonds that possess high BDE/BDH.

2.2. Plastics

Plastics consist of repeating monomer units connected by covalent bonds, including C–C, C–O, and C–N, with diverse pendant functional groups that influence their properties.[25] Common thermoplastic polymers linked by C–C bonds include PE, PP, polyvinyl chloride (PVC), polystyrene (PS), polymethyl methacrylate (PMMA), and poly-acrylonitrile-butadiene-styrene (ABS) (Fig. 2). C–C linked thermosets mainly include natural or synthetic rubbers.

Functional groups often polarize the adjacent C_{alkyl}–C_{alkyl} bonds and stabilize specific radical or carbocation intermediates, thereby acting as reactive centers for C–C bond activation. This substitution effect can similarly be approximated *via* BDE analysis (Fig. 2, bottom).[92–94] Bond dissociation energies were determined using complementary approaches such as density functional theory methods where BDE = $H_{radicals}$ − H_{parent},[92] and CBS-QB3 *ab initio* methods to derive enthalpies of formation, from which BDEs were subsequently extracted.[93] According to computational studies on model compounds, the BDE of homolytic C–C bond cleavage *via* carbocation intermediates follows the trend PE > PP > PS (BDE ∼ 86–88, 84–86, and 78–80 kcal mol^{-1}, respectively).[92] In PVC, the presence of Cl substituents increases the BDE to ∼88–90 kcal mol^{-1}, due to a cleavage mechanism that relies on the extraction of a HCl molecule.[92] The cleavage of C_{aryl}–C_{alkyl}, C_{aryl}–CN, and C_{alkyl}=C_{alkyl} bonds (∼110 kcal mol^{-1}, ∼130 kcal mol^{-1}, and ∼170 kcal mol^{-1}, respectively), which are present in PS, ABS, are more difficult due to their partial sp^2/sp or full sp^2 character. C_{aryl}–CO bonds in PMMA exhibit a BDE of ∼90 kcal mol^{-1}, due to the electron-withdrawing capacity of the ester groups. To conclude, similar considerations made for lignin can be drawn for plastic substrates, as BDE relate with the energy content of C–C bonds without accounting for steric hindrance and presence of functionalities (*e.g.*, unsaturations or tertiary sites) that facilitate catalyst binding and/or radical stability. In general, BDE are more relevant for thermal and radical processes compared to catalyzed reactions.

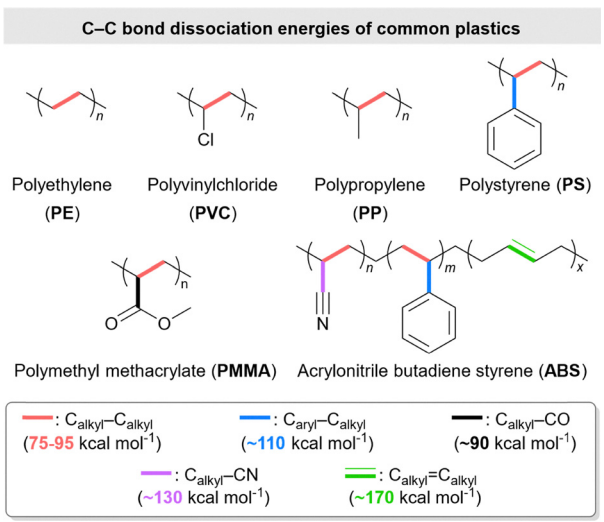

Fig. 2 Structure of common C–C linked plastics and the corresponding bond dissociation energies (BDE) at 298 K of key C–C bonds.[92–94]

3. General approaches for C–C cleavage

Several approaches exist for C–C bond cleavage in the context of small molecules including: transition metal C–C bond activation,[27,28,95,96] synergistic C–C/C–H activation,[97,98] cleavage of unstrained (linear) systems,[29–31,99] cleavage of cyclic systems,[32–35,100] photoinduced and radical reactions,[36,101–103] oxidative C–C cleavage,[104,105] and decarboxylation/decarbonylation pathways,[106,107] among others. Additional methods, such as (hydro-)cracking,[108–113] retro Diels–Alder reactions,[114] electrochemical[115,116] and enzymatic[117] cleavage, and retro aldol condensations[118,119] may not require transition metal catalysts, although some variants may employ them. This section discusses the most relevant approaches that apply towards lignin and plastics deconstruction targeting the cleavage of single, double, and aromatic C–C bonds and their mechanisms. Throughout the text, if not otherwise stated, colored circles indicate general functional groups while cleaved C–C bonds are highlighted in red.

3.1. Metal catalyzed reactions

3.1.1. C–C single bond cleavage. Strain release of small rings is one of the most common strategies for C–C bond activation in metal-catalyzed reactions (Fig. 3A-i).[120] However, the inherent structures of both plastics and lignin preclude this method from being directly applicable. Instead, more relevant strategies include the conversion of unstrained linear systems using reactive precursors or *via* cracking (Fig. 3A-ii and iii).[121] Metal-catalyzed C–C single bond cleavage occurs *via* two main general reaction mechanisms, namely (i) oxidative addition and (ii) β-carbon elimination (Fig. 3B).[120] C–C bond activation *via*

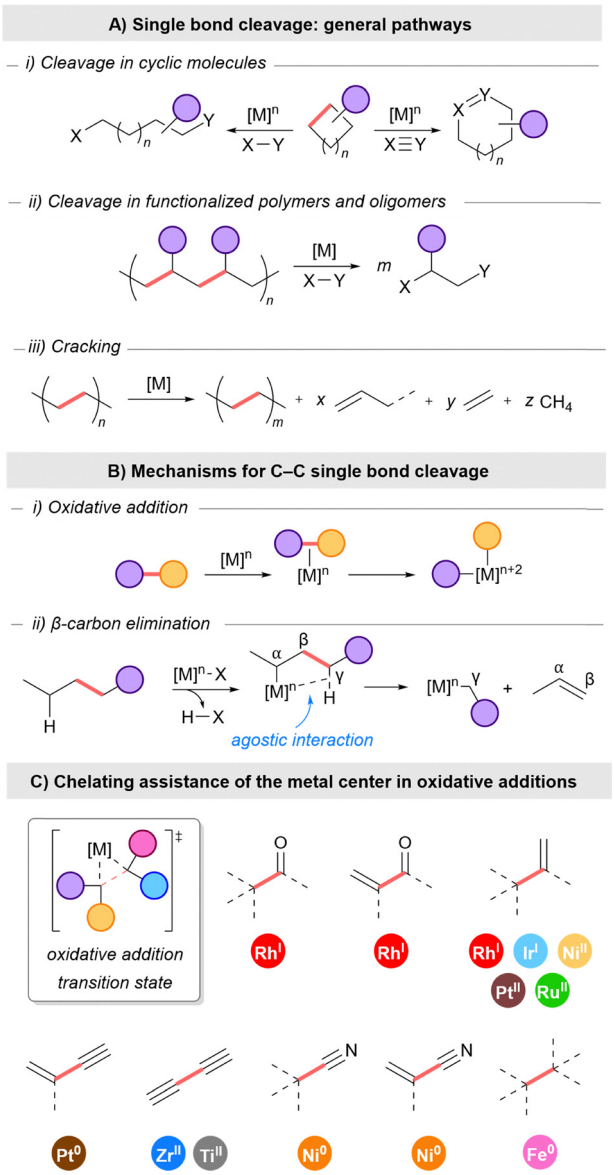

Fig. 3 (A) General pathways for metal mediated C–C single bond cleavage. (B) The mechanisms for metal-mediated C–C single bond cleavage.[120] (C) Metal chelating assistance is key for the cleavage of C–C single bonds *via* metal-catalyzed reactions. Cleaved C–C bonds are highlighted in red; M = metal center; colored circles indicate general functional groups.

oxidative addition is the microscopic reverse of C–C bond formation *via* reductive elimination (Fig. 3B-i). Unlike reductive elimination, which is typically thermodynamically favorable, oxidative addition of unstrained C–C single bonds requires metal-chelating assistance (*e.g.*, σ-bonds, π-bonds, directing groups, and polarized bonds; Fig. 3C).[122] Electron-rich late transition metals in low oxidation states are most commonly applied for oxidative additions, albeit with a few exceptions, such as Ti(II) and Zr(II).[122]

C–C single bond cleavage can also occur *via* β-carbon elimination in substrates such as alcohols, alkoxides, amines, and amides.[97,123] This reaction proceeds *via* coordination of the substrate to a metal center followed by elimination of an alkene and the simultaneous formation of a new metal-bonded alkyl (or aryl) fragment (Fig. 3B-ii).[124] β–Carbon elimination is generally catalyzed by electron-poor early transition metals and, in the case of alkoxides, often proceeds through metal-mediated cyclobutanolate intermediates. This involves an interaction of the β-C–C σ-bond with the metal center, which can then undergo β–carbon elimination to cleave the C–C single bond between the β and γ positions (Fig. 3B-ii).[122] β–Carbon elimination preferentially cleaves C–C bonds that lead to more stable alkenes, following the general trend sp > sp^2 > sp^3 at the γ-carbons.

3.1.2. C=C double bond cleavage. The cleavage of C=C double bonds can occur *via* several processes, including (i) alkene metathesis, addition of C=C bond to yield (ii) carbene complexes, or (iii) carbyne species with the addition of hydrogen gas, and (iv) oxidative cleavage of C=C double bonds typically to generate carbonyl compounds (Fig. 4A).[121] There are also a number of miscellaneous C=C cleavage approaches that are an integral part of more complex functionalization processes, which are reviewed elsewhere and not discussed here.[125–130]

Alkene metathesis, or alkene disproportionation, involves the cleavage and reformation of C=C bonds to give a statistical redistribution of alkyl substituents in the produced olefins (Fig. 4A-i).[131,133–135] The catalytic cycle initiates with a metal carbene [2+2] cycloaddition of the substrate alkene to form a metallacyclobutane intermediate (Fig. 4B-step i). Ring opening of the metallacyclobutane yields a new carbene complex and the redistributed alkene product (Fig. 4B-step ii). Following the same pathway, the reaction of the carbene species with a second equivalent of alkene forms a metallocycle intermediate followed by the release of an alkene (Fig. 4B-steps iii, iv). All steps are reversible and the overall product distribution is dependent on the thermodynamic stability of the products as well as on the reaction conditions.

Grubbs and Schrock's Ru-/Mo-based catalysts are standard catalysts for a wide variety of metathesis reactions,[132,133,136] with detailed reviews of catalysts employed in olefin metathesis available.[134,135] Direct metal insertion into a C=C bond to form a carbene intermediate (Fig. 4A-ii) is less reported compared to the insertion into C–C bonds due to the higher BDEs of C=C double bonds (174 kcal mol^{-1} in $H_2C{=}CH_2$) compared to C–C single bonds (90 kcal mol^{-1} in $H_3C{-}CH_3$).[137] This metal-mediated cleavage of a strong alkene bond is accompanied by the formation of two strong metal–carbene bonds (up to 96 kcal mol^{-1} each).[138] However, substrates that result in stable carbene complexes are suitable for such a transformation.[139] For instance, the scission of diphenyl ketene by an Ir(I) complex is triggered by a metal insertion to give the corresponding carbonyl carbene complex.[140,141] Alkenes that do not contain a weakened C=C bond, or a directing group, undergo C=C cleavage through initial activation of the more accessible C–H bonds to yield H_2 as a co-product and generate a carbyne intermediate (Fig. 4A-iii). Specific examples include the cleavage of ethylene into two metal–methyne fragments by a W(III) species (or similar Ru, Os, Ni complexes) in the presence of a reductant.[142]

Oxidative cleavage is among the most common metal-mediated pathways for C=C bond scission, due to its broad

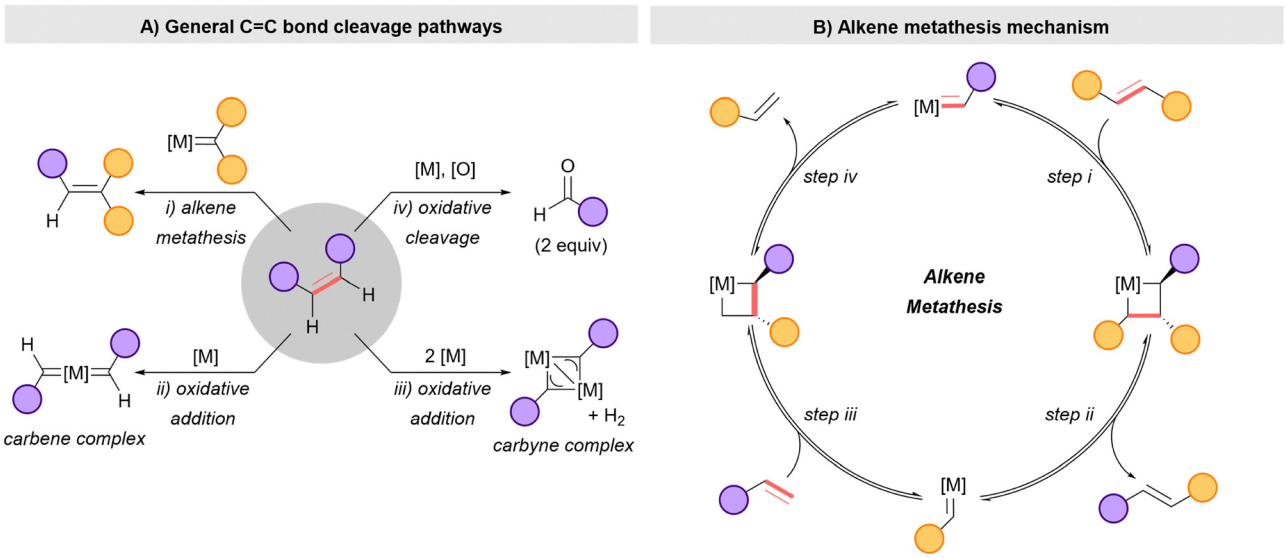

Fig. 4 (A) General pathways for C=C double bond cleavage,[121] (i) alkene metathesis, (ii) oxidative addition, (iii) carbyne intermediate, and (iv) oxygenation. (B) Mechanism of alkene metathesis.[131,132] Alkene metathesis proceeds *via* a metal–carbene intermediate that undergoes a [2+2] cycloaddition with an alkene to form a metallacyclobutane, followed by C–C bond cleavage to give a new alkene and regenerate a new metal–carbene. This cycle "scrambles" the alkene fragments, leading to exchange of substituents between double bonds. M = metal center; colored circles indicate general functional groups.

substrate scope and useful synthetic route to carbonyl compounds (Fig. 4A-iv). Foundational examples of metal-induced cleavage of C=C bonds involve oxidation with permanganate and chromate anions and/or a combination of MnO_4^-, OsO_4, or RuO_4 catalysts with IO_4^- as a terminal oxidant.[143–146] It is well known that these oxidants are associated with environmental and hazard concerns, and greener options are available, such as hydrogen peroxide, molecular oxygen, oxone, ozone, and electrochemical oxidation, which avoid metal waste and typically generate benign by-products such as water. These oxidations convert cyclic alkenes into ketones, diols, epoxides, and carboxylic acids. More recent examples employ less toxic metal catalysts and more convenient oxidants, such as ozone,[147,148] cerium–ammonium nitrate,[149] and cleaner oxidants such as hydroperoxides,[150–153] and hypervalent iodine.[154] Additional catalysts for these transformations are based on Co, Mn, Cu, Au, Pd, Ru, Fe, Cr, Mo, and Ni metal centers.[155–158] Alkene–carbonyl oxidative metathesis also represents an appealing strategy of which stoichiometric Mo and Ti-based catalysts have been developed for this purpose.[134]

3.1.3. Cleavage of aromatic C–C bonds. Metal-mediated cleavage of C–C bonds in aromatic rings can proceed in either an oxidative or non-oxidative fashion through ring expansion, contraction, or opening following loss of aromaticity (Fig. 5). Non-oxidative cleavages are rare because they require thermodynamically unfavorable dearomatization and stabilization of highly strained or reactive intermediates prior to C–C bond scission. Reported pathways include metal insertion into the aromatic ring to form a metallacycle (Fig. 5A-i), ring contraction to five-membered carbocycles or related derivatives (Fig. 5A-ii), ring opening to generate linear conjugated products (Fig. 5A-iii), and carbene-mediated ring expansion reactions (Fig. 5A-iv).[159–168] Conversely, oxidative cleavage of aromatic rings to yield acyclic oxygenated products is far more prevalent (Fig. 5B).[121]

Direct insertion of a metal into an aromatic ring has been developed using electron-rich Pt(0),[159] Ru(II),[160] Ir(I),[161,162,169] and Al(I)[163] complexes, often facilitated by directing substituents or chelation effects (Fig. 5A-i, compound **1**). In the absence of metal insertion, arene C–C bond scission may proceed through alternative non-oxidative pathways.[121] One case is when the metal center activates the aromatic ring for nucleophilic functionalization to yield an intermediate that rearranges through ring contraction (Fig. 5A-ii, compound **2**). A second case is the formation of a metal carbene species that cyclopropanates the aromatic ring and triggers ring expansion rearrangement (Fig. 5A-iv; compound **4**). An example of arene ring contraction was reported using cationic Re-complexes upon treatment with sodium hydroxide,[170] whereas Cu and Rh catalysts facilitate arene ring expansion through carbene insertion into the aromatic ring.[171,172]

Additional non-oxidative pathways to cleave arene C–C bonds include the formation of linear conjugated compounds following de-aromatization (Fig. 5A-iii; compound **3**). Representative examples include arene-opening metathesis polymerization,[161] insertion of an Al-complex in the aromatic ring,[163] and formation of Ti-benzenes from alkylbenzenes.[168] Other non-oxidative bio-catalyzed strategies for aromatic ring opening are also possible pathways but are outside the scope of this review.[173]

Aerobic oxidative cleavage of aromatic rings (Fig. 5B) *via* enzymes is an important biochemical pathway for converting recalcitrant aromatic compounds to acyclic products, which has been extensively reviewed.[174–177] Key aspects of the reaction generally undergo activation by dioxygenase enzymes and the use of Fe ions as cofactors. Chemo-catalytic routes include the oxidative cleavage of bio-derived catechols as appealing precursors for the

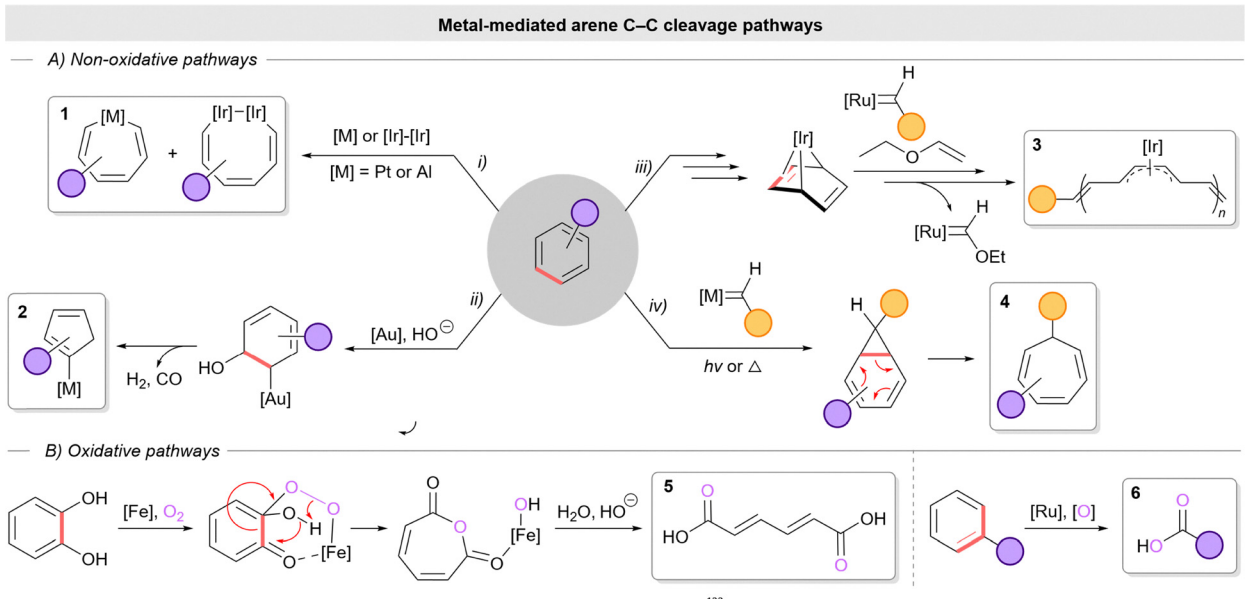

Fig. 5 (A) Non-oxidative (B) and oxidative pathways for the cleavage of C–C bonds in arenes.[121] (A-i) metal insertion into the aromatic ring to form a metallacycle; (A-ii) ring contraction to five-membered carbocycles or their derivatives; (A-iii) ring opening by metathesis reactions; (A-iv): ring expansion to carbocycles. (B) The metal, assisted by O_2 or other oxidants, first coordinates catechol and undergoes an intramolecular rearrangement involving C–C bond cleavage. Subsequently, ring opening provides muconic acid (**5**) as the product. M = metal center; cleaved C–C bonds are highlighted in red; colored circles indicate general functional groups.

sustainable synthesis of several C_6 industrial chemicals (*e.g.*, adipic acid and caprolactam).[178–180] Ozonolysis has also been developed for the cleavage of arene C–C bonds although its application remains limited by harsh reaction conditions and substrate scope (*vide infra*).[175]

3.2. Radical reactions

C–C cleavage through radical reactions has been widely investigated for single bonds, while less attention has been given to the cleavage of C=C double and arene bonds.[36,101] The most widespread radical routes involve radical addition–migration–fragmentation cascades and radical C–C fragmentation reactions (Fig. 6).

Tandem radical migrations involve an initial radical addition followed by its transfer to a reactive functional group (*i.e.*, an alkene or aromatic ring), which then can undergo C–H migration prior to C–C cleavage, and lastly single electron transfer (SET) to generate the product (Fig. 6A). They are generally catalyzed by metal complexes, such as Cu or Ag, and/or radical precursors/traps, such as Togni's, Langlois', Umemoto's reagents, Ph_2PO-/$(OR)_2PO$-/SCF_3-/silyl-ethers, acetonitriles, dimethylsulfoxide, aldehydes, *t*-butyl-hydroperoxide, or *t*-butyl-ammonium iodide.[36]

In general, radical C–C fragmentation reactions occur *via* two different mechanisms (Fig. 6B): (i) C–C bond cleavage proceeding through homolytic radical fragmentation or (ii) a radical oxidative rearrangement.[181] Reactions occurring *via* a fragmentation pathway include radical-mediated cleavage of unstrained $C(sp^3)$–$C(sp^3)$ bonds, C–CO bonds, and radical decarboxylation of carboxylic acid derivatives.

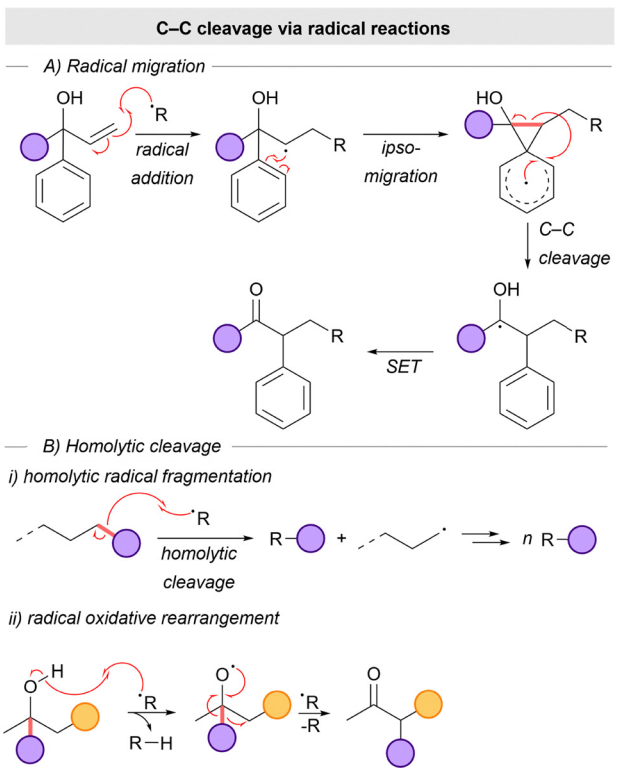

Fig. 6 (A) General mechanism for tandem radical migration reactions.[36] A carbon radical is first transferred to the substrates and then it migrates in a substituent or aryl group, providing a more stable radical intermediate, followed by β-scission (C–C cleavage). (B) Pathways for radical fragmentation reactions: (i) homolytic radical fragmentation and (ii) radical oxidative semi-pinacol type rearrangement.[181] Cleaved C–C bonds are highlighted in red; colored circles indicate general functional groups; SET = single electron transfer.

3.3. Retro Diels–Alder, retro aldol condensation, and Baeyer–Villiger oxidation

A retro Diels–Alder reaction, formally a [4+2] cycloelimination, is a specific class of concerted pericylic reactions in which two σ-bonds are broken to form one new π-bond (Fig. 7A). Such a transformation involves the dissociation of the Diels–Alder adduct back to its original components, the diene and the dienophile.[114] A common example of a retro Diels–Alder reaction is the synthesis of 1,3-butadiene and ethylene from cyclohexene, which illustrates the nature of the reaction. Retro Diels–Alder reactions are generally conducted thermally using flash vacuum pyrolysis, shock tube, photochemical (laser) activation, or gamma-radiation.[114] The conditions required to carry out retro Diels–Alder may result in several byproducts depending on the substrate. Alternative ways to carry out a retro Diels–Alder reaction under milder conditions have utilized (i) strained substrates, (ii) substrate activation with a trimethylsilyl (TMS) functional group, and (iii) the addition of heteroatoms within the system to polarize/activate the bonds. However, these methods require meticulous substrate design and are not generally applicable to most olefins. For a more detailed overview of such techniques, we refer to comprehensive reviews on the topic.[114,182,183]

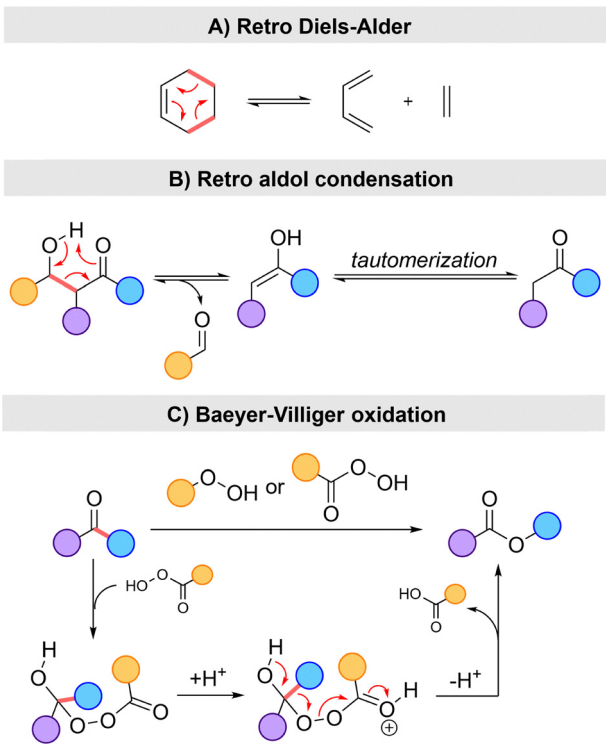

Fig. 7 (A) Model example of retro Diels–Alder of cyclohexene to form 1,3-butadiene and ethylene. (B) General mechanism of the retro aldol condensation. (C) Conversion of ketones into esters *via* Baeyer–Villiger oxidation and the mechanism of the reaction. A peroxyacid first adds to the ketone to form a Criegee intermediate, which then undergoes a concerted rearrangement where an adjacent substituent migrates (C–C cleavage) with simultaneous O–O bond cleavage, yielding an ester (or lactone). Colored circles indicate general functional groups.

Retro aldol condensation is the reverse reaction of aldol condensation. The reaction can be acid- or base-catalyzed and involves the cleavage of a C–C single bond to generate an aldehyde and enol intermediate (Fig. 7B). Examples of enzyme-,[184,185] peptide-,[186] Cu-,[187] Pd-,[188] Rh-,[189] biomimetic-,[190] photo-,[191] and N-heterocyclic carbene-catalyzed[192] processes are present in the literature. The equilibrium is sensitive and can be readily shifted by varying the reaction conditions (mainly heat and reagent excess). Retro aldol condensation is substrate specific, as a hydroxyl group must be adjacent to an unsaturated synthon. For instance, it occurs when carbohydrate-like compounds,[193,194] β-hydroxyl ketones/aldehydes or nitriles,[187,188,195] or nitroketones[196] are involved.

Lastly, Baeyer–Villiger oxidation represents an additional C–C cleavage method that involves the formation of an ester starting from a ketone (or a lactone from a cyclic ketone) *via* an oxidative rearrangement involving migration of an alkyl or aryl group (Fig. 7C).[197,198] The reaction is promoted by peroxyacids or peroxides, such as *meta*-chloroperbenzoic acid (*m*CPBA), trifluoroperacetic acid, and peroxides such as hydrogen peroxide (H_2O_2) or *tert*-butyl hydroperoxide.[198] This transformation can be catalyzed by Se-, Pt-, Ni-, Sn-, Cu-, Zr-, Al-based catalysts, among others, or by biocatalysis, and generally proceeds under mild conditions ($T < 100$ °C) following the Criegee mechanism (*vide infra*).[199]

4. Reported routes for the C–C cleavage in lignin and plastics

Having reviewed the general C–C cleavage methods and mechanisms relevant for lignin and plastics deconstruction, we showcase and discuss reports on the cleavage of C–C bonds in lignin/plastics substrates and their model compounds, with a focus on their mechanism, when available. Tables 1 and 2 summarize the main approaches complemented with substrate type, reaction conditions, catalyst used and yield of main products starting from lignin and plastic substrates, respectively.

4.1. Lignin

Significant efforts have been devoted to lignin depolymerization *via* targeted C–C bond cleavage using strategies such as hydrogenolysis, oxidative cleavage, reductive fragmentation, acid/base-catalyzed depolymerization, and radical-mediated pathways (Table 1). In particular, the cleavage of C–C bonds in lignin has been achieved through mechanisms including oxidative addition, β-scission, radical fragmentation, Baeyer–Villiger oxidation, and retro-aldol condensation, among other approaches, which are discussed in the following sections.

4.1.1. Oxidative addition. The cleavage of lignin C–C bonds *via* oxidative addition has been relatively underexplored, with only a single example to date targeting the cleavage of 5–5 bonds. Dong and coworkers showcased a Rh-catalyzed cleavage of C_{aryl}–C_{aryl} bonds in lignin model substrates mimicking 5–5 lignin bonds *via* oxidative addition (Fig. 8A).[200] These particular linkages are among the most difficult lignin bonds to cleave, as

Table 1 Main reported works on the depolymerization of lignin *via* C–C bond cleavage

Entry	Substrate	Method	Catalytic system	T; p; t (°C; bar; s/min/h)	Major products; yield	Ref.
1	Protected phenols, 5–5 linked	Hydrogenolysis	Rh + directing group	150; 7; 24 h	Phenols; 55–85 mol%	200
2	Protected phenols, methylene linked	Hydrogenolysis	Rh	150; 10; 12 h	Phenols; 54–87 mol%	201
3	β–5, β–1, and 5–5 models	Hydrogenolysis	NbO_x-supported Ru	310; 5; 40 h	Aliphatic and aromatic hydrocarbons; 124–153 mol% (theor.; C–O + C–C cleavage)	202
4	Lignin and model compounds	Hydrogenolysis	Pt/H–MOR	300; 40; 24 h	Aromatic and aliphatic cycloalkanes; 77 wt% (C–O + C–C cleavage)	203
5	Beech sawdust	Hydrogenolysis	Ni–Al alloy	200; 5; 5 h	Functionalized monophenolics; 62.9 wt% (initial lignin; C–O + C–C cleavage)	204
6	Pine-derived pyrolytic lignin	Ozonolysis	Cat.-free	0; 1; 4 h	Mono-/di-carboxylic acids; 45 wt% (initial lignin substrate)	205
7	Various lignins	Ozonolysis	Cat.-free	r.t.; 1; 10 s	Vanillin and p-hydroxybenzaldehyde; 5 wt% (initial lignin, C=C cleavage)	206
8	Diluted-acid corn stover lignin and steam exploded spruce lignin	H_2O_2 oxidation	Chalcopyrite	60; 1; 5 h	Dicarboxylic acids; 11–14 wt% (initial lignin)	207
9	Corn stover lignin	Bioconversion	*Pseudomonas putida*	r.t.; 1; 24 h	B-ketoadipic acid; 10 wt% (initial lignin)	208
10	Organosolv bagasse lignin	O_2 oxidation	$[BSmim]CuPW_{12}O_{40}$	160; 5; 5 h	Diethyl maleate; 40.5 wt% (lignin substrate)	209
11	Acetyl protected poplar RCF oil	O_2 oxidation + bioconversion	Co/Mn/Br + *Pseudomonas putida*	120; 1; 2 h	*cis*-/*cis*-muconic acid; 13 wt% (initial lignin)	210
12	Methyl protected pine and poplar RCF oil	O_2 oxidation	Mn/Zr	150; 6; 1.5 h	Aromatic acids and aldehydes; 23 wt% (initial lignin)	211
13	Deoxygenated pine, poplar and birch RCF oil	O_2 oxidation + bioconversion	Co/Mn/Br + *Pseudomonas putida*	220; 6; 3 h	73 wt% aromatic monomer yields (initial substrate) Adipic acid; 26 wt% (initial lignin)	212
14	Pine and poplar lignin RCF oligomers	O_2 oxidation	$CuSO_4$, NaOH	210; 3.4; 3 h	Aromatic acids and aldehydes; 19–34 wt% (lignin substrate)	213
15	Pine, cedrela, poplar, willow, eucalyptus, peach, applewood and cedar, and herbaceous plant *Phyllostachys pubescens*	Hydrogenolysis	RuW/HY_{30}	240; 1; 10 min	Benzene; 18.8 wt% (initial lignin)	214
16	Pine and birch wood RCF oil	Gas-phase hydroprocessing	Ni/SiO_2	410; 1; n.a.	Phenol and propylene; 20 wt% and 9 wt%, respectively (initial lignin)	215

n.a. = not available

they exhibit a partial sp^2 character, a high BDE of 112–118 kcal mol^{-1},[91] and are difficult to access kinetically. Bond cleavage was achieved by substituting the hydroxyl groups on **5** with catalytic amounts of phosphinite directing groups for the Rh center (A) to coordinate to and access the C_{aryl}–C_{aryl} bond of interest in reaction with H_2 to generate a putative Rh–H active catalyst (B, Fig. 8).

The authors investigated the 5–5 cleavage reaction mechanism *via* both model compound experiments and density functional theory (DFT) calculations. The proposed mechanism is shown in Fig. 8B and is as follows:[200] the starting Rh complex (A) is activated by H_2 to form a Rh–H species (B, step i), which cleaves the C_{aryl}–C_{aryl} bond *via* an oxidative addition step to form C (step ii). This is followed by reductive elimination of the hydride to form D (step iii) and oxidative addition by another equivalent of H_2 to generate E (step iv). Another hydride insertion step follows (step v) leading to a ligand exchange with the incoming substrate **6** to liberate the product **7** and regenerate B. DFT calculations also suggest that the Rh–H pathway is the most energetically favorable C–C bond cleavage route, and their detailed mechanistic investigation supports the proposed pathway.

Using the same Rh catalyst in tandem with the phosphinite-directing groups, the same group showcased an expanded reactivity to encompass the cleavage of C_{alkyl}–C_{aryl} methylene bridges shown in Fig. 8C.[201] Various mechanistic experiments such as deuterium labelling studies, rate order determination, and DFT calculations were conducted to conclude that the catalyst follows the same C–C bond cleavage pathway previously reported *via* oxidative addition.

While the use of stoichiometric amounts of phosphinite directing groups likely limits the scalability of this approach, the study provides important mechanistic insights into how functionalization of phenolic groups can facilitate access to otherwise inert 5–5 linkages. Future efforts may focus on finding alternative, more atom-efficient strategies that achieve similar substrate activation without the need of stoichiometric directing groups. Overall, the reported studies indicate that C–C bond cleavage in lignin *via* oxidative addition can be accomplished using noble metal pincer catalysts (*e.g.*, Rh), which can coordinate lignin bearing functionalized phenolic hydroxyl groups under relatively mild temperatures (T = 150 °C) and reductive conditions.

4.1.2. β-carbon elimination. In the lignin literature, the term β-carbon elimination is often used broadly to describe either β-elimination or β-scission pathways, though the two mechanisms are different. β-elimination generally proceeds through carbocation intermediates on acidic supports, while β-scission requires radical C–C bond homolytic cleavage. β-elimination regularly

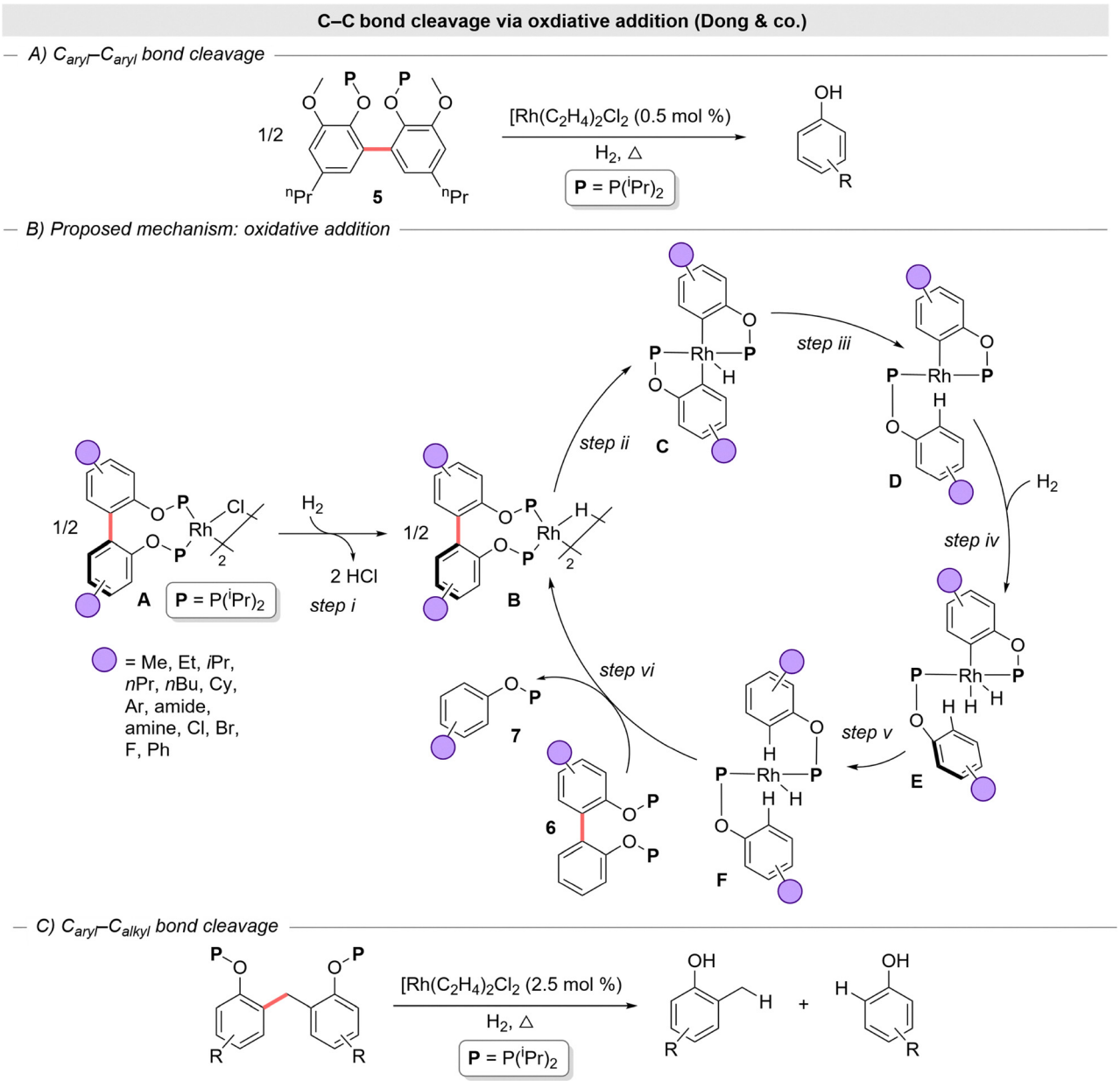

Fig. 8 (A) The synthesis of substituted phenols *via* the cleavage of C_{aryl}–C_{aryl} bonds.[200] (B) Dong and coworkers' mechanism of the reaction involving oxidative addition. The Rh catalyst is first activated by H_2 to form a Rh–H species, which undergoes oxidative addition into the C_{aryl}–C_{aryl} bond followed by reductive elimination to form a reorganized intermediate. A second H_2 activation and hydride insertion then occur, and ligand exchange with the substrate releases the product while regenerating the active Rh–H species. (C) Dong and coworkers' mechanistic experiments to validate their mechanism. (D) Dong and coworkers' follow-up work on the cleavage of methylene linked arenes.

invokes organometallic catalysts and is fundamentally the reverse of migratory insertion across a metal bond, producing a metal–alkyl intermediate. β-scission, on the other hand, often is described in free radical chemistries and thermal cracking and it involves the homolytic radical cleavage of single bonds. Both processes ultimately generate alkene substrates and this challenges mechanistic evaluations and distinction. For these reasons, this section combines these two pathways under the term "β-carbon elimination," as in most cases a rigorous distinction is difficult to establish based on the mechanistic evidence provided in the literature. β-carbon elimination has been a widely explored pathway for C–C bond cleavage in lignin or lignin models, comprising β–5, β–1, and 5–5 bonds. The reactions are generally carried out under reductive conditions (mainly H_2) using noble metal (Pt, Pd, Ru, *etc.*) catalysts to yield saturated cyclic or linear alkanes and aromatics (*e.g.*, benzene).[203,214,232]

β-Carbon elimination was suggested by Wang and coworkers as the pathway for C_{aryl}–C_{alkyl} bond cleavage in lignin models (Fig. 9A).[202,232] Utilizing a NbO_x-supported Ru catalyst, they investigated the reaction of different model compounds containing β–5, β–1, and 5–5 lignin bonds.[202] They used biphenyl (**8**) as a model compound for the cleavage of C_{aryl}–C_{aryl} (5–5) bonds and

observed a 97 mol% conversion of **8** to yield 25 mol% **9**, 24 mol% **10**, 19 mol% **11**, 3 mol% **12**, 14 mol% **13**, and <1 mol% **15** (Fig. 9A).[202] The authors combined the use of inelastic neutron scattering, diffuse reflectance infrared Fourier Transform spectroscopy, and DFT calculations to suggest that NbO_x strongly adsorbs phenyl cyclohexane *via* the aromatic substituent, thus leading to the activation of the C_{aryl}–C_{alkyl} bond between the benzene ring and the cyclohexane group, based on the suggested catalyst's ability to significantly reduce the energy barrier to cleave the C_{aryl}–C_{alkyl} bond of the carbocation intermediates. According to the authors, the reaction occurs *via* two main pathways (Fig. 9A): (i) hydrogenation of an aromatic ring in **8** followed by C_{aryl}–C_{aryl} cleavage of **9** *via* β-alkyl elimination and (ii) partial hydrogenation of a ring to the cyclohexene intermediate **14** followed by isomerization to **15** and C_{aryl}–C_{aryl} cleavage *via* β-alkyl elimination to form **10**

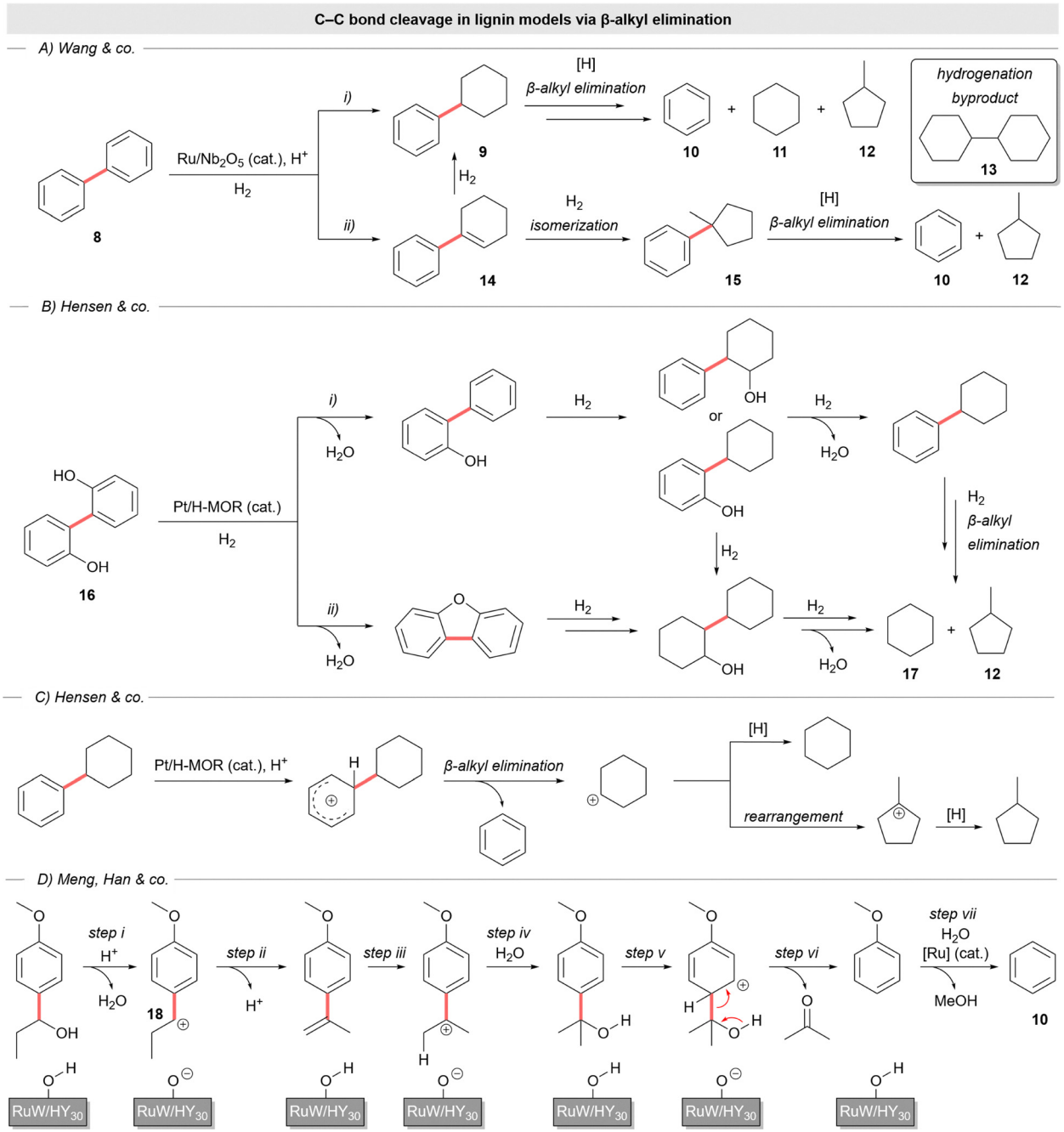

Fig. 9 (A) Wang and co.[202,232] and (B) Hensen and co.[203] pathways for the cleavage of C_{aryl}–C_{alkyl} bond and/or C_{alkyl}–C_{alkyl} bonds. (C) Plausible reaction mechanism for the conversion of phenylcyclohexane into benzene and other cyclic compounds *via* C–C cleavage mediated by Ru/Nb and Pt/H–MOR catalysts under acidic conditions.[203] (D) Mechanism to produce benzene from lignin promoted by a HY zeolite supported RuW alloy catalyst.[214] A Brønsted acid-catalyzed sequence generates a carbocation that undergoes subsequent rearrangement, hydration, protonation, followed by β-elimination to cleave the C_{aryl}–C_{alkyl} bond.

and **12**. Their proposed reaction pathway was supported experimentally and by DFT calculations.

Hensen and coworkers employed a Pt/H–MOR (MOR = mordenite) catalyst to convert lignin into monomers (Fig. 9B and C).[203] Shown in Fig. 9B, 2,2-biphenol (**16**) was used as a model substrate to represent a 5–5 linkage and was subjected to C–C cleavage facilitated by a Pt/H–MOR catalyst. Subjecting **16** to optimal conditions resulted in 100% conversion and gave an estimated yield of 70 mol% **17**, 16 mol% **12**, and 7 mol% dimers. DFT was used to investigate the pathway by which Pt/H–MOR cleaves C–C bonds. They found that the Brønsted acidic sites of H–MOR promoted the cleavage of C_{aryl}–C_{alkyl} bonds (Fig. 9C),[203] cleaving both C_{aryl}–C_{aryl} and C_{alkyl}–C_{alkyl} bonds *via* bifunctional catalysis. The catalyst can also simultaneously dehydroxylate aryl moieties, promote cyclization to generate furan-like compounds, hydrogenate arene rings, and perform C–C cleavage of dicyclohexyl moieties (Fig. 9B). Their mechanistic proposal was experimentally supported and aligned with Wang and coworkers studies.[232] The ability to dehydrogenate the fully reduced bicyclic compound to activate the substrates was key to increase reaction yields. The utility of this strategy was demonstrated on a real lignin substrate obtained through an RCF step that gave 42 wt% monomers followed by C–C scission to give a total monomer yield of 77 wt%. Notably, techno-economic analysis demonstrates the viability of the process, achieving a minimum fuel selling price of $1.51 GGE (Gasoline Gallon Equivalent), with an internal rate of return of 23.0% and a payback time of 6.6 years enabled by ~54 wt% lignin valorization into fuel-range products.[232] In parallel, life-cycle assessment reveals emission of 0.47 g CO_2 eq MJ^{-1}, which translates in a 55.0–77.1% reduction compared to synthetic paraffin kerosene.[232]

Meng, Han and coworkers developed a high-silica HY_{30} (hydrogen-type faujasite Y) zeolite-supported RuW alloy catalyst that simultaneously cleaves C_{aryl}–C_{alkyl} lignin bonds and promotes the hydrogenolysis of methoxy groups to yield benzene as the major product in *ca.* 19 wt%.[214] The mechanism was studied using DFT calculations (Fig. 9D). The reaction pathway is proposed to be initiated by an acid catalyzed dehydration to generate a carbonium ion (step i) followed by a methyl shift assisted by the Brønsted acid center on the catalyst to form intermediate **18** (step ii). Steps iii and iv show an alkene hydration, followed by protonation of the aryl ring to generate a reactive carbonium ion (step v) and resulting in a β-elimination C–C cleavage step (step vi). Acetone is produced as a co-product and anisole as the intermediate. Anisole is further transformed into benzene (**10**) through the hydrogenolysis of the methoxy groups (step vii). The ability of the catalyst to promote both C–C bond cleavage and deoxygenation is a strength of this approach. Additionally, Lu and coworkers developed a Ni_2Al_3 alloy catalyst for the cleavage of β–β and β–5 bonds of lignin in raw biomass to produce monomers in 63 wt% yield, including monomers also obtained *via* C–O bond cleavage.[204] Although no mechanistic studies were performed, a C–C cleavage *via* β-carbon elimination was proposed. It would be worthwhile to study this reaction pathway further.

Overall, the reported studies suggest that the acidity of the support and the capacity of the metal catalyst to work under reductive conditions are key elements for a successful cleavage of C–C bonds *via* β-carbon elimination. This approach is versatile and applicable to diverse lignins and common catalysts include noble metals like Ru or Pt deposited on acidic supports which are active at relatively high temperatures (T = 200–300 °C). However, attention should be given to catalyst deactivation due to impurities, for instance sulphur and ash in Kraft lignin.

4.1.3. Aromatic ring opening. Aromatic ring opening of lignin substrates has been carried out mainly under oxidative conditions, using O_2, O_3, or other oxidants.[180,205,206,233–235] The reaction involves the formation of unsaturated mono- or dicarboxylic acids as the main products and consequent loss of aromaticity. Both catalyst-free protocols and systems using non noble metal catalysts, such as Fe, have been reported, with radical-initiation frequently proposed. A major challenge of this strategy is overoxidation, which can lead to extensive degradation or CO_2 formation, thus emphasizing the importance of kinetic and thermodynamic control for success.

One method for the aromatic ring opening of lignin and lignin model compounds is ozonolysis.[206,236–239] Heeres and coworkers demonstrated oxidative aromatic ring opening using O_3 to valorize pyrolytic lignin fractions and model components (yield of dicarboxylic acids 4–40 wt%),[205] to depolymerize lignins into dicarboxylic acids/esters (yields up to 40 wt%) and a mixture of organic monomers (yields 20–80 wt%),[238,240] and to convert technical lignins into biofuels (yields 10–46 wt%).[241] Their proposed mechanism of C–C bond cleavage for these systems was studied through the ozonolysis of lignin and lignin-like compounds. Electrophilic O_3 addition to activated aromatic substrates generates a zwitterion intermediate (Fig. 10A-i; compound **19**). In acidic media, guaiacolic compounds (R = H; **20**) favor the heterolytic O–O bond cleavage over homolytic O–O cleavage to generate intermediate **21** resulting in arene ring opening to form alkyl oxygenates. Similarly, nonphenolic compounds (R = OCH_3) undergo heterolytic C–C cleavage of **22** *via* the Criegee mechanism[242] to generate similar oxygenates. Alternatively shown in path ii, an unproductive outer-sphere electron transfer between the lignin compounds and O_3 produces a phenoxy radical (Fig. 10A-ii; compound **23**), which is highly unstable and can readily polymerize. The proposed pathways were based on previous studies with model compounds, quantum mechanical calculations[243–246] and kinetics of ozonolysis.[239,247–250]

Examples of ozonolysis not involving aromatic ring opening are also present in the literature.[206,236,237] Subramaniam and coworkers demonstrated the cleavage of C–C bonds in lignin *via* ozonolysis.[206] Utilizing a spray reactor to mix acid-dissolved grass lignin with ozone, they found they could produce up to 5 wt% of aromatic monomers, including vanillin and *p*-hydroxybenzaldehyde. Notably, the spray reactor allowed for significantly improved monomer yields compared to similar ozonolysis reactions in a continuous stirred tank reactor.[237] While ozone typically oxidizes C=C double bonds through the Criegee mechanism (*vide supra*), the authors note that they believe the acid solvent participates in the lignin reactions, disrupting the standard mechanism.

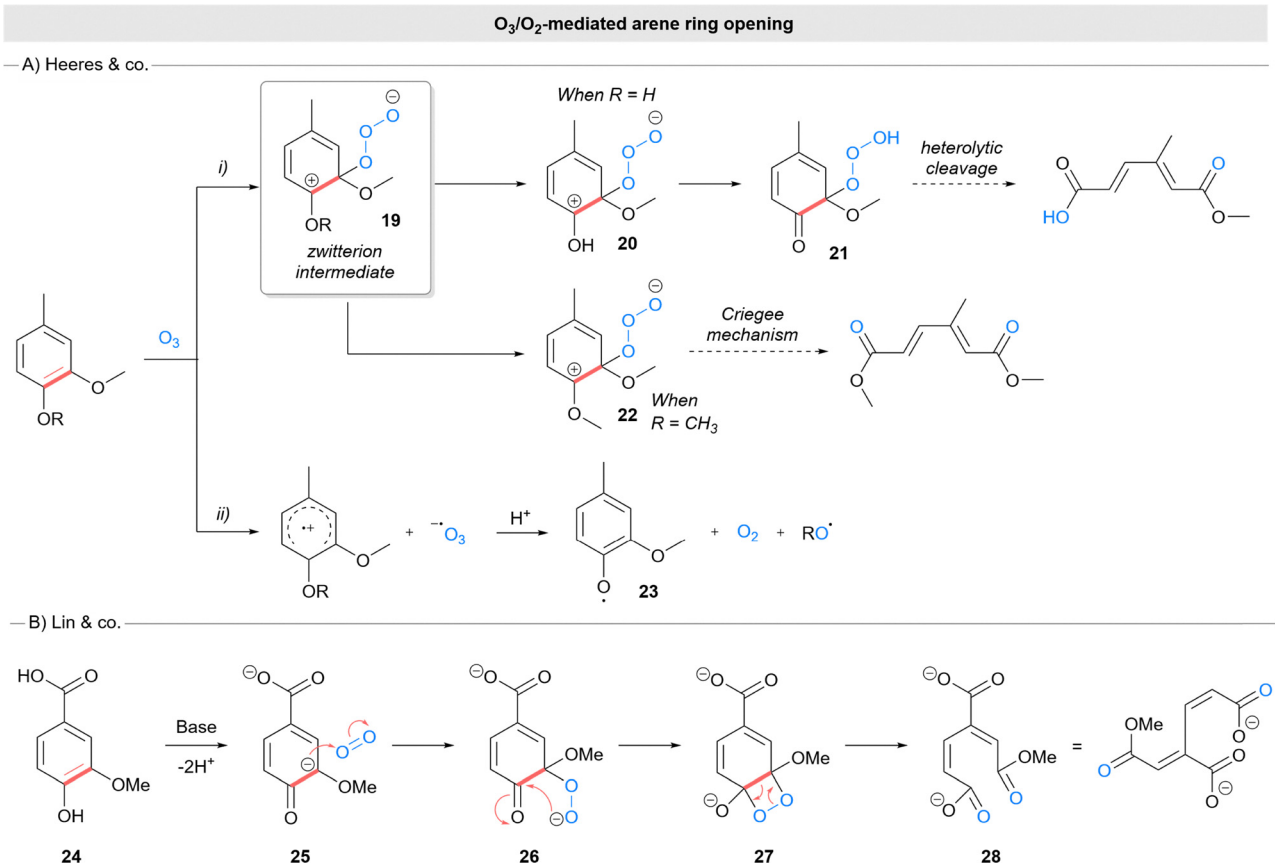

Fig. 10 (A) Possible mechanisms for the O_3-mediated arene ring opening: (i) C–C cleavage, and (ii) an undesirable side reaction that generates phenoxy radicals.[205,240] O_3 adds to the aromatic ring to form a reactive zwitterion intermediate which ultimately opens the ring aromatic ring *via* the Criegee mechanism. (B) Lin and coworkers proposed plausible mechanism for the arene ring opening mediated by molecular oxygen.[251] Base-promoted deprotonation activates the aromatic ring for oxygen addition, leading to an intramolecular cyclization and subsequent C–C bond cleavage that yields a polycarboxylate product.

Additional examples of ozonolysis of lignin and/or lignin model compounds are ozonation to convert lignosulfonates into sulfonated muconic acid-like carboxylic acids,[252] to upgrade lignin-derived products[253] and almond shell lignin,[254] among others. The mechanism was not given in the latter works. Overall, the ozone chemistry of aromatic compounds remains, in general, poorly understood and further studies could focus on better understanding the mechanism of these reactions.

Oxidative lignin conversion to aromatic monomers using O_2 as the oxidant has also been reported.[233,251,255,256] Lin and coworkers investigated the mechanism of lignin degradation under O_2 in alkali conditions (T = 160 °C, O_2 = 20 bar, Cat. = MgO).[251] They selected syringic, vanillic acid, and *p*-hydroxybenzoic acids as lignin models, to better understand the aromatic ring opening pathway, with the example of vanillic acid (**24**) shown in Fig. 10B. Deprotonation of both the carboxylic acid and the phenolic moieties activates the aromatic ring (compound **25**) to undergo a nucleophilic attack on oxygen, forming compound **26**. Oxygen then supports an intramolecular nucleophilic attack to form a cyclobutane structure (compound **27**), which then undergoes C–C cleavage to form the corresponding poly-carboxylate **28**. This pathway was proposed based on model compound experiments and would benefit from further validation. A similar path involving a superoxo intermediate was proposed by Xueqing and coworkers during their studies on the H_2O_2-promoted, microwave-assisted degradation of soda lignin, although the product yield was not reported.[234]

Quinone intermediates represent another important class of species in aromatic ring opening. Zhang and coworkers reported on the chalcopyrite-catalyzed oxidative conversion of lignin into dicarboxylic acids *via* quinone intermediates (Fig. 11A).[207] Lignin-derived monophenolics were first transformed into quinones and they subsequently underwent arene C–C cleavage to afford the desired dicarboxylic acids, according to their proposed mechanism (11–14 wt% yield from lignin). It would be of interest to further study the reaction mechanism from phenolic monomers into quinones. Beckham and coworkers suggested that a possible mechanism for arene ring-opening involves the oxidation of monomeric compounds into the corresponding benzoquinone derivatives, which can be converted into maleic acid derivatives (Fig. 11B).[208,210,257] Also in this case further mechanistic studies are required to gain insights into the reaction pathway.

Li and coworkers reported on the oxidative aerobic C–C cleavage for the selective production of diethyl maleate (yield:

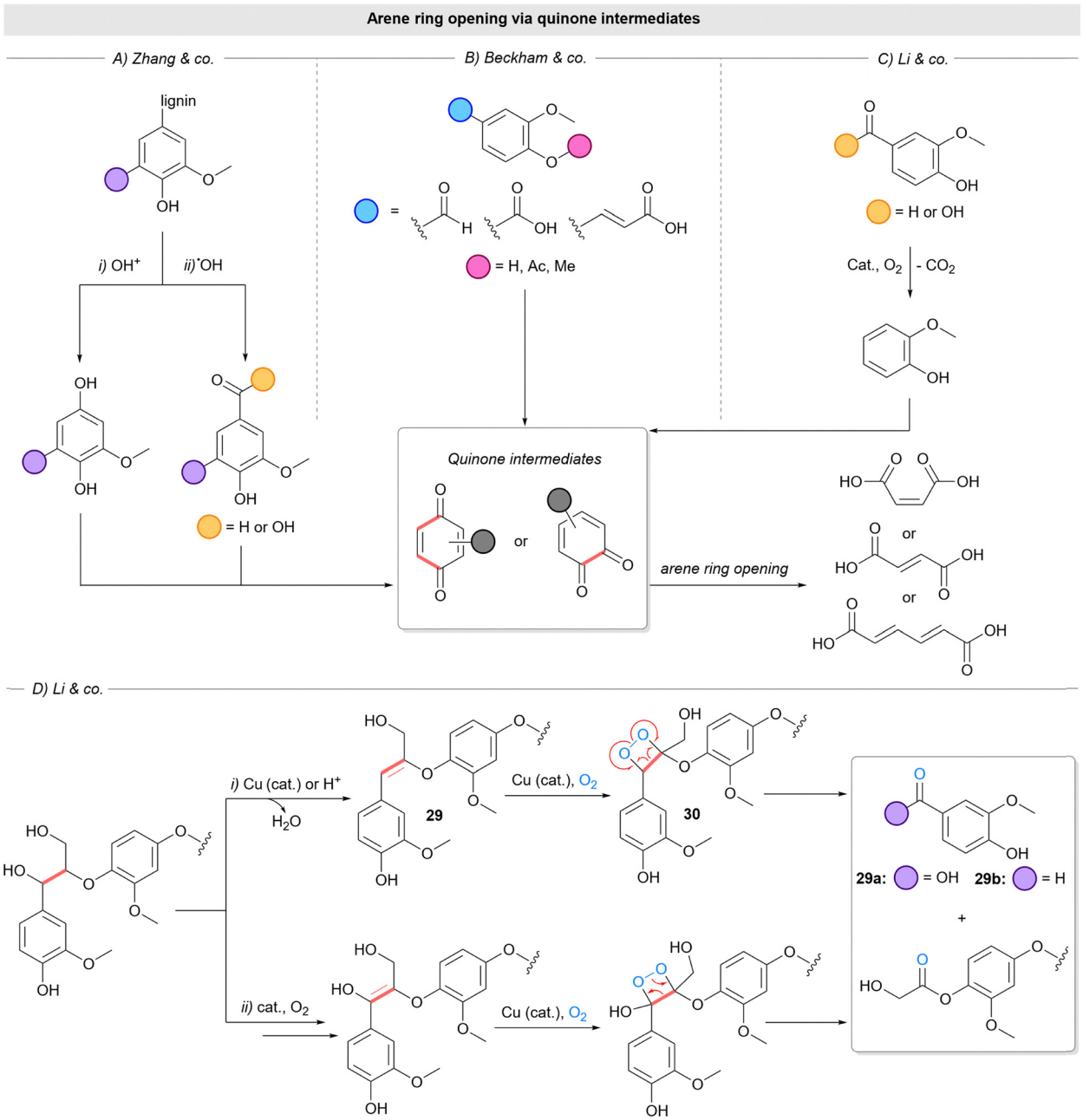

Fig. 11 Pathways for arene ring-opening (C–C cleavage) *via* quinone intermediates. The aromatic substrates are first oxidized to a quinone intermediate *via* different pathways and then undergo arene ring-opening to linear dicarboxylic acids. (A) Chalcopyrite-catalyzed oxidative conversion of lignin. (B) Bioconversion of monomeric lignin derivatives into dicarboxylic acids. (C) Initial and (D) final steps of the polyoxometalate ionic liquid ([BSmim]-$CuPW_{12}O_{40}$)-catalyzed oxidative process. If not otherwise stated, colored circles indicate general functional groups.

404.8 mg g^{-1}) from lignin aromatic units using a polyoxometalate ionic liquid ([BSmim]$CuPW_{12}O_{40}$) catalyst (Fig. 11C).[209] They proposed that the formation of a quinone intermediate was crucial because it facilitates the subsequent C–C bond cleavage (Fig. 11D). In brief, the reaction was proposed to occur *via* dehydration under strong acidic condition to form vinyl ethers (**29**; path i). The authors proposed that in the presence of a Cu^{2+} polyoxometalate under aerobic conditions, the vinyl ether reacts with superoxo species on the Cu active site to produce a dioxetane intermediate (**30**). Subsequently, the C–C and O–O bonds are simultaneously cleaved to form the corresponding acid and aldehyde (**29a** and **29b**, respectively). As a final step before arene C–C cleavage, the decarboxylation and oxidation to the benzoquinone intermediates proceeds, thus promoting arene ring-opening (Fig. 11C). An improved understanding and further validation of the mechanistic pathway leading quinones towards dicarboxylic acids would be desirable. Hensen and coworkers also proposed a quinone intermediate leading to aromatic ring opening in their studies on lignin oxidation with organic peroxides.[258] Quinones were also

proposed as intermediates in the conversion of lignin *via* the electro-Fenton reaction.[259] It would be of interest to gain more insights into the reaction mechanism of these pathways.

The groups of Bugg and Bruijnincx separately investigated the Fe-catalyzed oxidative cleavage of catechols and provided insights into the mechanism of the reaction (Fig. 12).[180,235,260] A similar pathway is found in enzymatic reactions.[261] The mechanism was supported by a combination of previous studies[262] and their results. First, catechol is coordinated to the Fe metal center through the two hydroxyl groups. The generated radical **31** complex then reacts with O_2 to form adduct **32**, which is either (i) protonated into **33** or (ii) converted into **34** *via* an intramolecular oxidative addition step by oxygen.

Following path (i), an acyl migration leads to the arene ring opening. In path (ii), the ring opening is triggered by a protonation of the bound oxygen followed by an intramolecular rearrangement. The produced lactones **33a** and **34a** are eventually trans-esterified by methanol into the corresponding linear products **33b** and **34b** in 7.5 mol% and 50 mol% yield, respectively. These reactions resemble the well-studied oxidations carried out by catechol dioxygenases.[261]

Other examples include arene ring opening promoted by UV-light and H_2O_2,[263] Cu(II)-mediated ring opening of catechols,[264] and electrochemical oxidation of lignin using Ti/$SbSnO_2$ and Ti/PbO_2 electrodes.[265] Of note, a comprehensive review that includes H_2O_2-mediated arene ring-opening reactions has been published.[266] Overall, optimal performance requires electron-rich phenolic substrates (*e.g.*, catechols/guaiacols), earth-abundant redox catalysts (*e.g.*, Fe, Cu, and POMs) enabling controlled O_2 activation, and finely tuned conditions (*e.g.*, pH, O_2/O_3 dosage, and residence time) to balance ring activation with suppression of CO_2 formation and re-polymerization.

4.1.4. Tandem radical migration mechanism. Only one example was found in the literature on the cleavage of C–C bonds (β–5, β–β, and β–1 types) *via* a tandem radical migration mechanism. Han and coworkers reported a NO_2-catalyzed aerobic oxidative cleavage of C(OH)–C bonds of various secondary alcohols present in lignin models and poplar lignin (Fig. 13).[267] According to the proposed mechanism, the *in situ* formed NO_2 both mediates a first oxidation of the secondary alcohol to a ketone (step i) and a subsequent C–C radical activation of the corresponding enol intermediate (step ii and iii). Lastly, O_2 is introduced and reacts with the intermediate from step iii to form a 4-membered ring, which undergoes C–C cleavage to yield the corresponding carboxylic acid as the final product in yields up to 95 mol%. It would be of interest to further study the reaction mechanism of this transformation. Advantages of the catalytic system include its effectiveness on a diverse range of secondary alcohols and lignin, mild reaction conditions, and atom economy.

4.1.5. Radical fragmentation mechanism. Radical fragmentations have been the most widely studied reactions for the cleavage of C–C bonds in lignin substrates. Methods involving chemo- and photo-catalysis have been reported.[210,213,257,268,269] One advantage of the approach is the wide applicability of radical fragmentations to different types of bonds, though controlling selectivity is a challenge. In oxidative radical processes, the formation of CO and CO_2 can occur, leading to over-oxidation of the desired products.[210,213,257] In addition, phenolic OH groups can scavenge radicals and, thus, quench radical-driven C–C bond cleavage reactions.

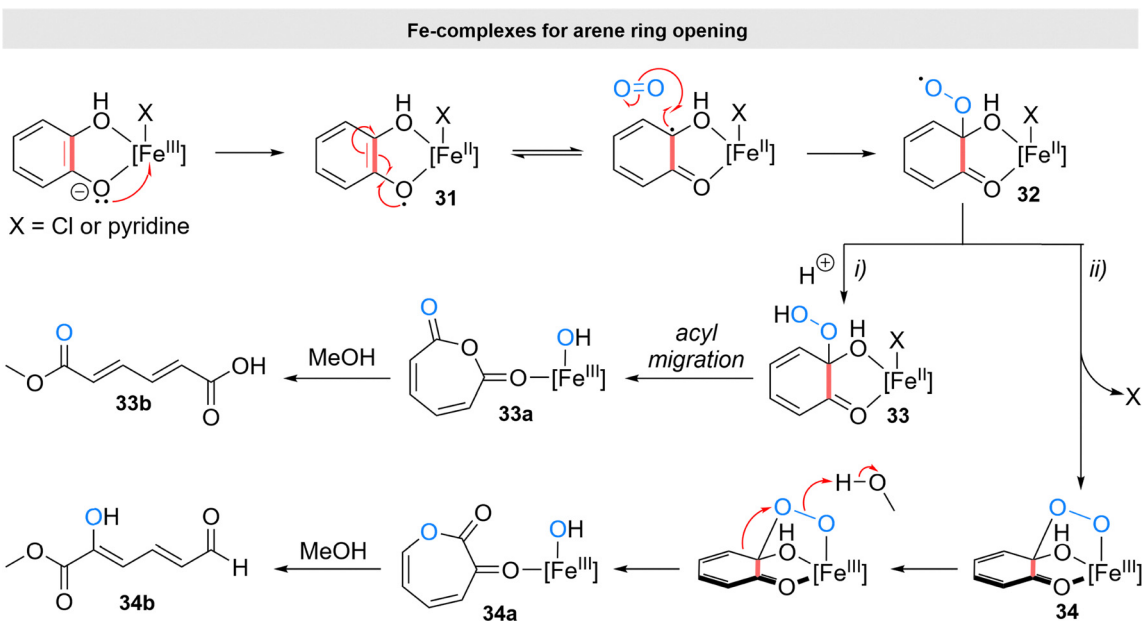

Fig. 12 Bugg and coworkers' proposed mechanism for the Fe-catalyzed arene ring opening of catechols.[235] Catechol coordinates to the Fe center and reacts with O_2 to form a peroxo intermediate that follows either (i) protonation and acyl migration or (ii) intramolecular rearrangement pathways, both leading to C–C bond cleavage and lactone formation. These intermediates are subsequently converted into linear products *via* transesterification.

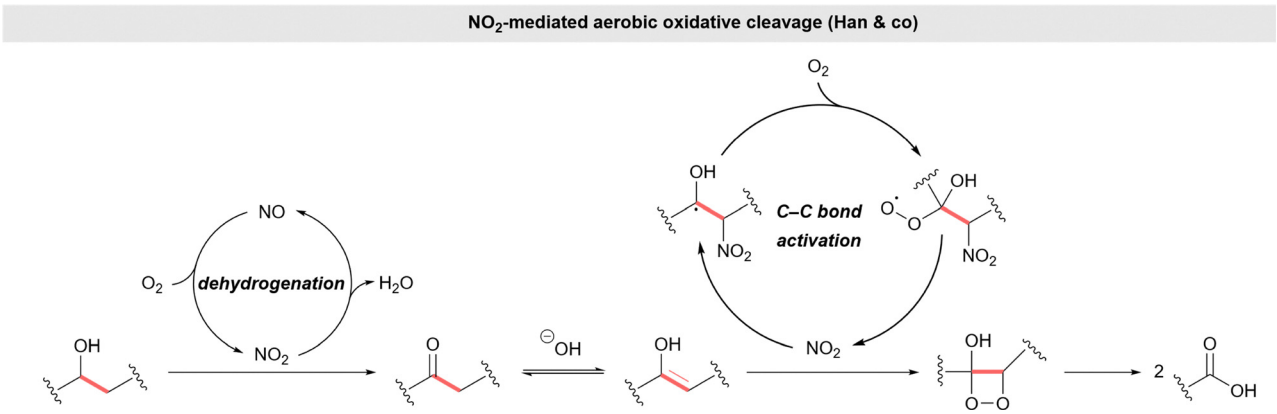

Fig. 13 Plausible reaction mechanism for the NO_2-mediated aerobic oxidative cleavage of C(OH)–C bonds.[267] The *in situ* generated NO_2 first oxidizes the secondary alcohol to a ketone, after which enolization enables C–C bond activation *via* a radical pathway promoted by NO_2. Subsequent reaction with O_2 forms a four-membered cycloadduct that undergoes C–C cleavage to deliver the corresponding carboxylic acid.

The radical fragmentation cleavage of lignin models and organosolv lignin has been observed using V-based catalysts. Using visible light irradiation, Wang and coworkers employed a V-based catalyst under aerobic conditions to selectively cleave the C–C bonds in β–1 (71–92 mol% yield) and β–O–4 interlinkages of lignin models. This SET process between the substrate and the catalyst led to the selective cleavage of the C_α–C_β bond through a radical homolytic process, similar to the pathway shown in Fig. 14A.[268] The same group also employed CuO_x clusters for the oxidative C–C cleavage ($\leq$96 mol% yield) using lignin models under visible light irradiation.[270] They also investigated the mechanism of the Cu–Mn-doped CeO_2 oxidative fractionation of biomass which yielded aromatic monomers in 29 wt% from birch (Fig. 14B).[271] Based on model compounds experiments, the authors suggested that under alkaline conditions, lignin undergoes deprotonation and

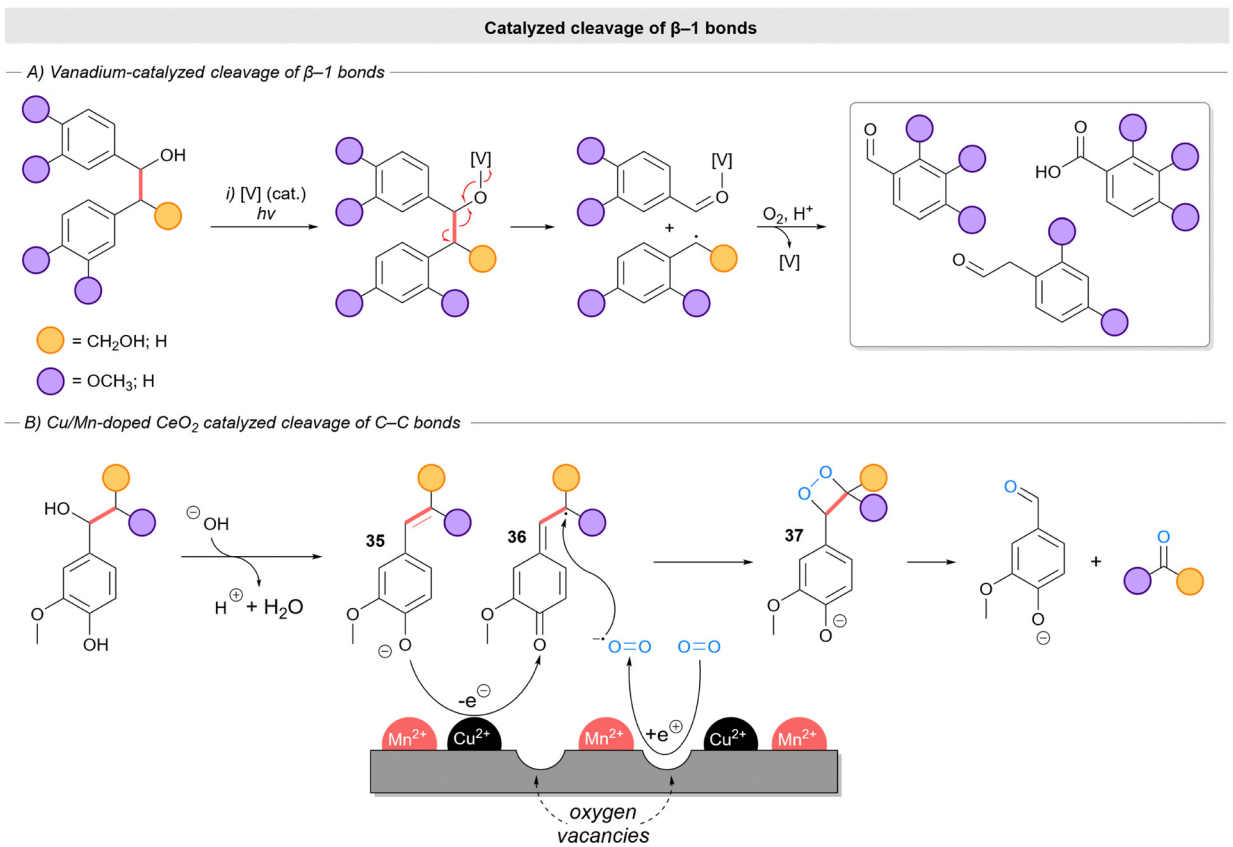

Fig. 14 Radical cleavage of β–1 lignin bonds *via* radical fragmentation. Possible mechanisms for (A) the V-[268] and (B) the Cu/Mn doped CeO_2-catalyzed processes.[271] Cleaved C–C bond is highlighted in red. Colored circles indicate general functional groups.

dehydration to form a stable phenoxy anion with a β-vinyl sidechain (compound **35**). In parallel, an O_2 absorption on the catalyst vacancies activates it to form $O_2^{\bullet -}$, while the oxidation of Cu^+ to Cu^{2+} occurs. Cu^{2+}, in turn, reduces back to Cu^+ *via* its interaction with the vicinal Mn species and oxidizes **35** into its corresponding quinone methide (**36**). Then, the $O_2^{\bullet -}$ reacts with the quinone methide radical, forming a 1,2-dioxetane intermediate (**37**). Eventually, the homolytic radical cleavage of the 1,2-dioxetane structure leads to the cleavage of the C_α–C_β bond, achieving aromatic aldehydes and carbonyl compounds.

Baker and Hanson also studied the V- and Cu-catalyzed cleavage of β–1 bonds in non-phenolic and phenolic lignin models.[272,273] Vanadium was found more suitable for non-phenolic substrates, while copper was active with both substrate types. The well-supported proposed mechanisms follow radical fragmentation pathways based on kinetic and computational studies involving two and one electron transfers for the V and Cu catalysts, respectively.

Other examples of SET-driven cleavages have been suggested. For example, Xu and coworkers reported the development of an Fe-doped graphene carbon nitride (g-C_3N_4) catalyst that is suggested to photocatalytically cleave C–C bonds in β–1 lignin models (yield of C–C cleavage in the range 91–99 mol%). They proposed that the reaction occurs *via* a C_β-radical and SET mechanism. This pathway is proposed to involve a homolytic radical fragmentation step. As the reaction is performed in micellar aqueous medium, hydroxyl radicals are generated through Fe-induced Fenton reactions, which promotes the cleavage of β–1 bonds.[274]

Shimada and coworkers studied the mechanism of the oxidative biomimetic Fe-catalyzed β–1 C–C cleavage of lignin models using ^{18}O-labelled compounds (C–C cleavage yield: 20–50 mol%).[275] According to the authors, the reaction follows a SET pathway. First, the electron deficient Fe(IV) porphyrin complex removes one electron from the aromatic ring to form a radical cation. The radical cation then concomitantly undergoes heterolytic C_α–C_β bond cleavage and deprotonation, which was supported by isotopic experiments.

Mariano and coworkers investigated the radical fragmentation reactions that occur *via* the formation of radical cations using lignin model compounds.[276] In this work, a SET reaction was proposed. The process was mediated by a Ce(IV) catalyst, or similarly by a Fe(III) heme peroxidase, resulting in the generation of lignin-derived radical intermediates. The C–C cleavage of β–1 and β–O–4 bonds in the lignin model compounds was proposed to occur *via* radical fragmentation. For β–1 models, they achieved yields of C–C cleavage up to 95 mol%. They also predicted through DFT calculations that the cleavage containing β–1 linkages was faster than for those containing β–O–4 linkages.[276] The same group later proposed a similar mechanism for C–C cleavage in tetrameric lignin model compounds using cation radical intermediates.[277]

Beckham and coworkers reported Co-/Mn-/Br-[210] and Mn-/Zr-promoted[257] autoxidation processes for the cleavage of different bonding motifs (β–5, β–β, and β–1) in phenol-protected lignin oligomers to yield monomers in 13–20 wt% (based on the lignin content in biomass; Fig. 15A-i). A similar process involving Co, Br and H_2O_2 was reported by Maschmeyer and co-workers for the oxidation of lignin model compounds.[278] The reactions are carried out in the presence of oxygen, and the mechanism involves radical fragmentation. The oxidized products of this reaction, benzaldehyde and benzoic acid derivatives, were then biologically converted to *cis*,*cis*-muconic acid. Such chemistry is based on the seminal work of Partenheimer.[279,280] Recently, the yield of monomers obtained *via* C–C bond cleavage was improved by starting from deoxygenated lignin oils (pine-, birch- and poplar-derived)[281,282] using the same Co/Mn/Br and O_2 catalytic system (Fig. 15A-ii).[212] Monomeric aromatic carboxylic acids were isolated in 73 wt% (based on the deoxygenated lignin oil) and then further converted to adipic acid with an overall yield of 26 wt% (57 wt% theoretical) based on the initial lignin content in biomass. This strategy overcomes the challenge of product instability observed for phenolic lignins. Though the catalyst system is based on the well-developed Mid-Century (or Amoco) Process,[283,284] the mechanistic pathways of these reactions are still underdeveloped, highlighting opportunities for future mechanistic investigations.

Additionally, Stahl and coworkers reported examples of conversion of lignin into monomers in flow *via* Cu-catalyzed aerobic oxidative processes.[213,269] Lignin depolymerization *via* both C–O and C–C bond cleavage was investigated in an O_2-permeable flow reactor achieving monomers in 43 wt% yield on a lignin basis (Fig. 15B-i).[269] The same authors later reported the conversion of lignin oligomers bearing only C–C bonds into aromatic monomers (yields 19–34 wt%) *via* radical reactions, followed by bioconversion to muconic acid or 2-pyrone-4,6-dicarboxylic acid, depending on the lignin feedstock origin, Fig. 15B-ii.[213]

Ni and coworkers reported a microwave-assisted Pt-catalyzed catalytic cracking strategy to cleave 5–5 C_{aryl}–C_{aryl} bonds in the lignin model substrate, 2,2′-biphenol (2-BP), using methanol vapor as the mediator.[285] Their optimized reaction yielded 49 wt% aromatic monomers (*e.g.*, benzene, phenol, and *o*-cresol) with 85% conversion of 2-BP. They proposed that under microwave irradiation, methanol vapor produces hydrogen and methyl radicals, leading to homolytic C–C bond cleavage. It would be worthwhile to perform a mechanistic study of this transformation.

Sheldrake and coworkers investigated the activity of TiO_2 for the photodegradation of a hexameric lignin model compound containing multiple C–C linkages, including 5–5 and β–5 bonds.[286] Cleavage of the β–5 linkages was observed, whereas 5–5 units remained stable under the tested conditions. Although the results clearly indicated the involvement of radical pathways, no detailed mechanistic proposal was provided. Notably, a review on photocatalytic lignin conversion has been published.[287]

Overall, radical fragmentations are among the most promising reactions for lignin depolymerization *via* C–C bond cleavage. Despite their high reactivity, radical processes remain challenging to characterize mechanistically. However, continued investigations are important given their high potential. In short, to achieve productive radical fragmentation conversions of lignin, phenolic groups should be protected or deoxygenated, to

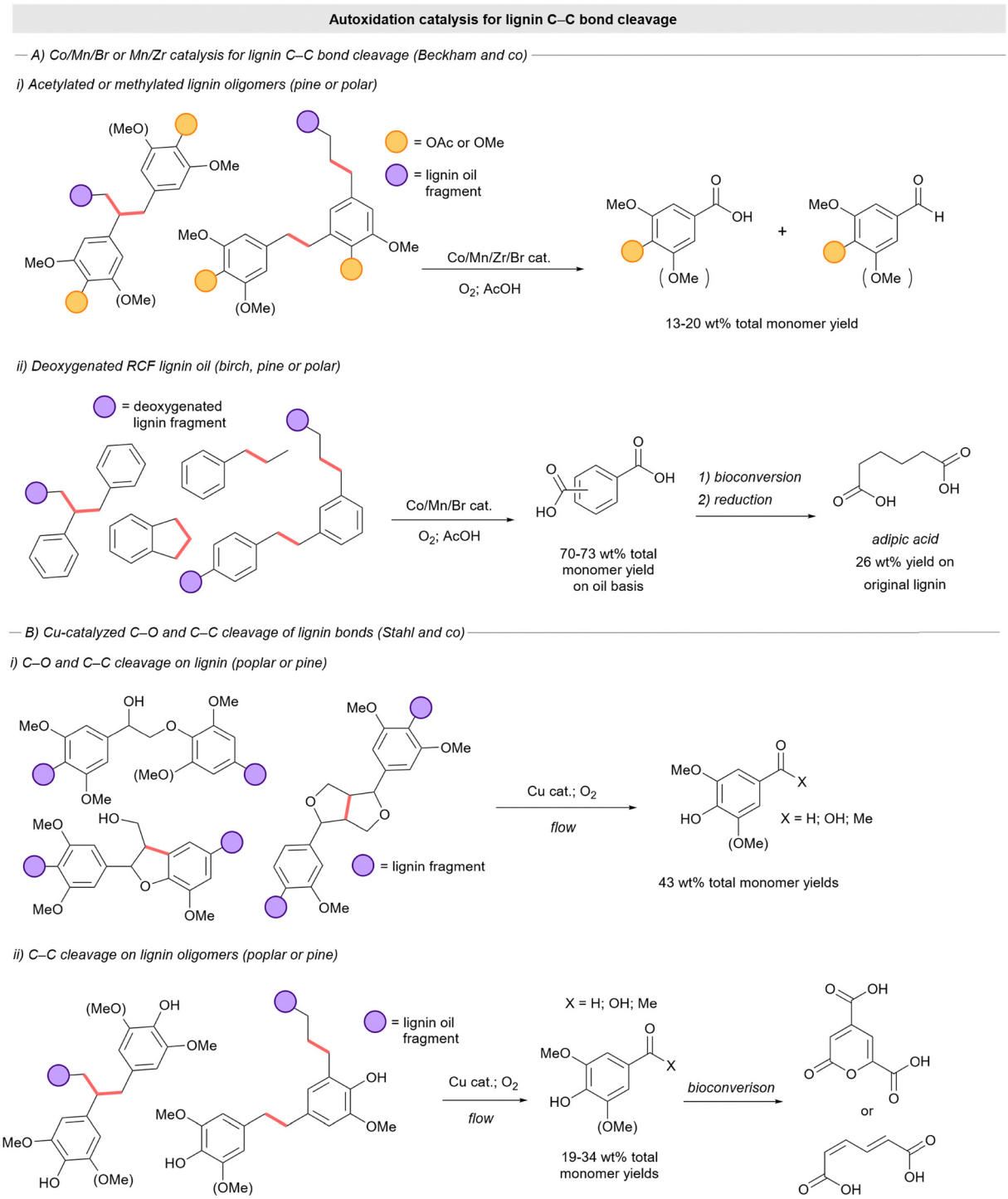

Fig. 15 Autoxidation for the cleavage of C–C lignin bond *via* radical pathways. (A) Co/Mn/Br and Mn/Zr catalysis.[210,212,257] (B) Cu-catalysis in flow.[213,269] The mechanisms of these reactions are not well understood but are proposed to involve radical reactions and β-scission.

minimize phenolic radical coupling and byproduct formation. Catalysts should also be selected to enable controlled single-electron transfer (*e.g.*, V, Cu, and Fe catalysts), and conditions must carefully regulate and control O_2 availability, pH, and light intensity to favor β-scission over unselective oxidation.

4.1.6. Organo-mediated C–C cleavage. Organo-mediated processes have been underexplored, with only two groups reporting studies in the field.[288,289] This strategy can be highly selective and target specific C–C bonds, but may require stoichiometric amounts of reactants. In some cases, this limitation may be mitigated by regeneration of the active species.[288]

Samec and coworkers demonstrated cleavage of β–β and β–1 C–C bonds in lignin through an oxidative organo-mediated strategy (Fig. 16A).[288] They developed a selective oxidation reaction to

give 2,6-dimethoxybenzoquinone (DMBQ) in 18 wt% yield from lignin using Bobbitt's salt as the oxidant. Their proposed mechanism begins with the deprotonation of the alcohol by Bobbitt's salt and consequent formation of an N–O bond (step i). The release of the reduced form of Bobbitt's salt in step ii generates a carbocation intermediate (**38**), which undergoes nucleophilic attack by MeOH (step iii), resulting in the formation of the corresponding methoxylated product (**39**). Post treatment with another equivalent of Bobbitt's salt yields DMBQ. The authors studied the reaction mechanism using model compounds.[290] This approach requires stoichiometric oxidant use, which could be partially regenerated *via* electrochemical means. Very recently similar chemistry was applied by Abu-Omar and coworkers to RCF oils.[291]

Jiao and coworkers reported on the selective dealkenylative functionalization of styrene derivatives *via* C–C bond cleavage (Fig. 16B-a).[292] Although lignin model compounds were not

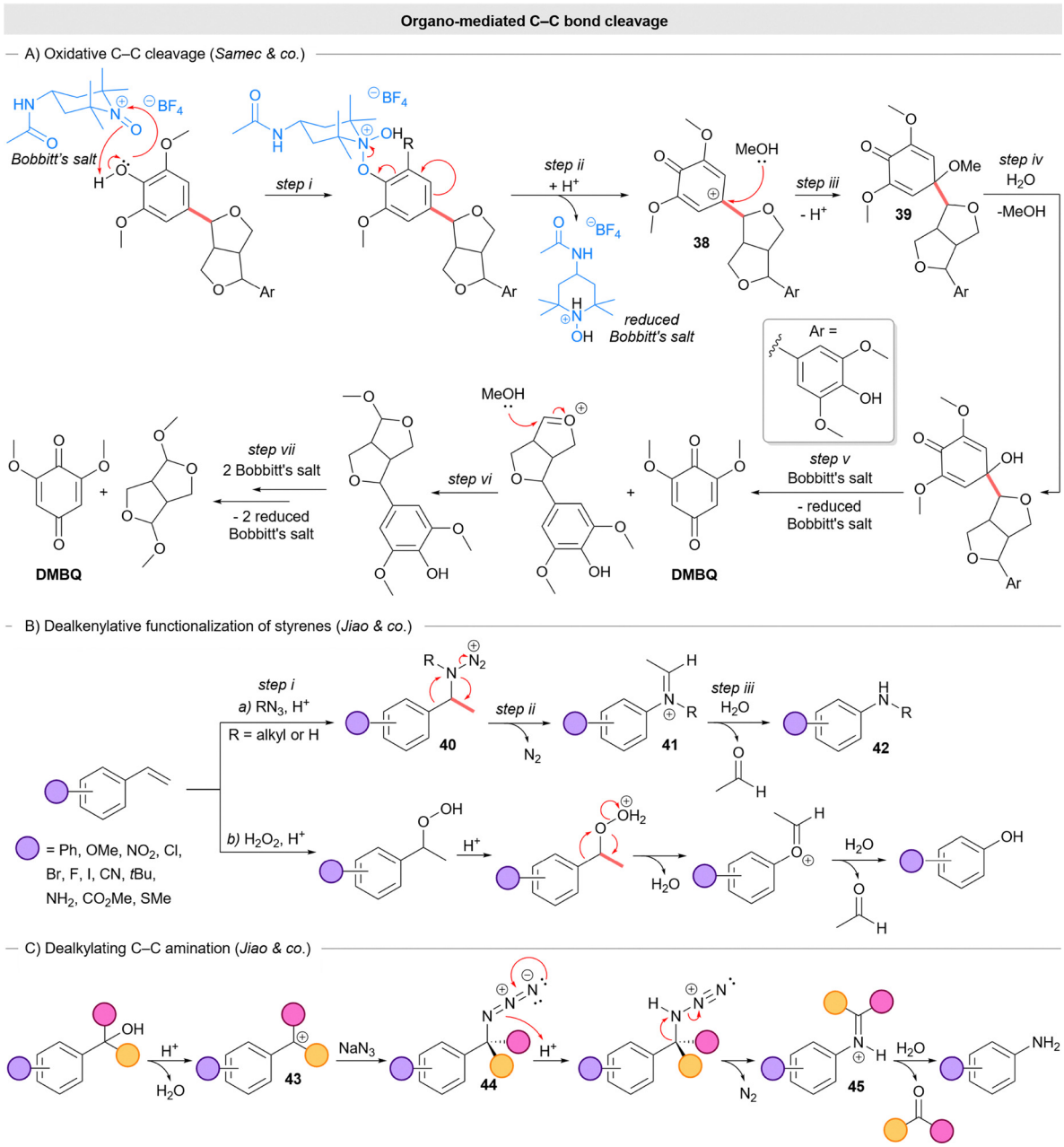

Fig. 16 Organo-mediated process for the cleavage of C–C bonds in lignin. (A) Mechanism proposed by Samec and coworkers for the oxidative C–C cleavage of β–β units in lignin. A similar pathway proceeds for the cleavage of β–1 bonds.[288] Bobbitts' salt first oxidizes the alcohol *via* N–O bond formation to generate a carbocation intermediate, which is then trapped by methanol to give a methoxylated product. Subsequent oxidation with another equivalent of the oxidant furnishes the final quinone product. DMBQ = 2,6-dimethoxy benzoquinone. (B) Dealkenylative functionalization of styrenes *via* C–C bond cleavage mediated by RN_3 or H_2O_2 proposed by Jiao and coworkers,[292] and (C) the mechanism of amination. Hydroazidation first generates an amine intermediate, which undergoes a Schmidt-type rearrangement to form an imine *via* C–C bond cleavage, followed by hydrolysis to yield the final amine product. If not otherwise stated, colored circles indicate general functional groups.

directly examined, several substrates have structural resemblance to lignin-derived motifs. One proposed pathway of their process begins with a hydroazidation step to form **40** (step i). A subsequent Schmidt-type rearrangement leads to imine **41** *via* a C–C bond cleavage shown in step ii. Lastly, a final hydrolysis step yields the corresponding amine product (**42**, step iii). Shown in Fig. 16B-b, a similar mechanism occurs using H_2O_2 in place of RN_3 leading to phenols as the product.

The same group developed a synthetic method to obtain anilines from alkylarenes through the cleavage of C_{aryl}–C_{alkyl} bonds using sodium azide (NaN_3) and 2,3-dichloro-5,6-dicyano-1,4-benzoquinone as an oxidant to cleave alkyl bonds or trifluoroacetic acid (TFA) as the acid additive to cleave C–C bonds containing secondary alcohols (Fig. 16C).[289] They displayed the versatility of their system by applying it onto lignin model substrates and cleaved β–1 and β–O–4 C–C bonds, which are proposed to proceed through the mechanism shown in Fig. 16C. The secondary alcohol is protonated by TFA to release water and generate the reactive carbocation intermediate (**43**, step i). This carbocation is nucleophilically attacked by NaN_3 and the resulting azide intermediate (**44**) is protonated to release N_2 as a byproduct. The resulting imine **45** reacts with water to generate the desired amine and ketone as a byproduct. This proposed mechanism was experimentally determined using control experiments confirming the involvement of the azide intermediate and stoichiometric reactions to capture reaction intermediates.

4.1.7. Retro-aldol C–C cleavage. One of the earliest mechanistic proposals for cleavage of C–C bonds in lignin came from Hibbert and coworkers, who proposed a retro-aldol mechanism as the key step in vanillin formation during oxidation of lignin in aqueous media.[293] A number of subsequent studies have corroborated this mechanism, particularly under strong alkaline conditions.[294,295] More recently, retro-aldol C–C bond cleavage has also been invoked under non-basic conditions when alternative catalytic systems are employed. For example, Zhou and coworkers used a Cu–NHC catalyst under aerobic conditions to cleave bonds in lignin model compounds with near quantitative conversion.[296] They propose a mechanism that begins with a Cu-catalyzed oxidation of an alcohol to generate a carbonyl intermediate, followed by C_α–C_β cleavage *via* a retro-aldol step.

4.1.8. Other strategies for lignin valorization *via* C–C cleavage. In this final section, we summarize the reported works on C–C cleavage where either no detailed mechanistic insights have been provided or the mechanism does not fall neatly into a prior category. Even though the reported routes use different conditions, many involve high temperatures for the conversion of lignin to monomers, particularly when heterogeneous catalysts are used.[297] The reaction schemes are condensed and summarized in Fig. 17.

Dealkylation of wood-derived lignin was reported by Sels and coworkers.[298] The authors developed a Ni/SiO_2 (64 wt% Ni) catalyst to convert lignin oil composed of a mixture of phenolic monomers into phenol (20 wt% yield) and propylene (9 wt% yield) *via* gas-phase hydroprocessing. The proposed mechanism follows well-established pathways of hydrogenolysis and hydrocracking. Notably, techno-economic analysis highlighted the efficiency of the process and revealed the potential for their strategy to be appealing for the market and life cycle assessment shows a reduced carbon footprint compared to fossil-based production, with lignin valorization contributing to lower net CO_2 emissions by replacing petrochemical routes and improving overall feedstock utilization efficiency.

Han and coworkers developed a demethoxylation and decarbonization reaction catalyzed by $La(OTf)_3$ to produce guaiacol in 26 wt% yield as the only liquid product sourced from lignin.[299] The formation of gaseous methane was proposed during the process, supporting cleavage of the C–C ethyl bond in 4-ethyl guaiacol.

Saha and coworkers reported a commercially available CoS_2 catalyst that can selectively cleave β–1 and 5–5 C–C bonds in methylene-linked lignin models and Kraft lignin.[300] In this reaction, β–1 and 5–5 C–C linked model dimers formed demethoxylated hydroxyl dimers as the major product, whereas

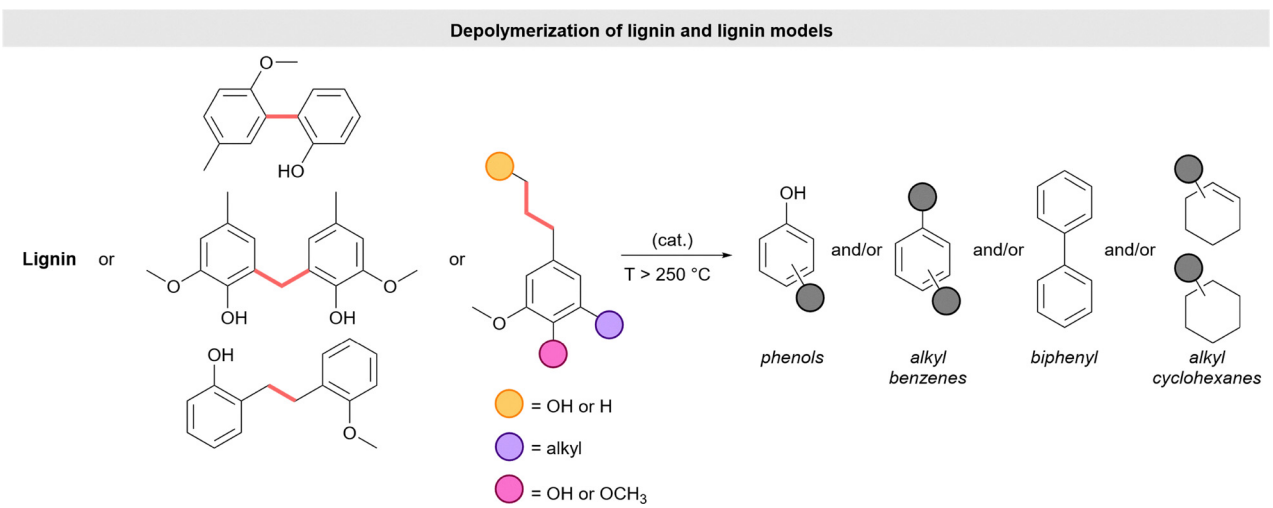

Fig. 17 General scheme for the depolymerization of lignin and lignin models *via* C–C cleavage under different conditions to yield aromatics, phenols and cyclohexane derivatives as the products.

five aromatic monomers (mainly *p*-methyl phenol and 2,4-dimethyl phenol) and lower-molecular-weight soluble products were achieved using a purified Kraft lignin fraction.

Li and coworkers reported on a similar, complex array of reactions to synthesize ethylbenzene through the catalytic transformation of lignin at temperatures >500 °C, where the consecutive reaction pathways for the transformation of lignin to ethylbenzene were proposed.[301] During the catalytic depolymerization of lignin, the oxygenated aromatic monomers were first produced *via* the pyrolysis of lignin. These aromatic monomers were further converted into aromatic hydrocarbons (mainly benzene) by deoxygenation routes and the removal of side chains over a Re-Y/H-ZSM-5 catalyst. The formation of benzene through the demethoxylation of anisole was the dominant reaction pathway. Similarly, the selective production of ethylbenzene from lignin oil over a FeO_x modified Ru/Nb_2O_5 catalyst involved dehydrogenative decarbonylation, hydrodeoxygenation, and C–C hydrogenolysis.[301] Additional examples of similar chemistries are present in the literature and have been extensively reviewed elsewhere.[302–305]

Another acid-catalyzed depolymerization was reported by Kong and coworkers, who used commercial zeolites to perform dual C–C cleavage of condensed lignins.[306] Reactions of lignin dimers/oligomers with Hβ zeolite at 300 °C produced aromatic monomers in 7–10 wt%. These monomers are in addition to the 8–15 wt% produced through C–O cleavage in an initial reductive depolymerization step. Cleavage of the methylene linkages in the condensed lignins is key to increase monomer yield, suggesting proton-induced C–C scission as an important mechanistic element. A similar process was applied by these researchers specifically to Kraft lignin as well.[307] Yan and coworkers also used zeolites to investigate the reductive single-step conversion of lignin monomers to phenol using Pt/C as a hydrodemethoxylation catalyst and a zeolite (H-ZSM-5) as a dealkylation catalyst, working in tandem.[308] However, no mechanism was proposed.

Han and coworkers reported on the production of 4-ethyltoluene from a reaction between lignin and CO using a $RhCl_3$–LiI–$LiBF_4$ catalyst.[309] Similar to previously discussed reports, demethoxylation and depolymerization of lignin took place to obtain 4-ethyltoluene. However, an extra methylation step using liberated methoxy groups from lignin was required to yield 4-ethyltoluene. A total yield of 9.5 wt% 4-ethyltoluene was achieved using γ-valerolactone lignin, whereas only 5.2 wt% yield was obtained when raw poplar was used as the starting material.

Practically, substrate pretreatment (*e.g.*, depolymerized or oil fractions), robust heterogeneous catalysts synthesis (*e.g.*, Ni, zeolites, and bifunctional metal–acid systems), and process conditions (*e.g.*, high temperature, controlled H_2/CO atmospheres, and acidity) should be targeted to maximize selective C–C cleavage while limiting excessive cracking and gas formation.

4.2. Plastics

The controlled deconstruction of synthetic plastics, especially linear polymers with carbon backbones, remains a critical challenge in the realization of a circular carbon economy. Plastics deconstruction *via* C–C bond cleavage has been performed using β-elimination/-scission, cross metathesis, radical fragmentation, Baeyer–Villiger oxidation, among other reactions (Table 2). In the following sections, these studies will be discussed with the emphasis on the reaction mechanism.

4.2.1. β-Elimination/-scission. β-Elimination/-scission is the mechanism proposed for most hydrogenolysis and hydrocracking reactions. Extensive research has been devoted to the design of efficient catalysts for the selective hydrogenolysis/hydrocracking of polyolefins.[14,310] Generally, such pathways involve a β–alkyl/β–carbon/β–scission step, which results in internal or terminal C–C cleavage along the polymer backbone to produce light alkanes or methane, respectively (Fig. 18).

Noble metals like Ru and Pt, and early transition organometallic complexes based on high oxidation state metals (*i.e.*, Zr, Ta, Hf, *etc.*) have been reported to be active at relatively mild reaction conditions ($T < 300$ °C) for the cleavage of C–C bonds in aliphatic plastics and operate *via* C–H σ-bond metathesis and subsequent β-alkyl elimination steps. Limited acidity of the catalyst is generally needed for hydrogenolysis reactions, while a higher acidity is requested for hydrocracking in most cases.

One of the earliest examples of this type of catalysis was reported by Dufaud and Basset in the 1990s, which proposed a Zr-based molecular catalyst for the conversion of PE and PP into hydrocarbons under a set of mild operational conditions (*i.e.*, T = 25–150 °C and 1 bar of H_2).[311] Key advantages of Zr catalysis are the milder reaction conditions and higher selectivity towards light alkanes compared, for instance, to noble metal catalysts that are more prone to over-cracking. Although the work only shows relative abundances for the products below a carbon chain length of 8 carbon atoms, the authors have qualitatively shown the possibility of tuning the product size distribution by controlling the extent of the depolymerization. The formation of methane was favored at longer times suggesting that internal and terminal cleavages occurred simultaneously.

The proposed mechanism (Fig. 19A), based on previous observations for this catalyst class,[216,312] initiates with a C–H σ-bond metathesis on the substrate with a Zr–H species (**46**) to generate H_2 and an alkylzirconium intermediate (**47**, step i). This is followed by β-alkyl elimination to form a π-bound alkene to the Zr center and a Zr–C_{alkyl} bond (**48**, step ii). The resulting Zr–C_{alkyl} bond undergoes another σ-bond metathesis step with H_2 to regenerate a Zr–H complex and releases a hydrocarbon product (**49**, step iii). The Zr–H proceeds with a hydride-insertion step to form a new Zr–C_{alkyl} bond (**50**, step iv), which reacts with another equivalent of H_2 to regenerate the active Zr–H catalyst (**46**) and desired product. The authors highlighted that the mechanism of hydrogenolysis reactions, and polymerization for that matter, are dependent on the equilibrium of β-alkyl transfer (elimination) *vs.* insertion (addition) which is generally thermodynamically unfavorable. However, they proposed that the subsequent hydrogenation of olefinic products pushes the equilibrium in favor of elimination by making the overall reaction exothermic.

Another example of such an induced C–C bond cleavage has been reported by Sadow and coworkers, which is mediated by a surface-supported organo-Zr catalyst followed by alkyl metathesis with an alkyl-aluminum species to deconstruct polyolefins

Table 2 Main reported works on the depolymerization of plastics *via* C–C bond cleavage

Entry	Substrate	Method	Catalytic system	*T*; *p*; *t* (°C; bar; s/min/h)	Major products; yield	Ref.
1	PE and PP	Hydrogenolysis	ZrH/silica	150; 1; several hours	Light alkanes; 100% conversion, yield not reported	216
2	Polyolefins	Alumination	$Zr(CH_2CMe_3)_n/SiAlO_x$ + AlX	200; 1; 12 h	Surfactants; 40–50 wt%	217
3	PE and PP	Hydrocracking	Ru nanoparticles on FAU	100, 30, 16 h	Liquid alkanes; 67 wt%	218
4	Polyolefins	Hydrogenolysis	Pt-nanoparticles $mSiO_2$/Pt–X/SiO_2	300; 9; 20	C23-centered distribution of hydrocarbons; ~80% mass balance	219
5	PE and PP	Cracking-alkylation	Ionic liquid $(C_4Py)Cl–AlCl_3$	70; 1; 6 h	Liquid iso-alkanes; 70 wt%	220
6	Aromatic plastic waste	Hydrogenolysis	Ru/Nb_2O_5	280–300; 5; 16 h	Arenes; 75–85 wt%	221
7	Polyolefins	Hydrogenolysis and isomerization	$Pt/WO_3/ZrO_2$ and HY zeolite	225; 30; 2–12 h	Liquid fuels; 85 wt%	112
8	PEs	Oxidation and bioconversion	Co, Mn, NHPI	150; 2; 11 h	Fungal metabolites; 52 mol% on carbon basis	222
9	PE	Pyrolysis, oxidation and bioconversion	Permanganate and *Pseudomonas putida*	100–140; 1; n.a.	medium-chain-length poly-hydroxyalkanoate; 83 g L^{-1}	223
10	Mixed plastic waste	Oxidation and bioconversion	Co/Mn/NHPI and *Pseudomonas putida*	160–210; 8; 2–5 h	B-ketoadipate 75.5 mol%	224
11	Plastic waste	Photocatalysis, oxidation	$V(acac)_2$	r.t.; 1; 120 h	Benzoic, acetic and formic acid; 77 mol% carbon recovery	225
12	Polystyrene	Photocatalysis	*p*TsOH and H_2O	r.t.; 1; 15 h	Formic and benzoic acid, acetophenone; 119 wt%	226
13	Plastic waste	Photocatalysis	NbO_2 layers	r.t.; 1; 40 h	Acetic acid; 40–50 g h^{-1} cat^{-1}	227
14	Polyolefins	Photothermal process	Ru/TiO_2	200–300; 40; 3 h	Liquid fuels; 83 wt%	228
15	PEs	Metathesis	Ir complex + Re_2O_7/γ-Al_2O_3	175; 1; 96 h	Liquid fuels and waxes; ~80 wt% fuels and 20 wt% waxes	229
16	PE	Metathesis	Ru and Ir complexes	130; 25; 16 h	Propylene; 80 mol%	230
17	Polyolefin waste	Cracking and metathesis	WO_3/SiO_2 + Na/γ-Al_2O_3	320; 10; 1.5 h	Light olefins; 95 mol%	231

n.a. = not available.

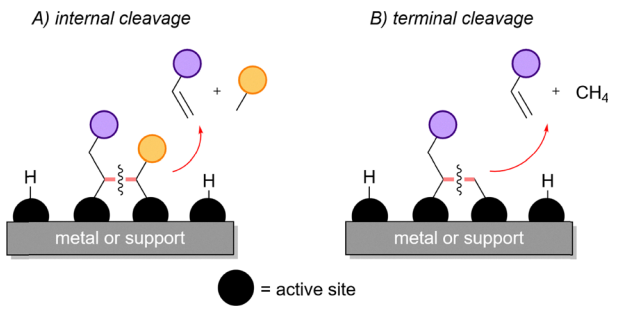

Fig. 18 Types of C–C bond cleavage occurring during hydrogenolysis *via* β-alkyl elimination.[14] (A) Internal cleavage providing light alkanes and (B) terminal cleavage providing methane. Colored circles indicate general functional groups.

to low molar mass unsaturated hydrocarbons (Fig. 19B).[217] In the temperature range of 150–200 °C, the authors report the conversion of HDPE to different functionalized alkanes with oil yields up to 85 wt% and selectivity ranging from 30–90%, depending on temperature, type of aluminum reagent, and other additives. Based on the experimental evidence provided by product analysis during catalytic tests, control experiments, and DRIFTS coupled with D_2 isotopic labelling, the authors proposed a sequence of elementary steps as shown in Fig. 19B. The process begins with the surface-grafted alkyl or hydride zirconium species **51** engaging in σ-bond metathesis to form a polymeryl–Zr species (**52**, step i). β-Alkyl elimination results in C–C cleavage to obtain a terminal olefin and a new alkylzirconium species (**53**, step ii). Finally, alkyl metathesis is facilitated by an alkylaluminum species in reaction with **53** to generate a new Al–C bond (step iii). Moreover, the authors performed techno-economic analysis, indicating that the process can produce fatty alcohols that are cost-competitive with conventional petrochemical routes, although no explicit cost metrics are reported. The life-cycle assessment was also qualitatively discussed, highlighting improved sustainability *via* waste valorization without providing quantitative CO_2 emission or GWP values.

Another approach is Ru-catalyzed hydrogenolysis of polyolefins, which has been among the most widely investigated.[313–324] For instance, Román-Leshkov and coworkers reported a relevant example of polyolefin deconstruction *via* β-scission/elimination using bifunctional Ru/H^+ catalysts (Fig. 20A).[218,325] The authors stated that the presence of branching within the products is indicative of an acid-catalyzed isomerization and subsequent β-scission of carbocation intermediates.

In another study, Lercher and coworkers explored the valorization of PE and PP into liquid hydrocarbons *via* tandem cracking-alkylation employing isopentane and an acidic chloroaluminate ionic liquid ($[C_4Py]Cl–AlCl_3$).[220] Under an atmosphere of 20 bar of N_2 and in the temperature range of 70–100 °C, the authors report selectivity values >70 wt% to C_6–C_{12} hydrocarbons with full polyolefin conversion. By performing a series of catalytic experiments, exploring the role of the initiator, and the addition of co-reagents, the authors propose a mechanism consisting in two independent but linked cracking and alkylation catalytic cycles, where the alkenes produced in the former *via*

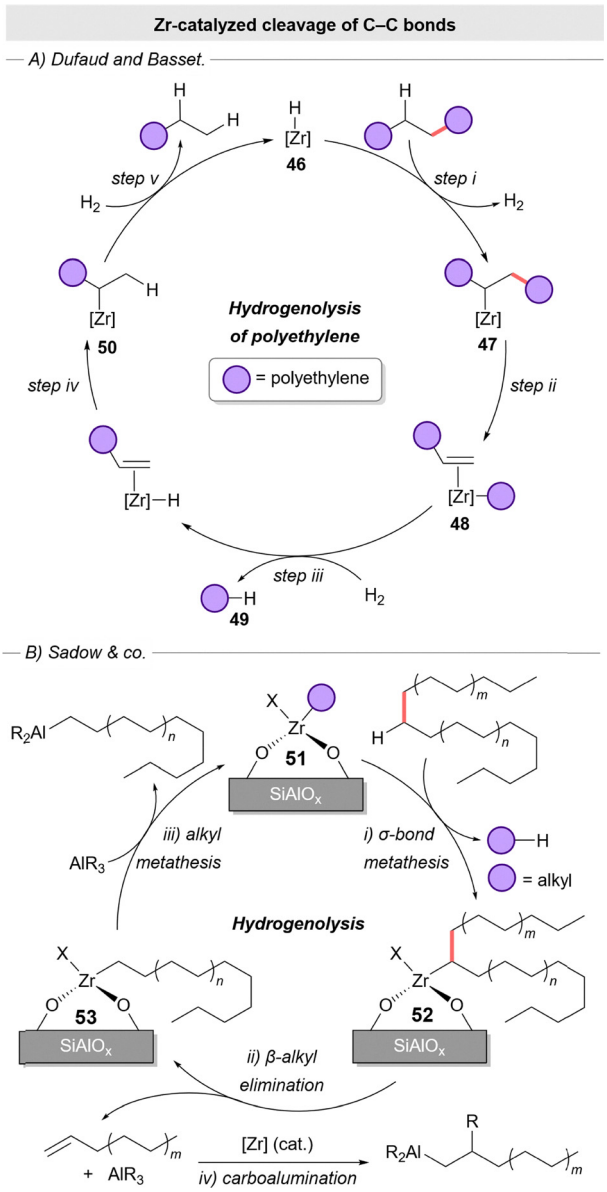

Fig. 19 (A) Dufaud and Basset's[311] and (B) Sadow and coworkers'[217] mechanisms for the Zr-catalyzed C–C cleavage of polyolefins *via* β-elimination. In A: the mechanism initiates with C–H σ-bond metathesis between the substrate and a Zr–H species to form an alkylzirconium intermediate, which undergoes β-alkyl elimination to cleave the C–C bond and generate an alkene. Subsequent hydrogenolysis and hydride insertion steps regenerate the active Zr–H catalyst while converting intermediates into the final hydrocarbon products. In B: the supported zirconium species first undergoes σ-bond metathesis with the polymer to form a polymeryl–zirconium adduct, which then undergoes β-alkyl elimination to cleave the C–C bond and generate a terminal olefin. Subsequent alkyl metathesis with an alkylaluminum species transfers the fragment, completing the catalytic cycle and forming the final products.

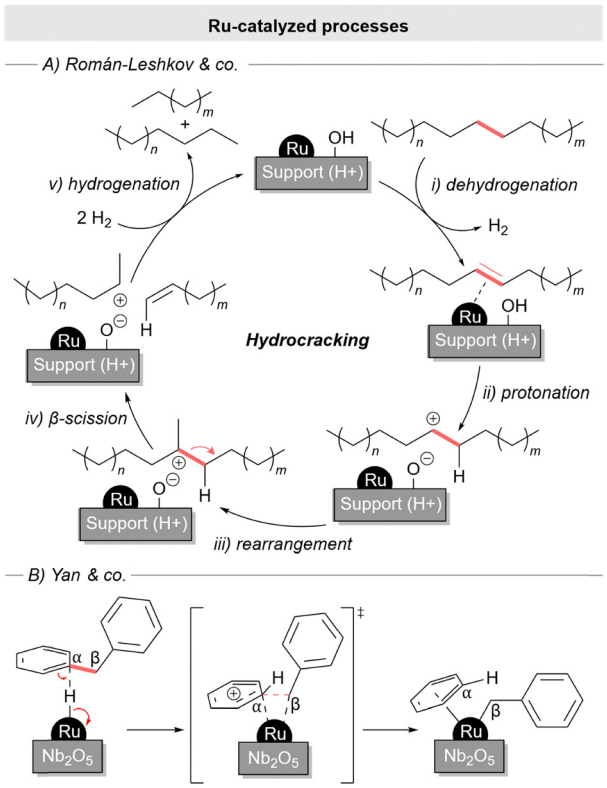

Fig. 20 Ru-catalyzed β-carbon elimination pathways for the cleavage of (A) polyolefins[218,325] and (B) aromatic plastic waste.[326] In (A) the dehydrogenated substrate is protonated by the Brønsted acidic sites of the support in cooperation with Ru, enabling C–C bond cleavage *via* β-scission. In (B) the aromatic ring is activated by the catalyst to generate a reactive intermediate which then undergoes selective C_{aryl}–C_{alkyl} bond cleavage.

β-scission serve as the substrate in the latter, similar to the studies from Román-Leshkov and coworkers.[218,325]

Yan and coworkers investigated the conversion of aromatic plastic wastes (PS, PET, polycarbonate and polyphenylene oxide) into alkyl arenes, such as benzene, toluene, xylene, *etc.*, using metal-supported heterogeneous catalysts.[326] In this work, the authors explored metal-support effects for a set of materials (Ru/Pd/Pt supported on ZrO_2,H-ZSM5, Nb_2O_5) and selected Ru/Nb_2O_5 as the optimized catalyst to produce yields up to 75–85 wt% at 280–320 °C with 50 bar of H_2. Combining catalytic experiments, spectroscopic investigations, and computational studies, the authors conclude that Ru/Nb_2O_5 shows superior performance due to synergism between the Lewis/Brønsted acidity and highly dispersed Ru sites, which enable the selective deconstruction of these O-containing plastics without hydrogenating the aromatic functional groups. Supported by DFT calculations, the authors propose a mechanism for the C–C cleavage. First, an incoming arene-containing substrate is adsorbed onto the Lewis acidic NbO_x sites followed by acid-catalyzed protonation of the aromatic ring (Fig. 20B). Notably, the Brønsted-acid sites allowed for selective cleavage of the challenging C_{aryl}–C_{alkyl} bond, a unique feature compared to other catalytic systems for hydrogenolysis.

Szanyi and coworkers investigated the effect of reaction conditions on the Ru-catalyzed hydrogenolysis of PP and PE.[327] They proposed that the first steps of the reaction are adsorption of the incoming substrate onto the Ru catalyst followed by dehydrogenation to form a Ru–C_{alkyl} bond, and then cleavage of the C_{alkyl}–C_{alkyl} bond mediated by Ru catalysis. In addition, they found that lighter products desorb preferentially, whereas heavier

hydrocarbon products remain on the catalyst surface. Additional examples of hydrogenolysis of polyolefins or model alkanes are the carbon-supported Pt-catalyzed conversion of PP,[328] the upcycling of PE under mild conditions with metal-free or metal-doped zeolite-catalyts,[329] or under nickel–aluminate catalysis,[330] and the use of Pt nanoparticles supported on silica to convert polyolefins into a C_{23}-centered distribution of hydrocarbons.[219] Perras and coworkers designed a hydrogenolysis catalyst composed of Pt nanoparticles located at the base of silica mesopores and employed it for the upcycling of HDPE.[331] Though the authors claimed that their ''enzyme-inspired'' type of catalyst follows a processive mechanism, their claims focused more on the chemo–physical interactions between the substrate and the catalyst than on the type of pathway the reaction was following.

Dehydrogenation, followed by C–C cleavage, was proposed for the Ir-, Rh-, and Pt-cluster catalyzed hydrogenolysis of *n*-alkanes by Flaherty and Iglesia.[332] They highlight that the key step for the C–C cleavage is the cooperation of adjacent metal centers. Additional examples from the same group have also been reported.[333,334] Another example of an unclear mechanism was given by Vlachos and coworkers for the Ni/SiO_2-catalyzed polyolefin deconstruction *via* divergent hydrogenolysis.[335] They suggest that single and multiple C–C scission events occur for both terminal and internal carbons. The reaction mechanism was also not clear for the conversion of PP using an industrial fluid catalytic cracking catalyst, as the authors suggested the need for a better understanding of this mechanism.[336]

Vlachos and coworkers investigated a combined $Pt/WO_3/ZrO_2$ catalyst for LDPE hydrocracking leading to higher value branched alkanes.[112,337] The depolymerization is proposed to occur *via* isomerization and hydrocracking of PE, where subsequent β-scission is involved. A similar mechanism was proposed by Liang and coworkers who reported a Rh/Nb_2O_5-catalyzed hydrogenolysis-isomerization of polyolefin plastics to liquid alkanes.[338] The authors suggested that this system follows a hydrocracking mechanism: the metal center activates C–C and H_2 bonds followed by an acid-catalyzed carbon positive ion isomerization and β-scission. However, a more rigorous study of the reaction mechanism is necessary.

Although extensive studies suggest that the reaction mechanism for C–C cleavage of small molecules (typically with $C_n < 30$) follows a β-elimination path, the macromolecular structure of polymers, the low relative abundance of intermediate species, and other challenges hinder the elucidation of the mechanism.[14,339] Therefore, for most of the examples documented in the literature, there is still evidence missing to truly assess the reaction mechanism relevant for C–C cleavage in plastic deconstruction. In contrast to linear polyolefins, which preferentially undergoes β-alkyl/β-scission pathways to form light alkanes, substrates containing branching or aromatic moieties require catalysts having finely tuned acidity (*e.g.*, Brønsted or Lewis sites) to enable isomerization and controlled C–C bond cleavage, while minimizing over-cracking. Catalyst choice should balance metal identity, loading (*e.g.*, Ru, Pt for hydrogenolysis; Zr-based systems for mild, selective β-elimination), and acidity (low for hydrogenolysis, higher for hydrocracking), while maintaining robustness to operate under relatively high temperatures (< 250–300 °C).

4.2.2. Cross metathesis. Cross metathesis is a powerful strategy for the cleavage of C–C bonds of polyolefins, by coupling co-reagents like light olefins/alkanes with plastic substrates. Such methods generally involve (i) dehydrogenation to generate coupling partners *in situ*, (ii) olefin metathesis, and (iii) hydrogenation of the olefin intermediates to generate the desired alkane products. PE metathesis can be coupled with either small molecule alkenes, such as ethylene (*i.e.*, ethenolysis), or light alkanes, which undergo β-alkyl elimination *in situ* and produce low-molecular weight olefins (Fig. 21A and B, respectively).

Cross metathesis requires careful catalyst selection and control of reaction rates to combine transfer dehydrogenation, olefin metathesis, and hydrogenation into a productive tandem process.[340,341] Alkane and alkene cross metathesis are two putative examples that undergo identical tandem reactions but differ due to the co-reagents identity, either an alkane or alkene, respectively (Fig. 21). Several methods have been developed for polyolefin deconstruction using both heterogeneous and homogenous catalysts.

Huang and coworkers reported an alkane metathesis reaction, co-catalyzed by an Ir-pincer dehydrogenation catalyst and Re_2O_7/Al_2O_3 olefin metathesis catalyst, to convert PE to liquid fuels and waxes. Synthesis of PE waxes remains a challenge in ethylene polymerization reactions, due to over-polymerization, and the production through PE waste deconstruction offers an attractive alternative strategy. The addition of short alkane metathesis partners (*n*-octane) was used to generate olefin coupling partners *in situ* (Fig. 22A).[342] Although, the mechanism is not reported in depth, the authors suggest that the distribution of degraded products could be controlled by reaction rate and different dehydrogenation catalysts. A similar tandem catalytic system with model substrates was used by Goldman and coworkers *via* a heterogeneous dehydrogenation Ir-pincer catalyst supported on alumina that converted long-chain alkanes to light alkanes an order of magnitude faster than homogenous catalysts.[343] Although both studies proposed the involvement of metathesis

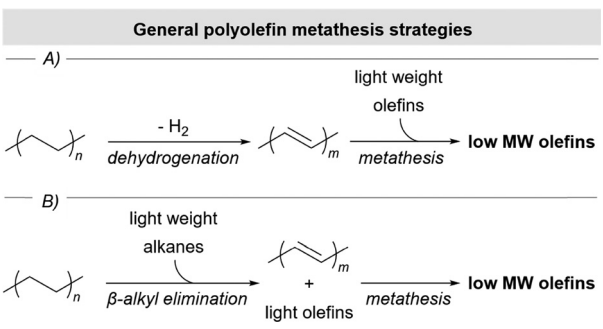

Fig. 21 General strategies for the C–C cleavage *via* polyolefins metathesis.[14] (A) β-elimination to form unsaturated products which are in turn converted into light weight olefins *via* olefin metathesis. (B) The addition of light alkanes to the initial polymer mixture results in the formation of light and high molecular weight olefins through β-alkyl elimination which then are converted to low molecular weight olefins *via* olefin metathesis.

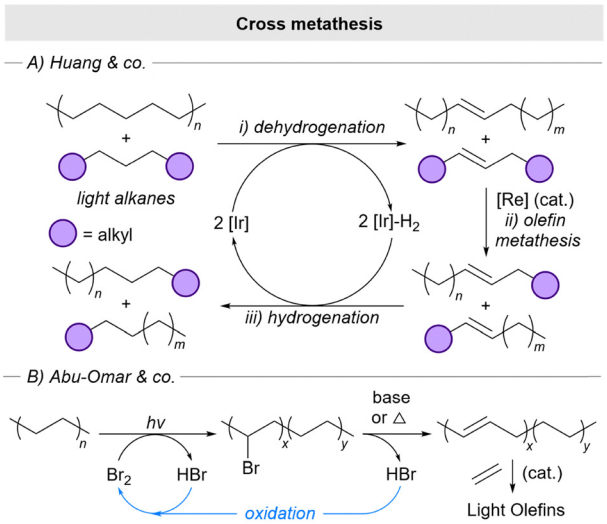

Fig. 22 (A) Cross alkane metathesis of polyolefins with the addition of light alkanes to the initial reaction mixture.[342] (B) Br-mediated method to produce C=C bonds into the polymer backbone.[344] The strategy involves initial bromination of the polymer backbone *via* photoactivated Br_2, followed by dehydrobromination to form olefinic sites that undergo ethenolysis with ethylene. The second step is C–C cleavage *via* olefin metathesis.

reactions, a more comprehensive understanding of the ongoing pathways would be of interest.

Abu-Omar and coworkers developed a unique three-step strategy involving olefin metathesis for the chemical upcycling of polyolefins to α,ω-divinyl-functionalized oligomers (Fig. 22B).[344] The strategy involves a sequence of bromination-dehydrobromination to generate the olefin coupling partner on the polymer backbone followed by olefin metathesis with ethylene. Direct bromination of PE was achieved in air, without oxidative cleavage side reactions, proposed *via* photoexcitation of Br_2 to produce brominated PE in good yields (86 wt%), followed by dehydrobromination and ethenolysis, from which the desired product was formed in 76 wt% yield.

Other examples of cross-metathesis for chemical deconstruction of PE were provided by the Scott's, Guironnet's, and Hartwig's groups, who utilized ethylene as a co-reagent.[230,231,345] Hartwig's strategy involved a combination of Ir-, Ru-, and Pd-based catalysts to perform sequential reactions and generate propylene in >60 wt% yields. Time course studies of the degradation of HDPE show a lengthy induction period and an increase in the formation of propylene – this fit well to an exponential function for the catalyst and showed a zero-order dependence on product until the substrate was depleted. The authors took these observations as evidence that the rate determining step in the reaction involved the ethylene co-reagent. Lastly, substrate unsaturation significantly affects the reaction performance, *via* catalyst poisoning due to chelation with conjugated dienes. To combat this, Hartwig and coworkers show hydrogenation of unsaturated polymers restores catalytic activity and propylene yields. Scott, Guironnet and coworkers developed a tandem ethenolysis/transfer dehydrogenation/isomerization catalytic system to convert PE in propylene.[345] Nevertheless, investigating the mechanism of these reactions was not the focus of their paper. Guironnet and Peters also exploited this strategy for the depolymerization of PE and develop a simple kinetic model for PE cross metathesis and isomerization to generate propylene.[346] The authors generated a Fokker–Planck type equation which allows for testable predictions including: the rate of propylene production, molecular weight distribution, and concentration dependences.

The groups of Beckham and Román-Leshkov further demonstrated tandem heterogeneous catalysts like $SnPt/\gamma\text{-}Al_2O_3$ and $Re_2O_7/\gamma\text{-}Al_2O_3$ to be effective for PE depolymerization *via* alkane metathesis.[347] First, the process occurs through dehydrogenation of both the co-reagent *n*-pentane (to *n*-pentene) and the polymer backbone. The products of this reaction are then converted into smaller homologues *via* olefin cross metathesis and finally are hydrogenated to form light alkane products in 99 wt% yield. In a similar study, a heterogeneous WO_x/SiO_2 catalyst also proved to be efficient for alkane or alkene metathesis reactions in the synthesis of waxes.[348] Although there were no detailed mechanistic studies, the addition of zeolites was found to be critical and reasoned necessary to prevent catalyst poisoning by *in situ* generated oxygenates. The heterogeneous catalyst was used for the synthesis of waxes with significant reduction in total reaction time, product molar mass, and dispersity compared to other heterogeneous analogues.

Catalytic cracking of polyolefins has also been shown to generate olefinic coupling partners *in situ* without the need for dehydrogenation of the starting polymer but operate at much harsher temperatures (>300 °C).[231] The combination of heterogeneous catalysts WO_3/SiO_2 and $Na/\text{–}Al_2O_3$ led to the deconstruction of a range of polyolefins, including HDPE and PP, in greater than 85 wt% conversion to form either propylene or a mixture of propylene and isobutylene, respectively. Critically, isotopic labeling experiments with ^{13}C-labeled polyolefin and ^{12}C-labeled ethylene produced enriched ^{13}C-propylene and helped to eliminate the possibility of propylene being produced from ethylene oligomerization and isomerization alone.

An example of HDPE open-loop recycling was achieved by Coates and coworkers by dehydrogenation of PE followed by cross-metathesis with 2-hydroxyethyl acrylate to generate telechelic macromonomers.[349] These macromonomers were then repolymerized through transesterification, after a diethanolamine-promoted aminolysis treatment, to generate a polymer with comparable mechanical properties to the starting post-consumer PE. Importantly, with the additional ester functionality the newly synthesized polymer is able to undergo facile depolymerization, allowing for closed-loop recyclability. While the authors discuss that the mechanism involves dehydrogenation and metathesis reactions, detailed insights are not provided.

Even though olefin metathesis is a well-studied reaction, the mechanism of polyolefin depolymerization involving metathesis reactions, coupled with dehydrogenation and hydrogenation, is more complex and less understood. For example, reaction rates of dehydrogenation *versus* metathesis, together with their stereo- and regio-selectivity, remain as mechanistic questions. Catalytic cross metathesis systems should integrate dehydrogenation, metathesis

(*e.g.*, Re_2O_7/Al_2O_3 and WO_x/SiO_2), and hydrogenation capability. This can be achieved through careful catalyst selection and loading, tuned to balance these tandem steps. In addition, the choice of light alkane or alkene coupling partners (*e.g.*, ethylene for ethenolysis) strongly influences kinetics, product distribution, and susceptibility to catalyst poisoning by unsaturated intermediates. Such aspects can be further exploited to steer catalyst selectivity towards the desired products.

4.2.3. Radical fragmentation. Radical fragmentation is the mechanism proposed for most O_2-/O_3-/peroxide-mediated processes, photochemical strategies, and electrochemical reactions for plastic substrates deconstruction reported to date.

Coupling radical fragmentations with bioconversion is a powerful strategy to upcycle plastic waste into high value products. A pyrolysis-oxidation–bioconversion strategy was adopted by O'Connor and coworkers for PE deconstruction. The authors initially produced hydrocarbon wax *via* pyrolysis which was subsequently oxidized using O_2 and a permanganate catalyst in a mixture of fatty acids that were fed to microorganisms (*P. Putida*).[350] A more recent example of chemical recycling of mixed plastics wastes *via* tandem chemical autoxidation and biological funneling, inspired by the Mid-Century Process for autoxidation catalyzed by homogeneous metal/bromide catalysts, typically Co, Mn, or Zr,[351] was reported by Beckham, Stahl and coworkers (Fig. 23A-i).[224] It was hypothesized that autoxidation of the polymer is initiated by C–H bond abstraction to generate alkyl radicals that react with O_2 to form peroxide intermediates. These peroxide intermediates, in turn, undergo homolytic cleavage of the O–O bond, mediated by the Co and Mn catalysts, and form alkoxyl radicals. Subsequently, the alkoxy radicals suffer C–C bond cleavage through β-scission ultimately producing low molecular weight oxygenated products (Fig. 23A-ii).[279,283,351,352] The autoxidative deconstruction was shown to be effective on PE, PS, and polyesters. Eventually, the oxidized products were subjected to biological funneling, wherein an engineered microbe converted a mixture of oxygenates to one exemplary product. More recently, the same group reported the conversion of PS waste to adipic acid *via* similar oxidation-bioconversion chemistry.[353] In another study, oxygenated products derived from the catalytic conversion of PE or PS to dicarboxylic acids and benzoic acid, respectively, were also used as a carbon source by the fungus *Aspergillus nidulans* to produce pharmacologically-active compounds.[354,355]

A photocatalytic radical fragmentation pathway using vanadium catalysts was developed by Soo and coworkers utilizing visible light to drive C–C bond cleavage of functionalized substrates.[356] The authors proposed that the reaction proceeds *via* a cascade of homolytic C–C bond cleavage wherein peroxide radicals are involved (Fig. 23B). V-photocatalysis using peroxides is well known,[357] however this transformation was not studied in detail. First, $V(O)(acac)_2$ is oxidized by O_2 to **54**, which is then photoexcited through a ligand-to-metal charge transfer mechanism, followed by the C–H oxidation of isopentane to form **55**. At this stage, a rearrangement of the peroxide radical species **55**, aided by photoexcitation, facilitates the subsequent homolytic C–C cleavage. An equivalent of O_2 helps regenerate the catalyst and finally the oxygenated products are released. A similar mechanism was proposed by the same group in a different system where the authors proposed that a radical fragmented C–C bond cleavage occurs for the

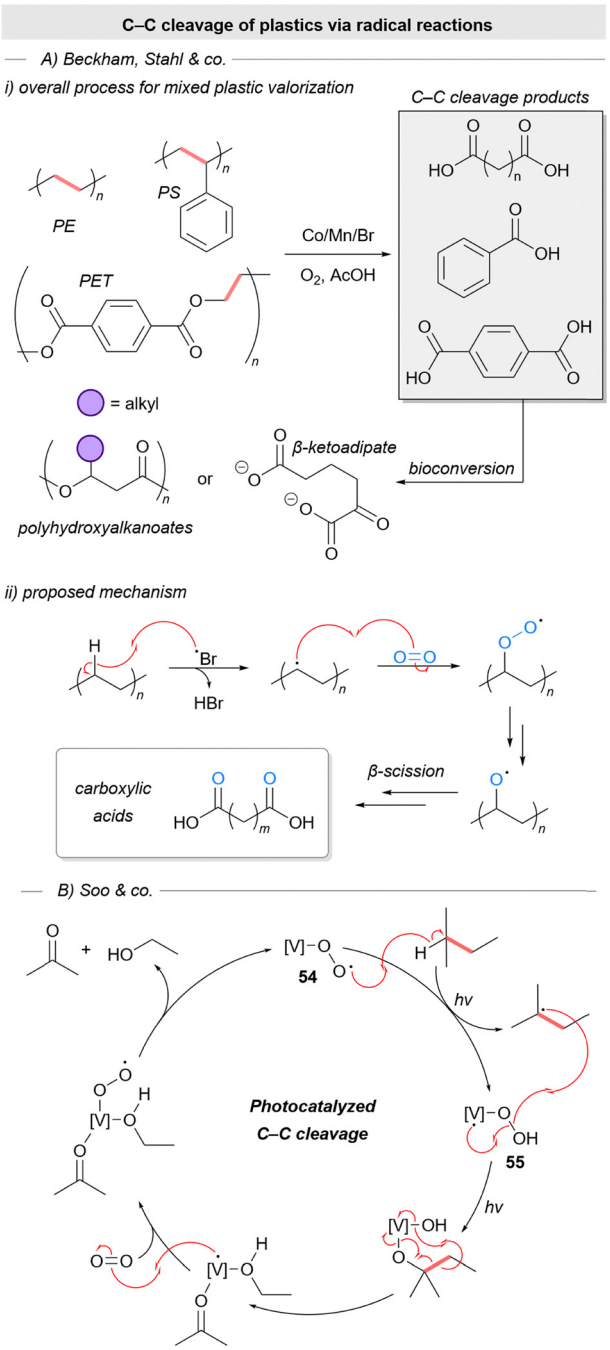

Fig. 23 (A) pathway for the oxidative C–C bond cleavage of plastics catalyzed by Co and Mn *via* β-scission.[224] The mechanism is believed to occur *via* first radical transfer from Br to the polymer backbone and subsequent β-scission. (B) Proposed mechanism for vanadium-mediated C–C homolytic radical cleavage in OH-functionalized PE.[356] The V complex is first oxidized by O_2 and photoexcited to generate a reactive species that abstracts a hydrogen atom from the substrate to form a peroxide radical intermediate. This intermediate then undergoes rearrangement and homolytic C–C bond cleavage, while O_2 regenerates the catalyst and yields the final oxygenated products. Colored circles indicate general functional groups.

deconstruction of mixed plastics including HDPE, LDPE, PVC, PP, PS, and other co-polymers *via* base metal photocatalysis.[225]

Photo-aerobic upcycling of PS is also an emerging field and has been proposed to proceed *via* similar C–H oxidation steps, peroxy radical intermediates, and β-scission events to ultimately produce benzoic acid. Organo-photocatalyst 9-fluorenone has been proposed to act as both a hydrogen atom transfer (HAT) agent and photocatalyst to produce benzoic acid from PS in 40 wt% yield.[358] Stern–Volmer studies show a linear relationship between the catalyst's fluorescence emission intensity and PS concentration, suggesting the excited state of the photocatalyst is quenched directly by PS. Separate HAT- and photo-catalysts can also deconstruct PS to benzoic acid, including the alkylhalide–thioxanthone system.[359] Alternatively, *p*-toluene sulfonic (*p*TsOH) acid-catalyzed photo-aerobic oxidation can also efficiently deconstruct PS to formic and benzoic acid without the explicit addition of a photosensitizer.[226] UV-visible studies show mixed PS and *p*TsOH form an UV-active adduct [PS–H^+] at 405 nm and likely accelerate the reaction. Lastly, through electron paramagnetic resonance (EPR) studies and DFT calculations, the reactive oxygen species was identified as singlet oxygen ($^1O_2$).

Studying the impact of natural environment conditions, such as oxygen, humidity, and UV radiation, on polymer degradation rates and product formation can be informative in iterations of reaction design.[360] Xie and coworkers simulated natural environment conditions for PE, PVC and PP photoconversion, with a Nb_2O_5 photocatalyst, and proved effective in the selective synthesis of C_2 products, without the need of any sacrificial co-reagents (Fig. 24).[227] Their proposed mechanism includes: (i) photodegradation of the polymer chain into CO_2; (ii) O_2 reduction to H_2O; and (iii) CO_2 conversion in CH_3COOH, concomitant with the simultaneous H_2O oxidation to regenerate O_2. *In situ* EPR spectroscopy, UV-vis absorption, and isotopic labelling experiments show evidence for hydroxy- and superoxide radicals generated from water oxidation and oxygen reduction, respectively. *In situ* FTIR and labeled $^{13}CO_2$ experiments confirm the acetic acid product is likely generated from photoreduction of CO_2, rather than direct photodegradation of PE (Fig. 24). The author's detailed mechanistic investigation supports their proposal.

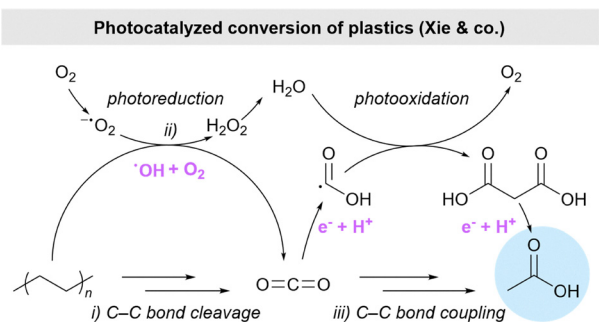

Fig. 24 Proposed radical pathway for the C–C cleavage in polyolefins and subsequent radical coupling towards acetic acid.[227] The proposed mechanism involves polymer photodegradation to CO_2 which is in turn converted into acetic acid while water oxidation regenerates O_2.

Lastly, inorganic photocatalysts, like Ru/TiO_2, can also be used for the conversion of waste polyolefin plastics to liquid fuels, as demonstrated by Zhang and coworkers.[228] The authors suggested that the photothermal heating of the Ru/TiO_2 catalyst results in a local heat increase of the catalyst and allowed melting of the polymer and triggering depolymerization. Treating the system with UV light ($\lambda < 365$ nm) activated the LDPE chains and created reaction sites for radical scission aided by Ru nanoparticles deposited on TiO_2. At 30 bar H_2/N_2 and 220 °C, 86 wt% yield of C_5–C_{21} hydrocarbons was obtained.

In summary, typical systems for autoxidation reactions involve transition-metal catalysts and a radical promoter (*e.g.*, Co/Mn/Br or Co/Mn/Zr/NHPI) under aerobic conditions (O_2 : 1–20 bar) and moderate temperatures (120–200 °C). Alternatively, autoxidative photocatalytic routes use metal oxide catalysts (Nb_2O_5, TiO_2, V complexes) or organic photosensitizers (*e.g.*, fluorenone, thioxanthone) under UV–visible light irradiation and aerobic conditions to generate reactive oxygen species ($^{\bullet}OH$, $O_2^{\bullet-}$, *etc.*) towards C–C cleavage. A major challenge in autoxidative valorization is controlling the reaction conditions to maximize selective C–C cleavage and formation of productive oxygenates (*e.g.*, acids, ketones) while limiting overoxidation to char, CO_2, or other small molecule products. Careful design of process conditions, such as through mild solubilization followed by downstream functionalization (either *via* chemo- or biological conversion) could provide more efficient routes to desired products.

4.2.4. Baeyer–Villiger oxidation. Baeyer–Villiger oxidation has been well explored with small molecules, but less attention has been given to its application for the cleavage of C–C bonds in plastics. The Baeyer–Villiger reaction is a selective transformation for polyolefin upcycling, but this typically requires the introduction of a carbonyl functional group *via* an initial oxidation step.

Hartwig and coworkers reacted PE in the presence of a Ni-based catalyst and *meta*-chloroperoxybenzoic acid (*m*CPBA) as the terminal oxidant, resulting in the hydroxylation of the polymer backbone.[361] In absence of the Ni catalyst, the authors observed 1.9 mol% formation of ester groups, which was proposed to arise from Baeyer–Villiger-type rearrangement following carbonyl formation. In a similar process, Wu and coworkers depolymerized PE *via* a combined chemical and biological method.[362] The authors first introduced ester groups *via* an *m*CPBA-mediated oxidation and then hydrolyzed the obtained ester groups using cutinase. In both cases, the mechanism was not clear, warranting further studies. Nevertheless, considering the ester products formed and the use of *m*CPBA as the oxidant, a Baeyer–Villiger mechanism is plausible.

More recently, Wang and coworkers converted PE to biodegradable adhesives by employing the Baeyer–Villiger oxidation as a key step in their procedure.[363] The authors proposed a reaction mechanism for their process, as shown in Fig. 25. Initially, thermal cleavage of the unstable peroxy bonds of *m*CPBA generates hydroxyl and carboxyl radicals (Fig. 25-i). The carboxy radical abstracts an H atom and forms a radical which, in turn, reacts with $OH^{\bullet}$ to form an alcohol (Fig. 25-ii). The same process occurs a second time, together with subsequent dehydration, yielding carbonyl groups along the polymer chain (Fig. 25-iii). Given the formation of the internal ketone, Baeyer–Villiger rearrangement can occur to

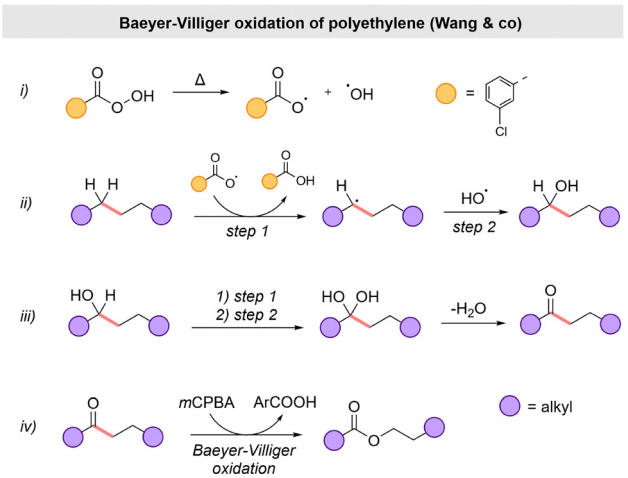

Fig. 25 Proposed pathways for the Baeyer–Villiger oxidation of PE by Wang and coworkers.[363] PE is first oxidized to produce an alcohol-functionality *via* radical oxidation with peracetic acid followed by additional oxidation to a ketone and finally a Baeyer–Villiger oxidation reaction.

form ester groups and formally cleave C–C bonds (Fig. 25-iv). Overall, Baeyer–Villiger oxidation is an underexplored approach in plastic depolymerization and an improved mechanistic understanding is important to increase its efficiency and to uncover more benign or sustainable oxidants.

4.2.5. Other routes: unclear or speculative mechanisms. In a certain number of reports, the mechanism for C–C cleavage is unclear, speculative, or not comprehensively discussed, and in this section such works are summarized.

Tomishige and coworkers investigated oxidative addition in the context of hydrogenolysis of squalene, model alkanes, and polyolefin plastics using heterogeneous Ru- and V-based catalysts (Fig. 26).[317,364–366] Throughout their studies, the authors proposed different pathways for two adjacent Ru metal centers for C–C cleavage. It is unclear if the mechanism follows either or both oxidative addition and β-elimination step(s).

The reaction rate and catalyst selectivity can be controlled *via* the reaction conditions and the catalyst composition.

In a similar catalytic system, Wang and coworkers reported the electronic-driven selectivity for the Ru/CeO_2-I catalyzed production of liquid alkanes from PE, such that more positively charged Ru sites favored hydrogenolysis.[367] The hydrogenolysis of PE starts with the oxidative addition of the C–H bond of alkanes on the Ru species. They proposed that the positions of the C–C bond cleavage are highly dependent on the charge of the Ru metal center and on the electron density of the carbon centers in the polymer backbone. Since the electron density of the secondary carbon is higher than that of a primary carbon, due to the electron-donating effect of adjacent alkyl species, more positively charged Ru species favorably bond to secondary carbon sites, resulting in C–C bond cleavage. Conversely, negatively charged Ru species favor the adsorption of primary carbons and produce methane.

Overall, understanding the mechanism of high-temperature processes for the chemical conversion of plastics is nontrivial. In that regard, an overview on the possible pathways has been recently given.[368]

5. Outlook

5.1. Overview

With the aim of finding cross-cutting opportunities between lignin and plastics deconstruction chemistries, we summarized

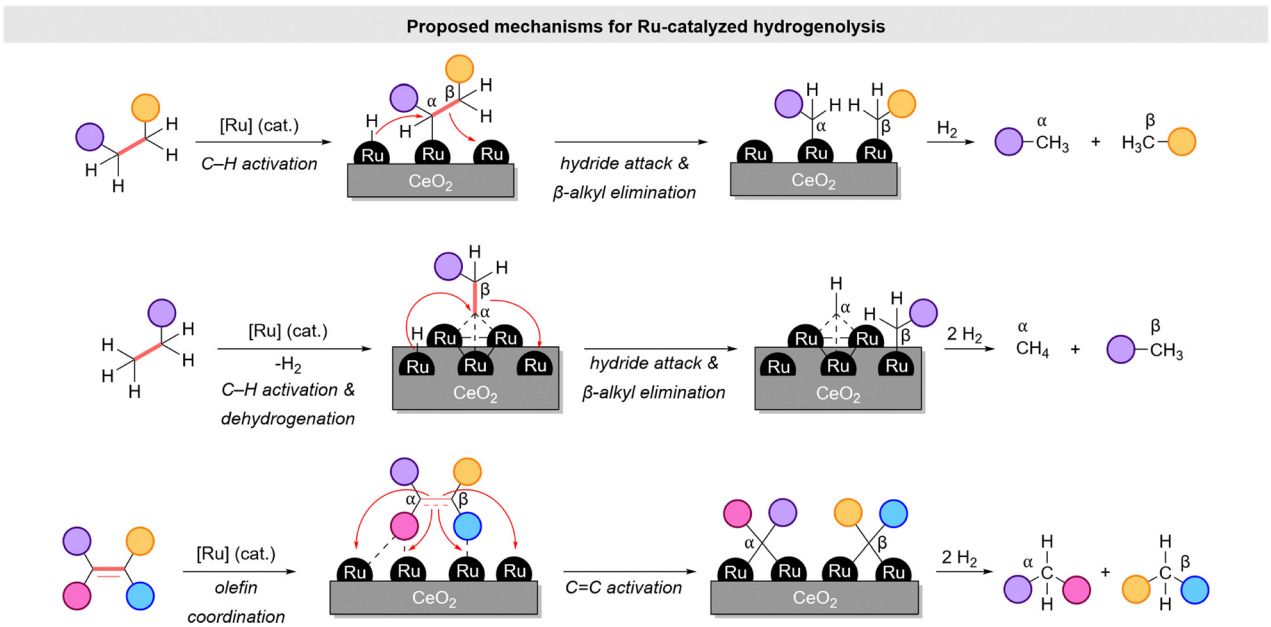

Fig. 26 Possible mechanistic pathways for the C–C cleavage of polyolefins by metal centers as the first step towards hydrogenolysis. The mechanisms of these reactions were proposed to occur *via* β-elimination. Colored circles indicate general functional groups.

catalytic procedures applied to both substrates and categorized them based on the mechanism of the reaction (Table 3). Such an effort facilitates identifying strategies that have or have not yet been applied to plastics and/or lignin. For instance, although olefin metathesis is intensively employed to cleave and re-form C=C bonds in plastics, to date, only one report has explored its use to target C=C bonds in lignin substrates.[369] Similarly, radical migration, oxidative addition, and organo–catalytic reactions have been applied to lignin, but not to plastics. Intriguingly, the well-known Baeyer–Villiger oxidation has been applied to lignin model compounds bearing C–O bonds[370,371] but with little attention to plastic substrates.[361–363] These gaps highlight clear opportunities for future cross-fertilization between the two fields.

5.2. Most promising methods

As presented above, there are many C–C bond cleavage methods available, both as general strategies and specific examples for lignin and plastics. In our opinion, certain approaches merit attention in future studies, as described in this section (Fig. 27A).

5.2.1. Radical fragmentations. Oxidations with molecular oxygen (or other oxidants) that generally occur *via* radical fragmentations are very promising for future studies. Indeed, to date the most efficient process for the cleavage of C–C bonds in lignin is *via* Co/Mn/Br aerobic oxidation of deoxygenated lignin substrates, with monomer yields up to 73 wt% (based on the deoxygenated lignin substrate).[212] This substrate agnostic chemistry produces aromatic carboxylic acids such as benzoic and terephthalic acids, key platform chemicals with applicability as chemical intermediates, pharma, cosmetics, and polymer chemistry. In addition, similar catalytic systems[210,257] and Cu-based catalysts[213,269] have proven effective for cleaving lignin C–C bonds. The very broad spectrum of targeted C–C bonds is a major strength, while the selectivity remains a challenge. A downside is the inevitable production of CO_2 as byproduct, which leads to loss of carbon. However, there is room for improvement considering the current yields of monophenols are typically around 50 wt% of the theoretical maximum yield.[212]

Similarly to lignin, aerobic oxidation and, more generally, radical fragmentation are also among the most promising methods for plastic deconstruction. Their wide applicability is a strength, as they can be applied to different plastic substrates and even to mixed plastics. Relevant examples in this regard are the combination of catalytic oxidative processing and bioconversion to funnel plastic waste in a single product (Table 2; entry 10),[224] and the $V(acac)_2$-catalyzed oxidative photocatalytic method to convert mixed plastics simultaneously into functional substrates like benzoic acid (aromatic chemical platform), acetic acid (commodity chemical), and formic acid (green source of H_2), not achievable *via* reductive protocols (Table 2; entry 11).[225] Both systems showed high catalytic performance for C–C bond cleavage, with yields of monomers up to 70–80%. A challenge is to control the reaction progress to avoid overoxidation towards undesired gaseous products (*vide infra*). Oxidation is also useful to provide functionality (*e.g.*, hydroxyls, carbonyls, *etc.*) to the polymer chain and make them more amenable for bioconversion and/or for high-value applications and chemicals.

5.2.2. β-Elimination/-scission. Methods involving β-alkyl elimination are also very promising. For instance, reductive processes mediated by Ru and Pt catalysts deposited on acidic supports afforded very high yields of reduced monomers from lignin.[203,214] Advantages include tolerance to phenolic OH groups and the production of reduced compounds similar to the conventional products of crude oil refining. C–C bond cleavage efficacy *versus* over-reduction of aromatics to fully saturated compounds is a challenge. Further catalyst development is needed to reach maximum monomer yields while avoiding over-cracking.

Additionally, one of the most suitable and promising methods for the deconstruction of plastics into light alkanes and waxes is *via* β-alkyl elimination. Plastics, and especially polyolefins, are mainly (or solely) composed of C–C and C–H bonds, which are among the most challenging to activate. Accordingly, catalyst systems capable of activating these bonds for β-alkyl elimination should be a major focus of future research. An alternative approach is the functionalization of the polymer chain (*e.g.*, *via* oxidative processes) followed by catalysis involving β-elimination to form unsaturated synthons. An example is the Pt/H–MOR-catalyzed hydrocracking strategy by Hensen and coworkers, which enables the production of aromatic and aliphatic hydrocarbons in 77 wt% yield *via* C–O and C–C bond cleavage with potential applications in sustainable fuels and bio-derived aromatic chemical platforms (Table 1, entry 4);[203] another relevant example among reductive processes is the gas-phase hydroprocessing of lignin over Ni/SiO_2 catalysts by Sels & coworkers, yielding phenol and propylene (yield: 20 wt% and 9 wt%, respectively), an approach particularly relevant for the generation of a limited product slate. The concurrent production of phenol and propylene offers potential as an alternative to conventional petrochemical routes, as both compounds serve as key platform chemicals: phenol for downstream chemical synthesis and propylene for polypropylene (PP) production (Table 1, entry 16).[215] In summary, fine tuning of porosity, metal dispersion and accessibility, and support acidity are key drivers of reaction outcomes.

5.2.3. Cross metathesis. These reactions are 100% atom economical and occur under relatively mild conditions ($T <$ 100 °C). Only one report is currently present in the literature related to lignin valorization[369] and future research could better exploit this reaction. Lignins rich in stilbenes and other double bonds are the most suitable substrates for this transformation. Conversely, plastics deconstruction *via* metathesis has been more widely explored and showed promising results. These methods generally involve a complex array of dehydrogenation and metathesis reactions, simultaneously occurring on molecules with different sizes and structures. Though the general mechanism of metathesis reactions is well known, the pathways in plastic deconstruction reactions involving metathesis are still poorly understood. This is pivotal to better design future catalysts and steer the reactions more selectively towards desired products.

Table 3 Summary of reported routes for the C–C bond cleavage in lignin and plastics

Entry	Mechanism	Feature	Lignin	Plastics	Ref.	
					Lignin	Plastics
1	β-Carbon elimination	Substrates	β–5, β–1, and 5–5 models, woody biomass	PE, PP	202–204, 214 and 232	112, 216–218, 220, 311, 312, 326, 337 and 338
		Catalysts	Ru/Nb, Pt/H–MOR, zeolite supported RuW, Ni_2Al_3 alloy	Zr-, organo-Zr + Alkyl-Al, bifunctional Ru/H^+, Ru/Nb_2O_5, $Pt/WO_3/ZrO_2$, Rh/Nb_2O_5		
		Typical conditions	H_2; 200–300 °C; 12–40 h	H_2; 100–300 °C; 12–24 h		
		Challenges & opportunities	Avoid cracking and gaseous products, provide functional groups, milder conditions, cleave different bonds and improve yields, develop multi-metallic catalysts, Pt/HMOR for plastics, Zr-catalysts for lignin, catalyst tolerate impurities (apply to Kraft lignin and plastic waste),			
2	Radical fragmentation	Substrates	Protected and deoxygenated RCF oils, several lignin models, lignocellulose	Mixed plastics, polystyrene, polyolefins	210, 212, 213, 257, 270, 271, 274–277, 279, 280, 285 and 286	225–228, 279, 280, 350–352, 354–356, 358–360 and 372
		Catalysts	V, CuO_x clusters, $Cu–Mn/CeO_2$, Fe-doped g-C_3N_4, Co/Mn/Br, Mn/Zr, Pt, TiO_2	Co/Mn/Br, V, V(acac)$_2$, 9-fluorenone, Nb_2O_5, Ru/TiO_2		
		Typical conditions	120–220 °C; 1–6 h; oxidative environment	25–160 °C; 1–40 h; oxidative or reductive environment		
		Challenges & opportunities	Avoid overoxidation, apply photocatalysts to lignin, control reaction kinetics, benign radical promoters, catalyst recycling, milder conditions, control selectivity			
3	Arene ring opening	Substrates	Pyrolysis, organosolv steam explosion, bagasse lignins	n.r.	205, 207–210, 234, 235, 238–254, 257–259, 262–265, 373 and 374	
		Catalysts	O_3, O_2 + MgO, chalcopyrite, [BSmim]$CuPW_{12}O_{40}$, *P. Putida*, Fe, UV + H_2O_2, $Ti/SbSnO_2$ and Ti/PbO_2 electrodes, Cu	n.r.		
		Typical conditions	0–160 °C; 0.1–24 h; low pressure	n.r.		
		Challenges & opportunities	Avoid overoxidation, control reaction kinetics, find greener oxidants, develop reductive processes, apply to plastics, develop catalysts, test Kraft and technical lignins, couple with other approaches, use as a pre-/post-treatment			
4	Oxidative addition	Substrates	Protected phenolic model compounds	n.r.	200 and 201	
		Catalysts	Rh complex	n.r.		
		Typical conditions	H_2; 150 °C, 12–24 h	n.r.		
		Challenges & opportunities	Apply to real lignin substrates, develop catalytic systems, apply to plastics, couple with other approaches, find other protection strategies, very important for cleaving $C_{aryl}–C_{aryl}$ bonds			
5	Cross metathesis	Substrates	Distilled RCF monomers	Polyolefins	369	230, 231, 340–344 and 346–348
		Catalysts	HGII Hoveyda Grubbs 2nd generation catalysts	Re_2O_7/Al_2O_3, Ir, Ru, Pd, SnPt/γ-Al_2O_3 and Re_2O_7/γ-Al_2O_3, WO_3/SiO_2 + Na/γ. -Al_2O_3		
		Typical conditions	rt, 22h, mild conditions	100–200 °C; 1–96 h; low to moderate pressure		
		Challenges & opportunities	Develop more for lignin, mild conditions, control selectivity, develop for polystyrene and mixed plastics, add double bond to lignin and then apply, tandem catalysis dehydrogenation + metathesis, tune catalyst acidity/basicity, high atom economy			
6	Organo-mediated	Substrates	Lignin oligomers	n.r.	288 and 292	
		Catalysts	Bobbitt's salt; NaN_3	n.r.		
		Typical conditions	25–100 °C; 0.5–1 h; ambient pressure	n.r.		
		Challenges & opportunities	Underdeveloped field, selective and targeted bonds, mild conditions, find catalytic methods, non-stoichiometric reagents, target different bonds, apply to plastics			
7	Radical migration	Substrates	Model compounds	n.r.	267	
		Catalysts	NO_2/O_2	n.r.		
		Typical conditions	130 °C; 5 bar, 24 h	n.r.		
		Challenges & opportunities	Underdeveloped method, apply to real lignin substrates and model compounds, apply to plastics, other catalytic systems and oxidants			

Table 3 (*continued*)

Entry	Mechanism	Feature	Lignin	Plastics	Ref. Lignin	Ref. Plastics
8	Retro aldol condensation	Substrates	β-1 lignin models	n.r.	296	
		Catalysts	copper–NHC	n.r.		
		Typical conditions	100 °C; 24 h; 1 bar	n.r.		
		Challenges & opportunities	Apply to other lignin substrates, find catalysts, atom economy, selective method, not really suitable for plastics			
9	Baeyer–Villiger oxidation	Substrates	Applied to model compounds bearing C–O bonds	PEs	370 and 371	361–363
		Catalysts	tin beta zeolite/hydrogen peroxide	mCPBA		
		Typical conditions	80 °C; mild conditions	Mild conditions		
		Challenges & opportunities	Underexplored method, find recyclable green oxidants, apply to real lignin substrates and plastic waste, plastics need functionalization, selective method, provides functionalized products			
10	Other approaches	Substrates	Model compounds, woody biomass and lignin	Polyolefins	297–301, 306–309 and 375	219, 280–284, 317 and 327–336
		Catalysts	Ni/SiO_2, La(OTf)$_3$, CoS_2, Pt/C + H-ZSM-5, Re-Y/H-ZSM-5, SiO_2–Al_2O_3, Hβ zeolite, $RhCl_3$–LiI–$LiBF_4$	Ru, V, Ru/CeO_2–I, Pt nanoparticles, Ir-/Rh-/Pt-clusters, Ni/SiO_2		
		Typical conditions	200–400 °C; high pressure, reduction	> 300 °C; high pressure, reduction		
		Challenges & opportunities	Catalyst is key, tuning acidity/basicity + metal, control selectivity, targets several bonds, applicable to lignin and plastics, avoid overcracking, apply WO_3/SiO_2 + Na/γ-Al_2O_3 to lignin, reaction kinetics, flow, gas phase			

n.r. = no reports

5.2.4. Baeyer–Villiger oxidation. This approach is a selective method to cleave C–C bonds under mild conditions, and lignin is a suitable substrate for such transformations given its inherent aliphatic OH-containing structure. Though the presence of phenolic OH groups can interfere with the transformation, it can be circumvented by phenol capping. Given its selectivity and limited exploration in lignin systems, Baeyer–Villiger oxidation represents an attractive candidate for future studies. Conversely with polyolefins, it is required to first provide functionality (*i.e.*, ketones within the polymer chain) prior to Baeyer–Villiger oxidation. Nevertheless, since this route has been underexplored on plastic substrates, it should be investigated in future studies.

For complex mixed plastics streams, one of the most promising approaches is the stepwise "orthogonal" approach that converts mixed plastic waste into multiple valuable products, ~51% benzoic acid from PS, 95% BPA (and ~86% carbonate) from PC, ~97% terephthalic acid from PET, and ~90% conversion of polyolefins to short alkanes under specific catalytic steps.[376] The approach integrates multiple catalytic systems tailored to each polymer, such as g-C_3N_4, ZnO/SiO_2, Ru/P25, and Pt/HBeta. The work highlights strong catalytic performance across different tailored systems and shows broad applicability to real mixed plastic streams, although it remains a proof-of-concept multi-step process requiring further optimization for industrial scalability.

5.3. Catalysis and process design

Given that lignin and mixed plastics waste are heterogeneous macromolecules with a variety of functional groups and properties, catalyst and process design requires detailed forethought (Fig. 27B). Waste plastics are often found as a mixture of different polymers and contain additives such as dyes and inorganic fillers, while lignin presents an aromatic backbone complemented with several functionalities, including phenolic and aliphatic hydroxyl groups, carboxylic acids, carbonyls, and heteroatoms among others. An ideal catalytic system would be able to simultaneously cleave C–O and C–C bonds, providing high selectivity towards the desired small molecule products while tolerating the mentioned functionalities. This remains a current challenge in both fields, where one-pot procedures are still heavily underdeveloped.

Cascade processes, by which substrates are reacted in sequential steps with or without purification, represent the majority of current methodologies for lignin and plastics valorization. For instance, thoughtful biomass pretreatment methods, such as lignin-first strategies, offer the opportunity to isolate less recalcitrant and condensed lignin, which can be selectively converted in subsequent catalytic steps. Such controlled pretreatments can produce lignin in a more processable form, as a liquid or "lignin oil," rather than as a highly condensed solid such as Kraft lignin. These lignin oils exhibit improved solubility, reduced molar mass, lower condensation extents, and enhanced chemical homogeneity, factors that facilitate downstream separation and catalytic conversion *via* C–C bond cleavage methods. Fractionation of lignin oils can be further used to separate monomers from oligomers that are rich in C–C bonds.[377,378] As a result, the isolated monomers can be

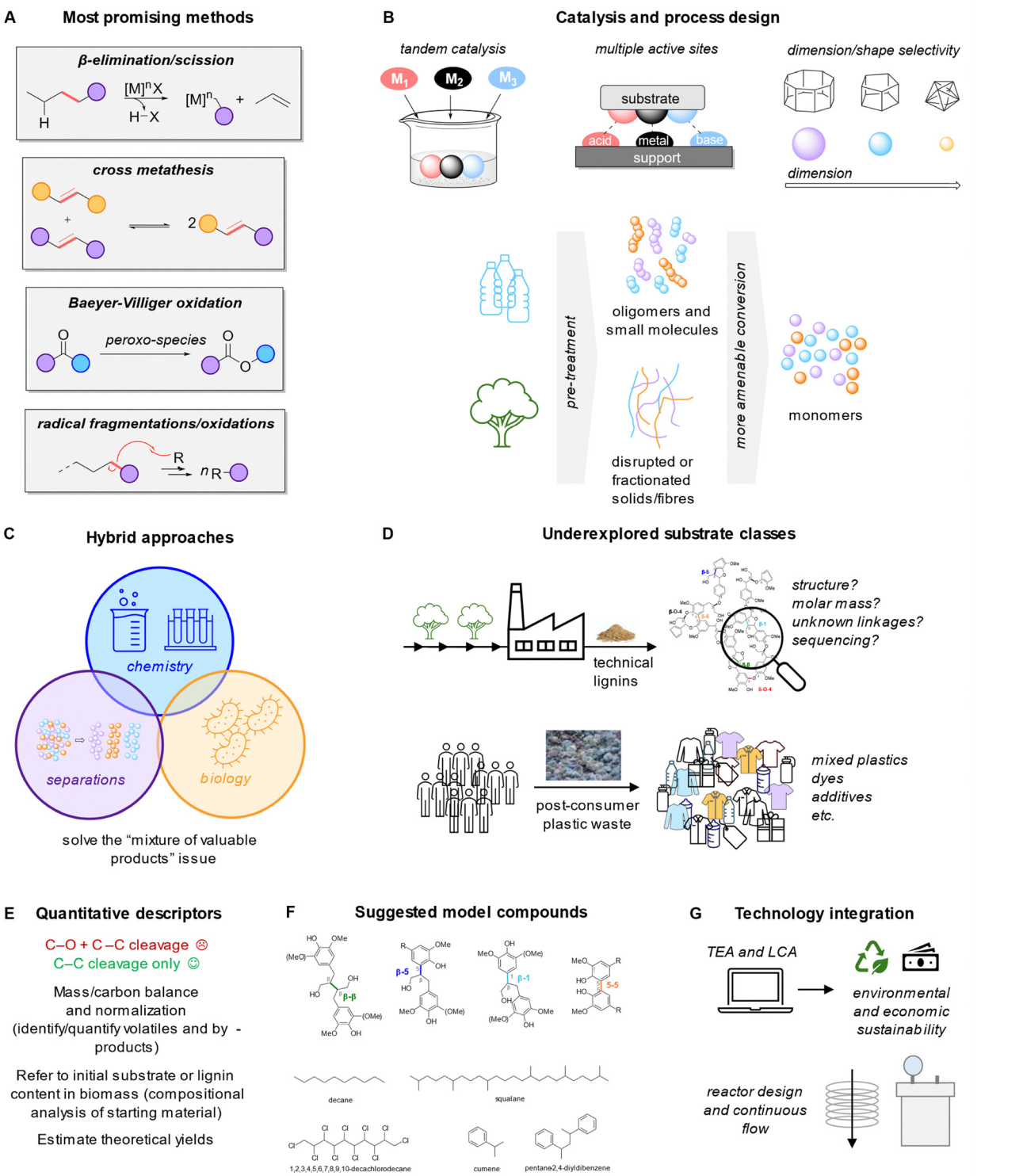

Fig. 27 Outlook summary. (A) Most promising methodologies for the cleavage of C–C bonds in lignin and plastic substrates based on the reviewed literature. (B) Opportunities for catalyst and process design: synergistic efforts by different homogeneous or heterogeneous catalysts and/or active sites/species and pre-treatments as a manner to facilitate the cleavage of C–C bonds. (C) Hybrid approaches combining chemo-/bio-catalysis and separations may overcome selectivity issues generally encountered during lignin and plastics deconstruction. (D) Technical lignins and mixed plastic waste (post-consumer) are the most underexplored class of substrates. An in depth characterization of technical lignins will be beneficial for future deconstruction studies. (E) The method by which monomer yields are calculated should be standardized to better compare across studies. The suggested pathway is stated. (F) Suggested lignin and plastic model compounds for C–C cleavage optimization and mechanistic investigations. The efficacy of a developed strategy should also be applied to real lignin and plastic substrates. (G) Techno-Economic Analysis is an excellent tool to aid in better understanding if a new technology for lignin and/or plastics deconstruction is financially viable and sustainable. Reactor design, including continuous flow systems, and technology integration have been so far underexplored and should be the objective of future studies.

more easily converted to value-added chemicals, while the oligomeric fractions are amenable to C–C bond cleavage to achieve higher monomer yields.

Oxidation is among the most successful and promising strategies for the chemical deconstruction of lignin and plastic substrates, yet they generally suffer selectivity issues. Substrates can be easily overoxidized to undesired gaseous products, such as CO and CO_2, partially due to lack of process control (such as the predominant use of batch reactors in academic laboratory settings). This is especially true for substrates like PE and PP that lack functional groups (*e.g.*, phenyl rings in PS) that form stable products, like benzoic acid.[353] Conversely, the inherent structure of lignin poses two main challenges: (i) the presence of phenolic groups inhibits radical oxidations[379] and (ii) the aromatic ring is susceptible to aromatic ring opening and subsequent over-oxidation with loss of aromaticity.[213,269] Continuous flow systems (*vide infra*) may help address these limitations by enabling precise control of residence time and temperature.[380]

In parallel, pretreatment and cascade reactions of plastics represent a strategy to (i) depolymerize and/or functionalize the polymer backbone, (ii) produce a homogeneous product that is a liquid or more soluble in conventional organic solvents, and (iii) separate additives or other components (*i.e.*, dyes, ash, and inorganic fillers).[381,382] This allows for facile processing and transformations of pretreated plastics, representing a pathway worth further exploration.[383] Such pretreatments could also provide intermediates with functional group handles (*i.e.*, carboxylic acids, carbonyls, alcohols, and others) that are more amenable to catalytic activation and upgrading. Additionally, improving the solubility and purity of plastic-derived intermediates creates opportunities for milder reaction temperatures, unrestrained by the physical properties of polymer substrates. This added solubility also facilitates better contact between the substrate and the catalyst, enhancing mass transfer and reaction efficiency. Overall, sequential processing strategies should be designed with step economy and process intensification in mind.[384,385]

Concurrent tandem catalysis (CTC)[386] is a promising option to overcome intensive sequential processes. Whereas CTC is prevalent in biological systems, often with multiple enzymatic functions operating simultaneously, it is far less studied in the context of heterogeneous lignin and plastics valorization. Amphoteric catalysts, species possessing both acidic and basic functionalities on the same surface, offer a versatile platform for CTC by enabling simultaneous activation of electrophilic and nucleophilic species/synthons. Increasing the amount of acidic and basic centers or metal clusters, can further extend this concept, as the proximity of multiple reactive sites can enable synergistic interactions, promote vicinal group(s) transfer between sites, and open new reaction pathways.

Moreover, size-exclusion catalysts, such as zeolites, metal–organic frameworks (MOFs), carbon-based supports (such as activated carbon, graphene, *etc.*), among others, provide shape- and size-selective environments, confining reactants and intermediates within well-defined pores and channels. This may not only enhance selectivity by controlling molecular access to reactive sites, but may also stabilize reactive intermediates, making mesoporous-based systems highly effective supports for tandem catalytic processes. These materials offer tunable porosity, surface chemistry, and electronic properties, which can be tailored to optimize metal dispersion, control acid–base behavior and enhance stability and reusability of the tandem catalytic systems.

5.4. Hybrid approaches combining chemo- and bio-catalysis

The separation of product mixtures derived from lignin or plastic depolymerization remains one of the most challenging aspects of biomass and polymer deconstruction (Fig. 27C). These reactions typically generate complex mixtures containing a wide range of compounds with overlapping physicochemical properties, including monomers, oligomers, char, gases, ashes, sulfur derivatives (*i.e.*, from Kraft lignin), and other by-products, along with residual additives, solvents, and catalyst residues. The similarity in polarity, molar mass, and functional groups of the products renders conventional separation techniques, such as distillation or liquid–liquid extraction, inefficient. As a result, achieving high purity in isolating valuable monomers, while minimizing carbon loss and degradation, remains difficult. This may require advanced and often multi-step separation strategies, such as membrane filtration, chromatography, or integrated hybrid processes. The complexity of these mixtures not only increases operational costs but also represents a major barrier to the scalability and economically viable conversion of lignin or plastic feedstocks to high-value chemicals.

Biocatalysis offers a promising approach to narrow the broad product distribution generally related to lignin and plastics deconstruction. Both lignin and plastics (unmodified) are largely non-bioavailable and resistant to microbial or enzymatic degradation, where lignin exhibits antimicrobial activity and most plastics, particularly polyolefins, lack functional groups accessible for efficient biocatalysts. Chemo-catalytic conversion of lignin and plastics into bio-available substrates is key for their subsequent bioconversion into a singular small molecule in high yield and selectivity. For plastics, introducing oxygen-containing functional groups can significantly enhance their bioavailability, as microbes generally prefer substrates with hydroxyl, carbonyl, or carboxyl groups over purely C–H-rich materials. In parallel, eliminating phenolic OH groups in lignin substrates may also help facilitate its subsequent bioconversion. Overall, procedures involving the combination of metal- and biocatalysis (*i.e.*, biological funneling)[210,224,257] are still in their infancy and represent a promising method to convert complex mixtures into a single/small array of products.

5.5. Technology integration

Reactor design provides an additional handle on product control through reaction kinetics (Fig. 27G). Continuous flow technologies are ranked among the most promising alternatives to increase efficiency *via* the controlled introduction of reactants and removal of products.[387] In addition, accessibility of flow or semi-continuous reactors enables the acquisition of

relevant kinetic data, which might be insightful in unveiling mechanisms and catalyst deactivation pathways. To date, there have been a limited number of examples of continuous flow or semi-continuous technologies reported in lignin and in plastics depolymerization work. We view continuous flow particularly advantageous in processes where the generated products are susceptible to overoxidation and result in carbon loss in the form of gases. Furthermore, the access to flow reactors also provides opportunities for process intensification while permitting rapid reaction optimization. We encourage future studies to focus on the development of continuous flow systems.

More generally, the design and implementation of bench-scale, lab-friendly high-pressure reactors is a valuable area of investigation. Examples are flow/flow-through reactors,[388–391] bench-scale continuous stirred tank reactors, and flow systems able to work with supercritical fluids, among others.[89] Engineering novel reactors facilitates the scale-up of efficient laboratory strategies.

Most studies focus primarily on reaction yields and selectivity, without fully considering the scalability, energy intensity, or cost implications of the processes.[392] Integrating techno-economic analysis (TEA) and life cycle assessment (LCA) with experimental development could identify the most promising catalytic routes, optimize operating conditions, and highlight trade-offs between performance, economic feasibility and sustainability (Fig. 27G). This approach is essential to move from laboratory-scale demonstrations to industrially viable solutions, ensuring that advances in depolymerization technologies translate into sustainable and cost-effective strategies.

Generally, the mechanisms presented are proposed with limited direct mechanistic studies, posing several opportunities for further inquiry. DFT computations, kinetic modeling/investigations, and *in situ* or *operando* spectroscopic techniques could provide deeper insight into the reaction pathways, intermediate species, and transition states involved in both lignin depolymerization and plastic deconstruction. Such mechanistic understanding would enable rational catalyst design, guide the optimization of reaction conditions, and help predict the selectivity and efficiency of different catalytic systems. Moreover, combining experimental and computational approaches could uncover previously unrecognized reaction pathways.

5.6. Quantitative descriptors and evaluation metrics

There is a general need for more consistent reporting of important metrics/descriptors/yields in both the plastics and lignin deconstruction fields, as this would allow easier evaluation of specific strategies and provide better comparability of potential C–C bond cleavage methods across both fields (Fig. 27E).[14,37,393,394] For example, the presence of both C–O and C–C bonds in most lignin/plastics substrates renders rational comparison of different procedures very challenging: it can be hard to accurately distinguish the product/monomer yields that are due to C–C cleavage as opposed to C–O cleavage. Thus, we recommend reporting clear and valid product yields, and to specifically report C–C cleavage yields whenever possible by explicitly quantifying C–C bond cleavage yields rather than combined C–O and C–C cleavage metrics. For meaningful comparisons across studies, yields should be normalized to the mass of substrate or the moles of cleaved C–C bonds and accompanied by selectivity metrics where applicable. It is also essential to specify the method of quantification (*e.g.*, isolated yields, GC-FID, NMR), to use internal standards and calibration curves, and to include standard deviations from repeated experiments. Collectively, these practices would significantly improve the reliability and comparability of data across different studies.

Monomer separation prior to catalysis is key to accurately reporting product yields, especially with lignin substrates. Examples of relevant separation techniques include distillation, liquid/liquid extraction, and chromatography. If monomers are already present in the lignin or plastic substrate, the reported total yield is inherently overestimated. Moreover, the textural properties (porosity) and/or metal dispersion/loading of a catalyst complicate fair comparison of the catalytic activity of different catalyst within the literature. Accordingly, we encourage normalization of product yields to metal content, catalyst surface area, and accessible active sites when applicable. In addition, we also encourage evaluating catalyst leaching when heterogeneous catalysts are used, as even small amounts of leached soluble catalyst can significantly modify the reaction outcome.

Though reporting yields from model compound studies is relatively simple relative to real substrates, this is still not trivial due to side reactions that generate char, other solid products and/or gases (*e.g.*, CO_2, CO, CH_4, and others). Closing the mass balance of a process is therefore critical, not only for accurate reporting but also for developing mechanistic understanding. Comprehensive characterization and quantification of by-products are thus strongly recommended. Furthermore, monomer yields obtained from model compounds are typically higher than those achieved with polymeric or oligomeric substrates. In light of this discrepancy, catalytic systems should be evaluated using both model compounds and realistic, well-characterized post-consumer or industrial feedstocks.[25,37,382]

To enable meaningful benchmarking, we also suggest the adoption of standardized model substrates reacted under the same/similar conditions. Examples of suggested model compounds for lignin are representative dimers (Fig. 27F), while for polyolefins ideal substrates include oligomers with controlled molecular weight or light un-functionalized or functionalized alkanes (*e.g.*, decane for PE, perchlorinated alkanes for PVC, cumene for PS, squalene for PP; Fig. 27F), and their mixtures to mimic plastic waste. It is also necessary to provide detailed characterization of plastic substrates, at minimum report M_w of plastics substrates used, FTIR to evaluate bulk functional groups and noticeable impurities, TGA to evaluate the inorganic composition from fillers, and CHN to quantify the total carbon moles. Further details and guidelines are found elsewhere.[25,69,393]

5.7. Underexplored substrate classes

Due to their recalcitrance, commercially available technical lignins have been less explored for their depolymerization, despite being a desirable type of lignin to convert (Fig. 27D).

Technical lignins represent one of the most abundant and underutilized sources of aromatic building blocks, and developing strategies to efficiently break them down into monomers could unlock significant economic and sustainability value. For instance, the depolymerization of Kraft lignin *via* C–C bond cleavage constitutes a long-lasting challenge in the pulping industry. In that regard, processes carried out under milder conditions than hydroprocessing may be suitable. Similarly, hydrolysis and organosolv lignins are underutilized, or not considered. The presence of sulfur poses additional challenges in Kraft lignin valorization as catalysts are prone to deactivation or inhibition pathways. As a result, de-sulfurization of lignins prior to catalytic conversion (sequential process, *vide supra*) may preferentially be carried out.

Open gaps are present in the characterization of technical lignins, with research mainly focused on studying Kraft lignin. A better understanding of the chemical linkages of hydrolysis, organosolv, and other emerging biorefinery lignins should be targeted in the future. Furthermore, in addition to the well-known β–β, β–5, β–1 and 5–5 motifs, several other types of uncharacterized bonds are suspected to be present in technical lignins[47,48,65–68] and future work should focus on identifying these. An additional challenge in lignin characterization is providing reliable quantitative data on the amount of specific motifs, which most of the time derive from non-quantitative techniques, such as HSQC NMR analysis.

Most of the literature concerning plastics deconstruction focuses on the depolymerization of a single or small array of substrates. However, in real-world scenarios, plastic waste streams are highly heterogeneous, containing complex mixtures of polymers, additives, fillers, dyes, and other contaminants. Thus, though being useful to understand a specific system, targeting isolated or well-defined plastics does not realistically address the scale and complexity of post-consumer plastics. To develop truly effective solutions, depolymerization and valorization strategies should be designed to handle mixed plastic streams, enabling simultaneous and/or sequential conversion of diverse polymer types into valuable monomers or intermediates (Fig. 27D). Importantly, there is a need to address post-consumer plastic waste, which is far more heterogeneous and contaminated than the well-defined, pure polymer substrates typically acquired from chemical suppliers.

5.8. Cross-cutting opportunities

While both lignin and plastics require C–C bond cleavage for effective depolymerization, the different nature of these bonds dictates distinct catalytic requirements. Lignin depolymerization is primarily governed by the cleavage of C–C linkages within an oxygen-rich, highly functionalized polymer, often proceeding *via* carbocationic and/or radical pathways. In contrast, polyolefins, for example, consist of chemically stable, non-functionalized C–C backbones, requiring initial activation through dehydrogenation, carbocation formation (acidic catalysis), metal–alkyl intermediates, or radical pathways to ultimately enact C–C bond cleavage. As a result, lignin valorization typically benefits from catalytic systems able to stabilize and coordinate oxygenated intermediates, whereas polyolefin deconstruction often relies on cooperative metal and acid support hydrogenolysis, acid-driven cracking, or radical pathways to overcome the high stability of aliphatic C–C bonds.

Despite these intrinsic differences, several catalytic concepts and cross-cutting opportunities can be translated between the two fields (Table 3). Bifunctional metal/acid systems, which are highly effective in lignin depolymerization for balancing bond cleavage and intermediate stabilization, could be further leveraged in polyolefin hydrocracking to improve selectivity and suppress over-cracking, while approaches developed for plastics, such as tandem catalysis or metathesis-based depolymerization, are valuable strategies for scaling lignin conversion. Additionally, photocatalytic methods, already explored in plastic upcycling, could provide milder and more versatile routes for lignin functionalization and depolymerization, particularly if coupled with downstream biological or catalytic upgrading. Finally, advances in polyolefin processing, such as catalytic cracking and tandem reaction engineering, highlight strategies for operating under continuous-flow and industrially relevant conditions that could be leveraged for lignin valorization.

6. Conclusions

The development of C–C bond cleavage reactions are emerging in plastic and lignin depolymerizations and as outlined in this review, have largely evolved independently of one another. Yet their structural and mechanistic similarities suggest a clear opportunity for methodology convergence. This review sheds light on the disparity of work done on the investigation of C–C scission reaction mechanisms within these types of systems. In summary:

(1) The most reported lignin methods: oxidations with O_2/O_3, radical reactions, metal- and acid-catalyzed hydrogenolysis, often applied to model compounds and with limited control over selectivity.

(2) Plastics methods: hydrogenolysis and hydrocracking occurring *via* β-elimination/scission, olefin metathesis, oxidative approaches.

(3) Overlapping C–C cleavage methods: despite few examples, most approaches have been separately applied to lignin and plastic substrates (*e.g.*, tandem catalysis in some cases), such as oxidation and hydrogenolysis, and demonstrate avenues for future exploration.

(4) Mechanistic understanding: mechanistic insights remain insufficient for both classes, with studies often limited to simplified models and lacking detailed experimental validation.

(5) Underexplored C–C cleavage methods: oxidative additions, retro aldol condensation, retro Diels–Alder, Baeyer–Villiger oxidation, flow chemistry, hybrid approaches, and tandem catalysis.

Future efforts should focus on improving atom efficiency (*e.g.*, directing-group-free oxidative addition), and developing bifunctional catalysts that simultaneously enable C–C cleavage and deoxygenation (tandem catalysis), particularly for lignin. In parallel, integrating cleavage with downstream upgrading and improving catalyst robustness against real-feedstock impurities

will be critical to advance applicability and scalability across both lignin and plastics systems.

Our hope is that this review provides a synergistic and cross-disciplinary approach – one that bridges insights from both lignin valorization and plastics recycling together – to accelerate the development of catalytic systems capable of efficiently cleaving diverse C–C linkages. We also hope this review serves as a foundation for future work aimed at coupling a molecular-level understanding with process-level innovation, enabling the transformation of complex feedstocks into well-defined product streams.

Conflicts of interest

There are no conflicts to declare.

Data availability

There are no data as this is a review article.

Acknowledgements

This work was authored by the National Laboratory of the Rockies for the U.S. Department of Energy (DOE) under Contract No. DE-AC36-08GO28308. For DR, MGF, YRL, and GTB, this material is based upon work supported by the Center for Bioenergy Innovation (CBI), U.S. Department of Energy, Office of Science, Biological and Environmental Research Program under Award Number ERKP886. Funding to ASC, MGF, ETO, YRL, and GTB was provided by the US DOE, Office of Critical Material and Energy Innovation (CMEI), Alternative Fuels and Feedstocks Office (AFFO). For BLF, MGF, YRL, and GTB, this work was performed as part of the Bio-Optimized Technologies to keep Thermoplastics out of Landfills and the Environment (BOTTLE) Consortium and was supported by the Advanced Materials and Manufacturing Technologies Office (AMMTO) and AFFO under contract no. DE-AC36-08GO28308 with the National Laboratory of the Rockies, which includes members from MIT. M. G. F. thanks Fundacion Ramon Areces for his postdoctoral fellowship. This work was supported by the Wallenberg Initiative Materials Science for Sustainability (WISE) funded by the Knut and Alice Wallenberg Foundation.

References

1 R. M. Peltzer, J. Gauss, O. Eisenstein and M. Cascella, *J. Am. Chem. Soc.*, 2020, **142**, 2984–2994.
2 K. C. Nicolaou, S. A. Snyder, T. Montagnon and G. Vassilikogiannakis, *Angew. Chem., Int. Ed.*, 2002, **41**, 1668–1698.
3 H. G. Alt and A. Köppl, *Chem. Rev.*, 2000, **100**, 1205–1222.
4 R. W. Hoffmann, *Angew. Chem., Int. Ed.*, 2001, **40**, 1411–1416.
5 G. Domínguez and J. Pérez-Castells, *Chem. Soc. Rev.*, 2011, **40**, 3430–3444.
6 G. C. Vougioukalakis and R. H. Grubbs, *Chem. Rev.*, 2010, **110**, 1746–1787.
7 L.-C. Campeau and N. Hazari, *Organometallics*, 2019, **38**, 3–35.
8 S.-H. Xiang and B. Tan, *Nat. Commun.*, 2020, **11**, 3786.
9 P. Tautorat, B. Tremolada, A. J. Martín, L. F. Santos, G. Guillén-Gosálbez, J. Pérez-Ramírez and B. Steffen, *Green Chem.*, 2025, **27**, 12985–13003.
10 I. T. Horváth, *Chem. Rev.*, 2018, **118**, 369–371.
11 C. Shi, E. C. Quinn, W. T. Diment and E. Y.-X. Chen, *Chem. Rev.*, 2024, **124**, 4393–4478.
12 F. Vidal, E. R. Van Der Marel, R. W. F. Kerr, C. McElroy, N. Schroeder, C. Mitchell, G. Rosetto, T. T. D. Chen, R. M. Bailey, C. Hepburn, C. Redgwell and C. K. Williams, *Nature*, 2024, **626**, 45–57.
13 A. J. Ragauskas, G. T. Beckham, M. J. Biddy, R. Chandra, F. Chen, M. F. Davis, B. H. Davison, R. A. Dixon, P. Gilna, M. Keller, P. Langan, A. K. Naskar, J. N. Saddler, T. J. Tschaplinski, G. A. Tuskan and C. E. Wyman, *Science*, 2014, **344**, 1246843.
14 J. Sun, J. Dong, L. Gao, Y.-Q. Zhao, H. Moon and S. L. Scott, *Chem. Rev.*, 2024, **124**, 9457–9579.
15 N. Tripathi, C. D. Hills, R. S. Singh and C. J. Atkinson, *npj Clim. Atmos. Sci.*, 2019, **2**, 35.
16 M. Mujtaba, L. Fernandes Fraceto, M. Fazeli, S. Mukherjee, S. M. Savassa, G. Araujo De Medeiros, A. Do Espírito Santo Pereira, S. D. Mancini, J. Lipponen and F. Vilaplana, *J. Cleaner Prod.*, 2023, **402**, 136815.
17 C. Li, X. Zhao, A. Wang, G. W. Huber and T. Zhang, *Chem. Rev.*, 2015, **115**, 11559–11624.
18 W. Schutyser, T. Renders, S. V. den Bosch, S.-F. Koelewijn, G. T. Beckham and B. F. Sels, *Chem. Soc. Rev.*, 2018, **47**, 852–908.
19 J. Zakzeski, P. C. A. Bruijnincx, A. L. Jongerius and B. M. Weckhuysen, *Chem. Rev.*, 2010, **110**, 3552–3599.
20 D. D. S. Argyropoulos, C. Crestini, C. Dahlstrand, E. Furusjö, C. Gioia, K. Jedvert, G. Henriksson, C. Hulteberg, M. Lawoko, C. Pierrou, J. S. M. Samec, E. Subbotina, H. Wallmo and M. Wimby, *ChemSusChem*, 2023, **16**, e202300492.
21 Plastics – the Facts 2022, Plastics Europe, https://plasticseurope.org/knowledge-hub/plastics-the-facts-2022/, (accessed September 26, 2025).
22 Global Plastics Outlook, https://www.oecd.org/en/publications/global-plastics-outlook_de747aef-en.html, (accessed September 26, 2025).
23 S. R. Nicholson, N. A. Rorrer, A. C. Carpenter and G. T. Beckham, *Joule*, 2021, **5**, 673–686.
24 K. Ragaert, L. Delva and K. Van Geem, *Waste Manage.*, 2017, **69**, 24–58.
25 L. D. Ellis, N. A. Rorrer, K. P. Sullivan, M. Otto, J. E. McGeehan, Y. Román-Leshkov, N. Wierckx and G. T. Beckham, *Nat. Catal.*, 2021, **4**, 539–556.
26 C. T. Palumbo, E. T. Ouellette, J. Zhu, Y. Román-Leshkov, S. S. Stahl and G. T. Beckham, *Nat. Rev. Chem.*, 2024, **8**, 799–816.
27 C.-H. Jun, *Chem. Soc. Rev.*, 2004, **33**, 610–618.
28 P. Chen, B. A. Billett, T. Tsukamoto and G. Dong, *ACS Catal.*, 2017, **7**, 1340–1360.

29 M. Tobisu and N. Chatani, *Chem. Soc. Rev.*, 2008, **37**, 300–307.
30 M. D. R. Lutz and B. Morandi, *Chem. Rev.*, 2021, **121**, 300–326.
31 K. Nogi and H. Yorimitsu, *Chem. Rev.*, 2021, **121**, 345–364.
32 T. R. McDonald, L. R. Mills, M. S. West and S. A. L. Rousseaux, *Chem. Rev.*, 2021, **121**, 3–79.
33 M. Murakami and N. Ishida, *Chem. Rev.*, 2021, **121**, 264–299.
34 O. O. Sokolova and J. F. Bower, *Chem. Rev.*, 2021, **121**, 80–109.
35 J. Wang, S. A. Blaszczyk, X. Li and W. Tang, *Chem. Rev.*, 2021, **121**, 110–139.
36 P. Sivaguru, Z. Wang, G. Zanoni and X. Bi, *Chem. Soc. Rev.*, 2019, **48**, 2615–2656.
37 C. T. Palumbo, E. T. Ouellette, J. Zhu, Y. Román-Leshkov, S. S. Stahl and G. T. Beckham, *Nat. Rev. Chem.*, 2024, **8**, 799–816.
38 C. Chio, M. Sain and W. Qin, *Renewable Sustainable Energy Rev.*, 2019, **107**, 232–249.
39 X. Liu, F. P. Bouxin, J. Fan, V. L. Budarin, C. Hu and J. H. Clark, *ChemSusChem*, 2020, **13**, 4296–4317.
40 T. Thiounn and R. C. Smith, *J. Polym. Sci.*, 2020, **58**, 1347–1364.
41 M. P. Pandey and C. S. Kim, *Chem. Eng. Technol.*, 2011, **34**, 29–41.
42 C. Zhang, X. Shen, Y. Jin, J. Cheng, C. Cai and F. Wang, *Chem. Rev.*, 2023, **123**, 4510–4601.
43 N. Yan, C. Zhao, P. J. Dyson, C. Wang, L. Liu and Y. Kou, *ChemSusChem*, 2008, **1**, 626–629.
44 R. Rinaldi, R. Jastrzebski, M. T. Clough, J. Ralph, M. Kennema, P. C. A. Bruijnincx and B. M. Weckhuysen, *Angew. Chem., Int. Ed.*, 2016, **55**, 8164–8215.
45 C. Xu, R. A. D. Arancon, J. Labidi and R. Luque, *Chem. Soc. Rev.*, 2014, **43**, 7485–7500.
46 M. Balakshin, E. A. Capanema, X. Zhu, I. Sulaeva, A. Potthast, T. Rosenau and O. J. Rojas, *Green Chem.*, 2020, **22**, 3985–4001.
47 P. Schlee, D. Tarasov, D. Rigo and M. Balakshin, *ChemSusChem*, 2023, **16**, e202300549.
48 M. Yu Balakshin, E. A. Capanema, C. L. Chen and H. S. Gracz, *J. Agric. Food Chem.*, 2003, **51**, 6116–6127.
49 C. Crestini, F. Melone, M. Sette and R. Saladino, *Biomacromolecules*, 2011, **12**, 3928–3935.
50 W. Boerjan, J. Ralph and M. Baucher, *Annu. Rev. Plant Biol.*, 2003, **54**, 519–546.
51 J. C. Del Río, J. Rencoret, A. Gutiérrez, T. Elder, H. Kim and J. Ralph, *ACS Sustainable Chem. Eng.*, 2020, **8**, 4997–5012.
52 H. Ito, T. Imai, K. Lundquist, T. Yokoyama and Y. Matsumoto, *J. Wood Chem. Technol.*, 2011, **31**, 172–182.
53 L. Knut, S. Tomas, B. Jannik, P. H. Nielsen, S. E. Rasmussen, S. Erling and N. A. Sørensen, *Acta Chem. Scand.*, 1970, **24**, 889–907.
54 L. Knut, L. Rolf, D. Jacob, H. Arne and S. Sigfrid, *Acta Chem. Scand.*, 1972, **26**, 2005–2023.
55 K. Lundquist, *Acta Chem. Scand.*, 1970, **24**, 3681–3686.
56 K. Lundquist, T. K. Kirk, F. Fredlund, P. Beronius, J. E. Engebretsen and L. Ehrenberg, *Acta Chem. Scand.*, 1971, **25**, 889–894.
57 S. Yasuda, *Mokuzai Gakkaishi*, 1981, **27**, 879–884.
58 S. Yasuda, *Mokuzai Gakkaishi*, 1981, **27**, 127–131.
59 S. Yasuda, *Mokuzai Gakkaishi*, 1981, **27**, 216–222.
60 T. Ito, *Mokuzai Gakkaishi*, 1981, **27**, 484–490.
61 S. Yasuda, *Mokuzai Gakkaishi*, 1986, **32**, 51–58.
62 S. Yasuda and K. Ota, *Holzforschung*, 1987, **41**, 59–65.
63 S. Yasuda and N. Murase, *Holzforschung*, 1995, **49**, 418–422.
64 H. D. Thi, K. V. Aelst, S. V. den Bosch, R. Katahira, G. T. Beckham, B. F. Sels and K. M. V. Geem, *Green Chem.*, 2022, **24**, 191–206.
65 M. Yu Balakshin, E. A. Capanema, I. Sulaeva, P. Schlee, Z. Huang, M. Feng, M. Borghei, O. J. Rojas, A. Potthast and T. Rosenau, *ChemSusChem*, 2021, **14**, 1016–1036.
66 C. S. Lancefield, H. L. J. Wienk, R. Boelens, B. M. Weckhuysen and P. C. A. Bruijnincx, *Chem. Sci.*, 2018, **9**, 6348–6360.
67 C. Crestini, H. Lange, M. Sette and D. S. Argyropoulos, *Green Chem.*, 2017, **19**, 4104–4121.
68 S. Constant, H. L. J. Wienk, A. E. Frissen, P. D. Peinder, R. Boelens, D. S. Van Es, R. J. H. Grisel, B. M. Weckhuysen, W. J. J. Huijgen, R. J. A. Gosselink and P. C. A. Bruijnincx, *Green Chem.*, 2016, **18**, 2651–2665.
69 M. M. Abu-Omar, K. Barta, G. T. Beckham, J. S. Luterbacher, J. Ralph, R. Rinaldi, Y. Román-Leshkov, J. S. M. Samec, B. F. Sels and F. Wang, *Energy Environ. Sci.*, 2021, **14**, 262–292.
70 Y. M. Questell-Santiago, M. V. Galkin, K. Barta and J. S. Luterbacher, *Nat. Rev. Chem.*, 2020, **4**, 311–330.
71 H. Luo, E. P. Weeda, M. Alherech, C. W. Anson, S. D. Karlen, Y. Cui, C. E. Foster and S. S. Stahl, *J. Am. Chem. Soc.*, 2021, **143**, 15462–15470.
72 M. V. Galkin and J. S. M. Samec, *ChemSusChem*, 2016, **9**, 1544–1558.
73 M. Talebi Amiri, G. R. Dick, Y. M. Questell-Santiago and J. S. Luterbacher, *Nat. Protoc.*, 2019, **14**, 921–954.
74 A. Rahimi, A. Ulbrich, J. J. Coon and S. S. Stahl, *Nature*, 2014, **515**, 249–252.
75 A. W. Bartling, M. L. Stone, R. J. Hanes, A. Bhatt, Y. Zhang, M. J. Biddy, R. Davis, J. S. Kruger, N. E. Thornburg, J. S. Luterbacher, R. Rinaldi, J. S. M. Samec, B. F. Sels, Y. Román-Leshkov and G. T. Beckham, *Energy Environ. Sci.*, 2021, **14**, 4147–4168.
76 M. Karlsson, N. Giummarella, P. A. Lindén and M. Lawoko, *ChemSusChem*, 2020, **13**, 4666–4677.
77 K. V. Aelst, E. V. Sinay, T. Vangeel, E. Cooreman, G. V. den Bossche, T. Renders, J. V. Aelst, S. V. den Bosch and B. F. Sels, *Chem. Sci.*, 2020, **11**, 11498–11508.
78 X. Dong, H. B. Mayes, K. Morreel, R. Katahira, Y. Li, J. Ralph, B. A. Black and G. T. Beckham, *ChemSusChem*, 2023, **16**, e202201441.
79 M. V. Galkin, A. T. Smit, E. Subbotina, K. A. Artemenko, J. Bergquist, W. J. J. Huijgen and J. S. M. Samec, *ChemSusChem*, 2016, **9**, 3280–3287.
80 M. Y. Balakshin, E. A. Capanema, R. B. Santos, H. Chang and H. Jameel, *Holzforschung*, 2016, **70**, 95–108.

81 J. Zeng, G. L. Helms, X. Gao and S. Chen, *J. Agric. Food Chem.*, 2013, **61**, 10848–10857.
82 S. Y. Lin and C. W. Dence, *Methods in Lignin Chemistry*, Springer Science & Business Media, 2012.
83 E. A. Capanema, M. Y. Balakshin and J. F. Kadla, *J. Agric. Food Chem.*, 2004, **52**, 1850–1860.
84 L. Zhang, G. Gellerstedt, J. Ralph and F. Lu, *J. Wood Chem. Technol.*, 2006, **26**, 65–79.
85 M. Sette, R. Wechselberger and C. Crestini, *Chem. – Eur. J.*, 2011, **17**, 9529–9535.
86 M. Y. Balakshin and E. A. Capanema, *RSC Adv.*, 2015, **5**, 87187–87199.
87 M. Karlsson, V. L. Vegunta, R. Deshpande and M. Lawoko, *Green Chem.*, 2022, **24**, 1211–1223.
88 M.-F. Li, S. Yang and R.-C. Sun, *Bioresour. Technol.*, 2016, **200**, 971–980.
89 D. Rigo, T. Fechter, E. Capanema, D. Diment, M. Alopaeus, D. Tarasov, D. Cantero and M. Balakshin, *ChemSusChem*, 2025, **18**, e202401683.
90 L. Zhu, C. Cui, M. Auersvald, J. Zhang, X. Kuang, X. Xiao, Y. Liao, Z. Zhou, K. M. Van Geem and F. Qi, *ACS Sustainable Chem. Eng.*, 2025, **13**, 5434–5443.
91 S. Kim, S. C. Chmely, M. R. Nimlos, Y. J. Bomble, T. D. Foust, R. S. Paton and G. T. Beckham, *J. Phys. Chem. Lett.*, 2011, **2**, 2846–2852.
92 J. B. Huang, G. S. Zeng, X. S. Li, X. C. Cheng and H. Tong, *IOP Conf. Ser.: Earth Environ. Sci.*, 2018, **167**, 012029.
93 A. M. El-Nahas, M. V. Navarro, J. M. Simmie, J. W. Bozzelli, H. J. Curran, S. Dooley and W. Metcalfe, *J. Phys. Chem. A*, 2007, **111**, 3727–3739.
94 A. A. Zavitsas, *J. Phys. Chem. A*, 2003, **107**, 897–898.
95 F. Song, T. Gou, B.-Q. Wang and Z.-J. Shi, *Chem. Soc. Rev.*, 2018, **47**, 7078–7115.
96 Y.-F. Liang and N. Jiao, *Acc. Chem. Res.*, 2017, **50**, 1640–1653.
97 D.-S. Kim, W.-J. Park and C.-H. Jun, *Chem. Rev.*, 2017, **117**, 8977–9015.
98 Z. Nairoukh, M. Cormier and I. Marek, *Nat. Rev. Chem.*, 2017, **1**, 1–17.
99 I. Marek, A. Masarwa, P.-O. Delaye and M. Leibeling, *Angew. Chem., Int. Ed.*, 2015, **54**, 414–429.
100 Y. Cohen, A. Cohen and I. Marek, *Chem. Rev.*, 2021, **121**, 140–161.
101 X.-Y. Yu, J.-R. Chen and W.-J. Xiao, *Chem. Rev.*, 2021, **121**, 506–561.
102 S. P. Morcillo, *Angew. Chem.*, 2019, **131**, 14182–14192.
103 L. Schanne and M. W. Haenel, *Tetrahedron Lett.*, 1979, **20**, 4245–4248.
104 C. J. Allpress and L. M. Berreau, *Coord. Chem. Rev.*, 2013, **257**, 3005–3029.
105 A. J. Smaligo, M. Swain, J. C. Quintana, M. F. Tan, D. A. Kim and O. Kwon, *Science*, 2019, **364**, 681–685.
106 A. Varenikov, E. Shapiro and M. Gandelman, *Chem. Rev.*, 2021, **121**, 412–484.
107 H. Lu, T.-Y. Yu, P.-F. Xu and H. Wei, *Chem. Rev.*, 2021, **121**, 365–411.
108 S. M. Sadrameli, *Fuel*, 2015, **140**, 102–115.
109 S. M. Sadrameli, *Fuel*, 2016, **173**, 285–297.
110 J. J. H. B. Sattler, J. Ruiz-Martinez, E. Santillan-Jimenez and B. M. Weckhuysen, *Chem. Rev.*, 2014, **114**, 10613–10653.
111 N. Rahimi and R. Karimzadeh, *Appl. Catal., A*, 2011, **398**, 1–17.
112 S. Liu, P. A. Kots, B. C. Vance, A. Danielson and D. G. Vlachos, *Sci. Adv.*, 2021, **7**, eabf8283.
113 J. Weitkamp, *ChemCatChem*, 2012, **4**, 292–306.
114 S. Kotha and S. Banerjee, *RSC Adv.*, 2013, **3**, 7642–7666.
115 S.-H. Shi, Y. Liang and N. Jiao, *Chem. Rev.*, 2021, **121**, 485–505.
116 W. Zhang, L. Killian and A. Thevenon, *Chem. Sci.*, 2024, **15**, 8606–8624.
117 F. P. Guengerich and F. K. Yoshimoto, *Chem. Rev.*, 2018, **118**, 6573–6655.
118 Y. Bao, N. Kumagai and M. Shibasaki, *Chem. Sci.*, 2015, **6**, 6124–6132.
119 A. More, T. Elder and Z. Jiang, *Int. J. Biol. Macromol.*, 2021, **183**, 1505–1513.
120 L. Souillart and N. Cramer, *Chem. Rev.*, 2015, **115**, 9410–9464.
121 A. P. Y. Chan and A. G. Sergeev, *Coord. Chem. Rev.*, 2020, **413**, 213213.
122 K. Ruhland, *Eur. J. Org. Chem.*, 2012, 2683–2706.
123 G. Smits, B. Audic, M. D. Wodrich, C. Corminboeuf and N. Cramer, *Chem. Sci.*, 2017, **8**, 7174–7179.
124 M. Murakami, M. Makino, S. Ashida and T. Matsuda, *Bull. Chem. Soc. Jpn.*, 2006, **79**, 1315–1321.
125 Y.-Y. Liu, R.-J. Song, C.-Y. Wu, L.-B. Gong, M. Hu, Z.-Q. Wang, Y.-X. Xie and J.-H. Li, *Adv. Synth. Catal.*, 2012, **354**, 347–353.
126 Y. Yang, L. Chen, Z. Zhang and Y. Zhang, *Org. Lett.*, 2011, **13**, 1342–1345.
127 C. Jia, D. Piao, J. Oyamada, W. Lu, T. Kitamura and Y. Fujiwara, *Science*, 2000, **287**, 1992–1995.
128 S.-G. Lim and C.-H. Jun, *Bull. Korean Chem. Soc.*, 2004, **25**, 1623–1624.
129 D. H. Lee, E.-A. Jo, J.-W. Park and C.-H. Jun, *Tetrahedron Lett.*, 2010, **51**, 160–163.
130 C. S. Chin, D. Chong, B. Maeng, J. Ryu, H. Kim, M. Kim and H. Lee, *Organometallics*, 2002, **21**, 1739–1742.
131 C. Copéret, Z. J. Berkson, K. W. Chan, J. de J. Silva, C. P. Gordon, M. Pucino and P. A. Zhizhko, *Chem. Sci.*, 2021, **12**, 3092–3115.
132 R. R. Schrock, *Angew. Chem., Int. Ed.*, 2006, **45**, 3748–3759.
133 R. R. Schrock, *Acc. Chem. Res.*, 1986, **19**, 342–348.
134 R. H. Grubbs and S. Chang, *Tetrahedron*, 1998, **54**, 4413–4450.
135 S. Lwin and I. E. Wachs, *ACS Catal.*, 2014, **4**, 2505–2520.
136 T. M. Trnka and R. H. Grubbs, *Acc. Chem. Res.*, 2001, **34**, 18–29.
137 Y.-R. Luo, *Comprehensive Handbook of Chemical Bond Energies*, CRC Press, Boca Raton, 2007.
138 P. B. Armentrout, L. F. Halle and J. L. Beauchamp, *J. Am. Chem. Soc.*, 1981, **103**, 6501–6502.

139 M. F. Lappert, *J. Organomet. Chem.*, 2005, **690**, 5467–5473.
140 H. Urtel, G. A. Bikzhanova, D. B. Grotjahn and P. Hofmann, *Organometallics*, 2001, **20**, 3938–3949.
141 D. B. Grotjahn, G. A. Bikzhanova, L. S. B. Collins, T. Concolino, K.-C. Lam and A. L. Rheingold, *J. Am. Chem. Soc.*, 2000, **122**, 5222–5223.
142 R. L. M. Chamberlin, D. C. Rosenfeld, P. T. Wolczanski and E. B. Lobkovsky, *Organometallics*, 2002, **21**, 2724–2735.
143 S. Dash, S. Patel and B. K. Mishra, *Tetrahedron*, 2009, **65**, 707–739.
144 F. Mecozzi, J. J. Dong, D. Angelone, W. R. Browne and N. N. H. M. Eisink, *Eur. J. Org. Chem.*, 2019, 7151–7158.
145 A. Sudalai, A. Khenkin and R. Neumann, *Org. Biomol. Chem.*, 2015, **13**, 4374–4394.
146 M. Balcı, *Reaction Mechanisms in Organic Chemistry*, John Wiley & Sons, 2021.
147 D. Yang and C. Zhang, *J. Org. Chem.*, 2001, **66**, 4814–4818.
148 S.-T. Liu, K. V. Reddy and R.-Y. Lai, *Tetrahedron*, 2007, **63**, 1821–1825.
149 A. Dhakshinamoorthy and K. Pitchumani, *Catal. Commun.*, 2009, **10**, 872–878.
150 D. Xing, B. Guan, G. Cai, Z. Fang, L. Yang and Z. Shi, *Org. Lett.*, 2006, **8**, 693–696.
151 S. Samanta, L. Adak, R. Jana, G. Mostafa, H. M. Tuononen, B. C. Ranu and S. Goswami, *Inorg. Chem.*, 2008, **47**, 11062–11070.
152 D. J. Lippincott, P. J. Trejo-Soto, F. Gallou and B. H. Lipshutz, *Org. Lett.*, 2018, **20**, 5094–5097.
153 A. Dhakshinamoorthy and K. Pitchumani, *Tetrahedron*, 2006, **62**, 9911–9918.
154 D. A. Chaudhari and R. A. Fernandes, *J. Org. Chem.*, 2016, **81**, 2113–2121.
155 A. Dhakshinamoorthy, M. Alvaro and H. Garcia, *ACS Catal.*, 2011, **1**, 836–840.
156 A. Wang and H. Jiang, *J. Org. Chem.*, 2010, **75**, 2321–2326.
157 A. Gonzalez-de-Castro and J. Xiao, *J. Am. Chem. Soc.*, 2015, **137**, 8206–8218.
158 F. Le Quéméner, S. Barman, N. Merle, M. A. Aljuhani, M. K. Samantaray, Y. Saih, K. C. Szeto, A. De Mallmann, Y. Minenkov, K.-W. Huang, L. Cavallo, M. Taoufik and J.-M. Basset, *ACS Catal.*, 2018, **8**, 7549–7555.
159 J. Browning, M. Green, A. Laguna, L. E. Smart, J. L. Spencer and F. G. A. Stone, *J. Chem. Soc., Chem. Commun.*, 1975, **0**, 723–724.
160 D. Ellis, D. McKay, S. A. Macgregor, G. M. Rosair and A. J. Welch, *Angew. Chem., Int. Ed.*, 2010, **49**, 4943–4945.
161 P. D. Zeits, T. Fiedler and J. A. Gladysz, *Chem. Commun.*, 2012, **48**, 7925–7927.
162 M. Jakoobi, N. Halcovitch, G. F. S. Whitehead and A. G. Sergeev, *Angew. Chem.*, 2017, **129**, 3314–3317.
163 J. Hicks, P. Vasko, J. M. Goicoechea and S. Aldridge, *J. Am. Chem. Soc.*, 2019, **141**, 11000–11003.
164 A. Sattler and G. Parkin, *Nature*, 2010, **463**, 523–526.
165 D. Frejka, J. Ulč, E. A. B. Kantchev, I. Císařová and M. Kotora, *ACS Catal.*, 2018, **8**, 10290–10299.
166 S. Tashiro, M. Yamada and M. Shionoya, *Angew. Chem.*, 2015, **127**, 5441–5444.
167 B. Zhu, W. Guan, L.-K. Yan and Z.-M. Su, *J. Am. Chem. Soc.*, 2016, **138**, 11069–11072.
168 S. Hu, T. Shima and Z. Hou, *Nature*, 2014, **512**, 413–415.
169 M. Jakoobi, Y. Tian, R. Boulatov and A. G. Sergeev, *J. Am. Chem. Soc.*, 2019, **141**, 6048–6053.
170 G. Meola, H. Braband, D. Hernández-Valdés, C. Gotzmann, T. Fox, B. Spingler and R. Alberto, *Inorg. Chem.*, 2017, **56**, 6297–6301.
171 A. Ford, H. Miel, A. Ring, C. N. Slattery, A. R. Maguire and M. A. McKervey, *Chem. Rev.*, 2015, **115**, 9981–10080.
172 S. E. Reisman, R. R. Nani and S. Levin, *Synlett*, 2011, 2437–2442.
173 G. Fuchs, M. Boll and J. Heider, *Nat. Rev. Microbiol.*, 2011, **9**, 803–816.
174 Y. Wang, J. Li and A. Liu, *JBIC, J. Biol. Inorg. Chem.*, 2017, **22**, 395–405.
175 L. N. Mander and C. M. Williams, *Tetrahedron*, 2003, **59**, 1105–1136.
176 P. J. Harrison and T. D. H. Bugg, *Arch. Biochem. Biophys.*, 2014, **544**, 105–111.
177 F. H. Vaillancourt, J. T. Bolin and L. D. Eltis, *Crit. Rev. Biochem. Mol. Biol.*, 2006, **41**, 241–267.
178 M. Palaniandavar and R. Mayilmurugan, *C. R. Chim.*, 2007, **10**, 366–379.
179 R. Yamahara, S. Ogo, H. Masuda and Y. Watanabe, *J. Inorg. Biochem.*, 2002, **88**, 284–294.
180 P. C. A. Bruijnincx, M. Lutz, A. L. Spek, W. R. Hagen, G. Van Koten and R. J. M. Klein Gebbink, *Inorg. Chem.*, 2007, **46**, 8391–8402.
181 J. A. Berson, *Angew. Chem., Int. Ed.*, 2002, **41**, 4655–4660.
182 A. J. H. Klunder, J. Zhu and B. Zwanenburg, *Chem. Rev.*, 1999, **99**, 1163–1190.
183 A. Ichihara, in *Studies in Natural Products Chemistry*, ed. Atta-ur-Rahman, Elsevier, 2008, vol. 34, pp. 129–171.
184 K. Fesko, *Front. Bioeng. Biotechnol.*, 2019, **7**, 119.
185 G. Zhong, D. Shabat, B. List, J. Anderson, S. C. Sinha, R. A. Lerner and C. F. Barbas III, *Angew. Chem., Int. Ed.*, 1998, **37**, 2481–2484.
186 K. Akagawa, J. Higuchi, I. Yoshikawa and K. Kudo, *Eur. J. Org. Chem.*, 2018, 5278–5281.
187 S.-L. Zhang and Z.-Q. Deng, *Org. Biomol. Chem.*, 2016, **14**, 7282–7294.
188 S.-L. Zhang and Z.-L. Yu, *J. Org. Chem.*, 2016, **81**, 57–65.
189 K. Murakami, H. Ohmiya, H. Yorimitsu and K. Oshima, *Tetrahedron Lett.*, 2008, **49**, 2388–2390.
190 S. Paladhi, S. J. Park, I.-S. Hwang, J. H. Park, H. Y. Bae, A. P. Jadhav and C. E. Song, *Org. Lett.*, 2023, **25**, 2713–2717.
191 P. Wan and S. Muralidharan, *J. Am. Chem. Soc.*, 1988, **110**, 4336–4345.
192 H. Leng, Q. Zhao, Q. Mao, S. Liu, M. Luo, R. Qin, W. Huang and G. Zhan, *Chin. Chem. Lett.*, 2021, **32**, 2567–2571.
193 A. Huyghues-Despointes and V. A. Yaylayan, *J. Agric. Food Chem.*, 1996, **44**, 672–681.
194 R. I. Mainil, N. Paksung and Y. Matsumura, *J. Supercrit. Fluids*, 2019, **143**, 370–377.
195 S.-L. Zhang and Z.-Q. Deng, *Org. Biomol. Chem.*, 2016, **14**, 8966–8970.

196 R. Maity, C. Gharui, A. K. Sil and S. C. Pan, *Org. Lett.*, 2017, **19**, 662–665.
197 R. A. Michelin, P. Sgarbossa, A. Scarso and G. Strukul, *Coord. Chem. Rev.*, 2010, **254**, 646–660.
198 M. Renz and B. Meunier, *Eur. J. Org. Chem.*, 1999, 737–750.
199 G.-J. Ten Brink, I. W. C. E. Arends and R. A. Sheldon, *Chem. Rev.*, 2004, **104**, 4105–4124.
200 J. Zhu, J. Wang and G. Dong, *Nat. Chem.*, 2019, **11**, 45–51.
201 J. Zhu, Y. Xue, R. Zhang, B. L. Ratchford and G. Dong, *J. Am. Chem. Soc.*, 2022, **144**, 3242–3249.
202 L. Dong, L. Lin, X. Han, X. Si, X. Liu, Y. Guo, F. Lu, S. Rudić, S. F. Parker, S. Yang and Y. Wang, *Chem*, 2019, **5**, 1521–1536.
203 Z. Luo, C. Liu, A. Radu, D. F. de Waard, Y. Wang, J. T. Behaghel de Bueren, P. D. Kouris, M. D. Boot, J. Xiao, H. Zhang, R. Xiao, J. S. Luterbacher and E. J. M. Hensen, *Nat. Chem. Eng.*, 2024, **1**, 61–72.
204 X. Si, R. Lu, X. Liu, J. Xu and F. Lu, *Ind. Crops Prod.*, 2023, **197**, 116659.
205 M. B. Figueirêdo, P. J. Deuss, R. H. Venderbosch and H. J. Heeres, *ACS Sustainable Chem. Eng.*, 2019, **7**, 4755–4765.
206 J. R. Silverman, A. M. Danby and B. Subramaniam, *React. Chem. Eng.*, 2019, **4**, 1421–1430.
207 R. Ma, M. Guo and X. Zhang, *ChemSusChem*, 2014, **7**, 412–415.
208 A. Z. Werner, W. T. Cordell, C. W. Lahive, B. C. Klein, C. A. Singer, E. C. D. Tan, M. A. Ingraham, K. J. Ramirez, D. H. Kim, J. N. Pedersen, C. W. Johnson, B. F. Pfleger, G. T. Beckham and D. Salvachúa, *Sci. Adv.*, 2023, **9**, eadj0053.
209 Z. Cai, J. Long, Y. Li, L. Ye, B. Yin, L. J. France, J. Dong, L. Zheng, H. He, S. Liu, S. C. E. Tsang and X. Li, *Chem*, 2019, **5**, 2365–2377.
210 N. X. Gu, C. T. Palumbo, A. C. Bleem, K. P. Sullivan, S. J. Haugen, S. P. Woodworth, K. J. Ramirez, J. K. Kenny, L. D. Stanley, R. Katahira, S. S. Stahl and G. T. Beckham, *ACS Cent. Sci.*, 2023, **9**, 2277–2285.
211 C. T. Palumbo, N. X. Gu, A. C. Bleem, K. P. Sullivan, R. Katahira, L. M. Stanley, J. K. Kenny, M. A. Ingraham, K. J. Ramirez, S. J. Haugen, C. R. Amendola, S. S. Stahl and G. T. Beckham, *Nat. Commun.*, 2024, **15**, 862.
212 K. M. Mains, C. T. Palumbo, D. Rigo, M. S. Webber, G. Rosetto, S. T. Bao, A. L. Carroll, N. R. Meyer, A. F. Benson, B. A. Boyle, S. J. Haugen, M. A. Ingraham, W. G. Alexander, M. Silberman, L. C. Myers, K. J. Ramirez, K. P. Sullivan, A. M. Guss, D. Salvachúa, Y. Román-Leshkov, S. S. Stahl, A. Z. Werner and G. T. Beckham, *Nature*, 2026, **654**, 668–675.
213 S. Omolabake, D. T. Hofsommer, K. M. Mains, C. T. Palumbo, D. Rigo, A. Z. Werner, G. T. Beckham and S. S. Stahl, *Angew. Chem., Int. Ed.*, 2025, e15588.
214 Q. Meng, J. Yan, R. Wu, H. Liu, Y. Sun, N. Wu, J. Xiang, L. Zheng, J. Zhang and B. Han, *Nat. Commun.*, 2021, **12**, 4534.
215 Y. Liao, S.-F. Koelewijn, G. Van den Bossche, J. Van Aelst, S. Van den Bosch, T. Renders, K. Navare, T. Nicolaï, K. Van Aelst, M. Maesen, H. Matsushima, J. M. Thevelein, K. Van Acker, B. Lagrain, D. Verboekend and B. F. Sels, *Science*, 2020, **367**, 1385–1390.
216 J. Corker, F. Lefebvre, C. Lécuyer, V. Dufaud, F. Quignard, A. Choplin, J. Evans and J.-M. Basset, *Science*, 1996, **271**, 966–969.
217 U. Kanbur, G. Zang, A. L. Paterson, P. Chatterjee, R. A. Hackler, M. Delferro, I. I. Slowing, F. A. Perras, P. Sun and A. D. Sadow, *Chem*, 2021, **7**, 1347–1362.
218 J. E. Rorrer, A. M. Ebrahim, Y. Questell-Santiago, J. Zhu, C. Troyano-Valls, A. S. Asundi, A. E. Brenner, S. R. Bare, C. J. Tassone, G. T. Beckham and Y. Román-Leshkov, *ACS Catal.*, 2022, **12**, 13969–13979.
219 X. Wu, A. Tennakoon, R. Yappert, M. Esveld, M. S. Ferrandon, R. A. Hackler, A. M. LaPointe, A. Heyden, M. Delferro, B. Peters, A. D. Sadow and W. Huang, *J. Am. Chem. Soc.*, 2022, **144**, 5323–5334.
220 W. Zhang, S. Kim, L. Wahl, R. Khare, L. Hale, J. Hu, D. M. Camaioni, O. Y. Gutiérrez, Y. Liu and J. A. Lercher, *Science*, 2023, **379**, 807–811.
221 Y. Jing, Y. Wang, S. Furukawa, J. Xia, C. Sun, M. J. Hülsey, H. Wang, Y. Guo, X. Liu and N. Yan, *Angew. Chem., Int. Ed.*, 2021, **60**, 5527–5535.
222 C. Rabot, Y. Chen, S. Bijlani, Y.-M. Chiang, C. E. Oakley, B. R. Oakley, T. J. Williams and C. C. C. Wang, *Angew. Chem., Int. Ed.*, 2023, **62**, e202214609.
223 M. W. Guzik, T. Nitkiewicz, M. Wojnarowska, M. Sołtysik, S. T. Kenny, R. P. Babu, M. Best and K. E. O'Connor, *Waste Manage.*, 2021, **135**, 60–69.
224 K. P. Sullivan, A. Z. Werner, K. J. Ramirez, L. D. Ellis, J. R. Bussard, B. A. Black, D. G. Brandner, F. Bratti, B. L. Buss, X. Dong, S. J. Haugen, M. A. Ingraham, M. O. Konev, W. E. Michener, J. Miscall, I. Pardo, S. P. Woodworth, A. M. Guss, Y. Román-Leshkov, S. S. Stahl and G. T. Beckham, *Science*, 2022, **378**, 207–211.
225 C. Li, X. Y. Kong, M. Lyu, X. T. Tay, M. Đokić, K. F. Chin, C. T. Yang, E. K. X. Lee, J. Zhang, C. Y. Tham, W. X. Chan, W. J. Lee, T. T. Lim, A. Goto, M. B. Sullivan and H. S. Soo, *Chem*, 2023, **9**, 2683–2700.
226 Z. Huang, M. Shanmugam, Z. Liu, A. Brookfield, E. L. Bennett, R. Guan, D. E. Vega Herrera, J. A. Lopez-Sanchez, A. G. Slater, E. J. L. McInnes, X. Qi and J. Xiao, *J. Am. Chem. Soc.*, 2022, **144**, 6532–6542.
227 X. Jiao, K. Zheng, Q. Chen, X. Li, Y. Li, W. Shao, J. Xu, J. Zhu, Y. Pan, Y. Sun and Y. Xie, *Angew. Chem., Int. Ed.*, 2020, **59**, 15497–15501.
228 Y. Miao, Y. Zhao, G. I. N. Waterhouse, R. Shi, L.-Z. Wu and T. Zhang, *Nat. Commun.*, 2023, **14**, 4242.
229 X. Jia, C. Qin, T. Friedberger, Z. Guan and Z. Huang, *Sci. Adv.*, 2016, **2**, e1501591.
230 R. J. Conk, S. Hanna, J. X. Shi, J. Yang, N. R. Ciccia, L. Qi, B. J. Bloomer, S. Heuvel, T. Wills, J. Su, A. T. Bell and J. F. Hartwig, *Science*, 2022, **377**, 1561–1566.
231 R. J. Conk, J. F. Stahler, J. X. Shi, J. Yang, N. G. Lefton, J. N. Brunn, A. T. Bell and J. F. Hartwig, *Science*, 2024, **385**, 1322–1327.

232 L. Dong, J. Xia, Y. Guo, X. Liu, H. Wang and Y. Wang, *J. Catal.*, 2021, **394**, 94–103.
233 P. C. Rodrigues Pinto, E. A. Borges da Silva and A. E. Rodrigues, *Ind. Eng. Chem. Res.*, 2011, **50**, 741–748.
234 X. Ouyang, Z. Lin, Y. Deng, D. Yang and X. Qiu, *Chin. J. Chem. Eng.*, 2010, **18**, 695–702.
235 G. Lin, G. Reid and T. D. H. Bugg, *J. Am. Chem. Soc.*, 2001, **123**, 5030–5039.
236 J. R. Silverman, A. M. Danby and B. Subramaniam, *ACS Sustainable Chem. Eng.*, 2020, **8**, 17001–17007.
237 A. M. Danby, M. D. Lundin and B. Subramaniam, *ACS Sustainable Chem. Eng.*, 2018, **6**, 71–76.
238 M. B. Figueirêdo, H. J. Heeres and P. J. Deuss, *Sustainable Energy Fuels*, 2019, **4**, 265–276.
239 R. a D. Mbachu and R. St. J. Manley, *J. Polym. Sci., Polym. Chem. Ed.*, 1981, **19**, 2053–2063.
240 M. B. Figueirêdo, F. W. Keij, A. Hommes, P. J. Deuss, R. H. Venderbosch, J. Yue and H. J. Heeres, *ACS Sustainable Chem. Eng.*, 2019, **7**, 18384–18394.
241 M. B. Figueirêdo, R. H. Venderbosch, P. J. Deuss and H. J. Heeres, *Adv. Sustainable Syst.*, 2020, **4**, 1900147.
242 R. Criegee, *Angew. Chem., Int. Ed. Engl.*, 1975, **14**, 745–752.
243 E. Mvula, S. Naumov and C. von Sonntag, *Environ. Sci. Technol.*, 2009, **43**, 6275–6282.
244 Y. Nakamura, M. Daidai and F. Kobayashi, *Water Sci. Technol.*, 2004, **50**, 167–172.
245 J. Sun, D. Han, D. E. Shallcross, H. Cao, B. Wei, Q. Mei, J. Xie, J. Zhan and M. He, *Chem. Eng. J.*, 2021, **404**, 126484.
246 Y. Sun, X. Chen, F. Xu and X. Wang, *Chemosphere*, 2020, **253**, 126744.
247 A. G. Khudoshin, A. N. Mitrofanova and V. V. Lunin, *Russ. Chem. Bull.*, 2008, **57**, 283–288.
248 N. A. Mamleeva, S. A. Autlov, A. V. Fionov, N. G. Bazarnova and V. V. Lunin, *Russ. J. Phys. Chem. A*, 2009, **83**, 745–751.
249 E. M. O'Neill, A. Z. Kawam, D. A. Van Ry and R. Z. Hinrichs, *Atmos. Chem. Phys.*, 2014, **14**, 47–60.
250 A. N. Mitrofanova, A. G. Khudoshin and V. V. Lunin, *Russ. J. Phys. Chem. A*, 2013, **87**, 1124–1128.
251 N. Ding, H. Liu, Y. Sun, X. Tang, T. Lei, F. Xu, X. Zeng and L. Lin, *J. Cleaner Prod.*, 2021, **278**, 123984.
252 D. Areskogh, J. Li, G. Gellerstedt and G. Henriksson, *Ind. Crops Prod.*, 2010, **32**, 458–466.
253 P. E. Montoneri, D. Rosso, G. Bucci, S. Berto, A. Baglieri, R. Mendichi, P. Quagliotto, M. Francavilla, D. Mainero and M. Negre, *ChemistrySelect*, 2016, **1**, 1613–1629.
254 J. Quesada, F. Teffo-Bertaud, J. P. Croué and M. Rubio, *Holzforschung*, 2002, **56**, 32–38.
255 M. I. F. Mota, P. C. Rodrigues Pinto, J. M. Loureiro and A. E. Rodrigues, *Sep. Purif. Rev.*, 2016, **45**, 227–259.
256 P. C. R. Pinto, C. E. Costa and A. E. Rodrigues, *Ind. Eng. Chem. Res.*, 2013, **52**, 4421–4428.
257 C. T. Palumbo, N. X. Gu, A. C. Bleem, K. P. Sullivan, R. Katahira, L. M. Stanley, J. K. Kenny, M. A. Ingraham, K. J. Ramirez, S. J. Haugen, C. R. Amendola, S. S. Stahl and G. T. Beckham, *Nat. Commun.*, 2024, **15**, 862.
258 M. R. C. Fernandes, X. Huang, H. C. L. Abbenhuis and E. J. M. Hensen, *Int. J. Biol. Macromol.*, 2019, **123**, 1044–1051.
259 S. Zhang, Z. Zhang, M. Ge, B. Liu, S. Chen, D. Zhang and L. Gao, *GCB Bioenergy*, 2021, **13**, 1290–1302.
260 R. Jastrzebski, M. G. Quesne, B. M. Weckhuysen, S. P. De Visser and P. C. A. Bruijnincx, *Chem. – Eur. J.*, 2014, **20**, 15686–15691.
261 J. B. Broderick, *Essays Biochem.*, 1999, **34**, 173–189.
262 E. L. Spence, G. J. Langley and T. D. H. Bugg, *J. Am. Chem. Soc.*, 1996, **118**, 8336–8343.
263 Y.-P. Sun, K. L. Nguyen and A. F. A. Wallis, *Holzforschung*, 1998, **52**, 61–66.
264 T. R. Demmin, M. D. Swerdloff and M. M. Rogic, *J. Am. Chem. Soc.*, 1981, **103**, 5795–5804.
265 D. Shao, J. Liang, X. Cui, H. Xu and W. Yan, *Chem. Eng. J.*, 2014, **244**, 288–295.
266 A. More, T. Elder and Z. Jiang, *Holzforschung*, 2021, **75**, 806–823.
267 M. Liu, Z. Zhang, J. Song, S. Liu, H. Liu and B. Han, *Angew. Chem.*, 2019, **131**, 17554–17559.
268 H. Liu, H. Li, N. Luo and F. Wang, *ACS Catal.*, 2020, **10**, 632–643.
269 E. P. Weeda, C. M. Holland, J. B. de Bueren, Z. Yuan, M. Alherech, J. Coplien, D. Haak, E. L. Hegg, J. Luterbacher, T. W. Root and S. S. Stahl, *Joule*, 2024, **8**, 3336–3346.
270 T. Hou, N. Luo, H. Li, M. Heggen, J. Lu, Y. Wang and F. Wang, *ACS Catal.*, 2017, **7**, 3850–3859.
271 Y. Zhu, N. Li, H. Liu, C. Cai, Y. Wang, J. Mu and F. Wang, *ACS Catal.*, 2024, **14**, 16872–16884.
272 B. Sedai, C. Díaz-Urrutia, R. T. Baker, R. Wu, L. A. P. Silks and S. K. Hanson, *ACS Catal.*, 2011, **1**, 794–804.
273 B. Sedai, C. Díaz-Urrutia, R. T. Baker, R. Wu, L. A. P. Silks and S. K. Hanson, *ACS Catal.*, 2013, **3**, 3111–3122.
274 J. Xu, T. Gong, X. Zhang, M. Liu and J. Wang, *Surf. Interfaces*, 2023, **41**, 103210.
275 M. Shimada, T. Habe, T. Higuchi, T. Okamoto and B. Panijpan, *Holzforschung*, 1987, **41**, 277–285.
276 D. W. Cho, R. Parthasarathi, A. S. Pimentel, G. D. Maestas, H. J. Park, U. C. Yoon, D. Dunaway-Mariano, S. Gnanakaran, P. Langan and P. S. Mariano, *J. Org. Chem.*, 2010, **75**, 6549–6562.
277 D. W. Cho, J. A. Latham, H. J. Park, U. C. Yoon, P. Langan, D. Dunaway-Mariano and P. S. Mariano, *J. Org. Chem.*, 2011, **76**, 2840–2852.
278 E. B. Clatworthy, J. L. Picone-Murray, A. K. L. Yuen, R. T. Maschmeyer, A. F. Masters and T. Maschmeyer, *Catal. Sci. Technol.*, 2019, **9**, 384–397.
279 W. Partenheimer, *J. Mol. Catal. A: Chem.*, 2003, **206**, 131–144.
280 W. Partenheimer, *Adv. Synth. Catal.*, 2009, **351**, 456–466.
281 M. L. Stone, M. S. Webber, W. P. Mounfield, D. C. Bell, E. Christensen, A. R. C. Morais, Y. Li, E. M. Anderson, J. S. Heyne, G. T. Beckham and Y. Román-Leshkov, *Joule*, 2022, **6**, 2324–2337.
282 M. S. Webber, Z. Yang, D. C. Bell, D. G. Brandner, J. R. Bussard, J. Watson, M. L. Stone, X. Wu, Q. S. Neuendorf, L. C. Myers, J. S. Heyne, G. T. Beckham and Y. Román-Leshkov, *Cell Rep. Phys. Sci.*, 2025, **6**, 102687.

283 W. Partenheimer, *Appl. Catal., A*, 2011, **409–410**, 48–54.
284 R. A. F. Tomás, J. C. M. Bordado and J. F. P. Gomes, *Chem. Rev.*, 2013, **113**, 7421–7469.
285 W. Wang, M. Wang, X. Li, L. Cai, S. Q. Shi, C. Duan and Y. Ni, *ACS Sustainable Chem. Eng.*, 2020, **8**, 38–43.
286 C. W. J. Murnaghan, N. Skillen, B. Hackett, J. Lafferty, P. K. J. Robertson and G. N. Sheldrake, *ACS Sustainable Chem. Eng.*, 2022, **10**, 12107–12116.
287 Z. Xiang, W. Han, J. Deng, W. Zhu, Y. Zhang and H. Wang, *ChemSusChem*, 2020, **13**, 4199–4213.
288 E. Subbotina, T. Rukkijakan, M. D. Marquez-Medina, X. Yu, M. Johnsson and J. S. M. Samec, *Nat. Chem.*, 2021, **13**, 1118–1125.
289 J. Liu, X. Qiu, X. Huang, X. Luo, C. Zhang, J. Wei, J. Pan, Y. Liang, Y. Zhu, Q. Qin, S. Song and N. Jiao, *Nat. Chem.*, 2019, **11**, 71–77.
290 J. M. Bray, S. M. Stephens, S. M. Weierbach, K. Vargas and K. M. Lambert, *Chem. Commun.*, 2023, **59**, 14063–14092.
291 X. Li, A. J. Chavez, H. Zhang, D. Andryushkina, P. C. Ford and M. M. Abu-Omar, *Green Chem.*, 2026, **28**, 4255–4262.
292 J. Liu, J. Pan, X. Luo, X. Qiu, C. Zhang and N. Jiao, *Research*, 2020, 7947029.
293 G. H. Tomlinson and H. Hibbert, *J. Am. Chem. Soc.*, 1936, **58**, 348–353.
294 V. E. Tarabanko, N. A. Fomova, B. N. Kuznetsov, N. M. Ivanchenko and A. V. Kudryashev, *React. Kinet. Catal. Lett.*, 1995, **55**, 161–170.
295 V. E. Tarabanko and N. Tarabanko, *Int. J. Mol. Sci.*, 2017, **18**, 2421.
296 Z. Zhou, M. Liu and C.-J. Li, *ACS Catal.*, 2017, **7**, 3344–3348.
297 M. Oregui-Bengoechea, I. Agirre, A. Iriondo, A. Lopez-Urionabarrenechea, J. M. Requies, I. Agirrezabal-Telleria, K. Bizkarra, V. L. Barrio and J. F. Cambra, in *Lignin Chemistry*, ed. L. Serrano, R. Luque and B. F. Sels, Springer International Publishing, Cham, 2020, pp. 197–271.
298 Y. Liao, S.-F. Koelewijn, G. Van den Bossche, J. Van Aelst, S. Van den Bosch, T. Renders, K. Navare, T. Nicolaï, K. Van Aelst, M. Maesen, H. Matsushima, J. M. Thevelein, K. Van Acker, B. Lagrain, D. Verboekend and B. F. Sels, *Science*, 2020, **367**, 1385–1390.
299 X. Shen, Q. Meng, Q. Mei, H. Liu, J. Yan, J. Song, D. Tan, B. Chen, Z. Zhang, G. Yang and B. Han, *Chem. Sci.*, 2020, **11**, 1347–1352.
300 L. Shuai, J. Sitison, S. Sadula, J. Ding, M. C. Thies and B. Saha, *ACS Catal.*, 2018, **8**, 6507–6512.
301 L. Li, L. Dong, X. Liu, Y. Guo and Y. Wang, *Appl. Catal., B*, 2020, **260**, 118143.
302 M. Saidi, F. Samimi, D. Karimipourfard, T. Nimmanwudipong, B. C. Gates and M. Reza Rahimpour, *Energy Environ. Sci.*, 2014, **7**, 103–129.
303 R. Shu, R. Li, B. Lin, C. Wang, Z. Cheng and Y. Chen, *Biomass Bioenergy*, 2020, **132**, 105432.
304 L. Shen, X. Xue, M. Wang, Y. Fan, D. Gu, L. Zhu, T. Jiang, D. Yuan, H. Wu and B. Wang, *Energy Fuels*, 2023, **37**, 15309–15347.
305 K. Ye, Y. Liu, S. Wu and J. Zhuang, *Ind. Crops Prod.*, 2021, **172**, 114008.
306 X. Kong, C. Liu, Y. Fan, M. Li and R. Xiao, *ACS Catal.*, 2023, **13**, 10048–10055.
307 X. Kong, C. Liu, H. Zeng, Y. Fan, H. Zhang and R. Xiao, *ChemSusChem*, 2024, **17**, e202300996.
308 J. Zhang, L. Lombardo, G. Gözaydın, P. J. Dyson and N. Yan, *Chin. J. Catal.*, 2018, **39**, 1445–1452.
309 X. Shen, Q. Meng, Q. Mei, J. Xiang, H. Liu and B. Han, *Green Chem.*, 2020, **22**, 2191–2196.
310 A. Musa, E. A. Jaseer, S. Barman and N. Garcia, *Energy Fuels*, 2024, **38**, 1676–1691.
311 V. Dufaud and J.-M. Basset, *Angew. Chem., Int. Ed.*, 1998, **37**, 806–810.
312 C. Lecuyer, F. Quignard, A. Choplin, D. Olivier and J.-M. Basset, *Angew. Chem., Int. Ed. Engl.*, 1991, **30**, 1660–1661.
313 W. Tu, M. Chu, X. Wang, X. Wang, Y. Li, W. Yang, M. Cao, L. Wang, Y. Li, T.-K. Sham, Y. Cui, Q. Zhang and J. Chen, *Appl. Catal., B*, 2023, **339**, 123122.
314 P. A. Kots, S. Liu, B. C. Vance, C. Wang, J. D. Sheehan and D. G. Vlachos, *ACS Catal.*, 2021, **11**, 8104–8115.
315 P. A. Kots, T. Xie, B. C. Vance, C. M. Quinn, M. D. de Mello, J. A. Boscoboinik, C. Wang, P. Kumar, E. A. Stach, N. S. Marinkovic, L. Ma, S. N. Ehrlich and D. G. Vlachos, *Nat. Commun.*, 2022, **13**, 5186.
316 L. Chen, L. C. Meyer, L. Kovarik, D. Meira, X. I. Pereira-Hernandez, H. Shi, K. Khivantsev, O. Y. Gutiérrez and J. Szanyi, *ACS Catal.*, 2022, **12**, 4618–4627.
317 Y. Nakaji, M. Tamura, S. Miyaoka, S. Kumagai, M. Tanji, Y. Nakagawa, T. Yoshioka and K. Tomishige, *Appl. Catal., B*, 2021, **285**, 119805.
318 H. Ji, X. Wang, X. Wei, Y. Peng, S. Zhang, S. Song and H. Zhang, *Small*, 2023, **19**, 2300903.
319 M. Chu, X. Wang, X. Wang, X. Lou, C. Zhang, M. Cao, L. Wang, Y. Li, S. Liu, T.-K. Sham, Q. Zhang and J. Chen, *Research*, 2023, **6**, 0032.
320 M. Tamura, S. Miyaoka, Y. Nakaji, M. Tanji, S. Kumagai, Y. Nakagawa, T. Yoshioka and K. Tomishige, *Appl. Catal., B*, 2022, **318**, 121870.
321 Q. Kang, M. Chu, P. Xu, X. Wang, S. Wang, M. Cao, O. Ivasenko, T.-K. Sham, Q. Zhang, Q. Sun and J. Chen, *Angew. Chem., Int. Ed.*, 2023, **62**, e202313174.
322 S. D. Jaydev, A. J. Martín, M.-E. Usteri, K. Chikri, H. Eliasson, R. Erni and J. Pérez-Ramírez, *Angew. Chem.*, 2024, **136**, e202317526.
323 C. Wang, K. Yu, B. Sheludko, T. Xie, P. A. Kots, B. C. Vance, P. Kumar, E. A. Stach, W. Zheng and D. G. Vlachos, *Appl. Catal., B*, 2022, **319**, 121899.
324 C. Wang, T. Xie, P. A. Kots, B. C. Vance, K. Yu, P. Kumar, J. Fu, S. Liu, G. Tsilomelekis, E. A. Stach, W. Zheng and D. G. Vlachos, *JACS Au*, 2021, **1**, 1422–1434.
325 J. E. Rorrer, C. Troyano-Valls, G. T. Beckham and Y. Román-Leshkov, *ACS Sustainable Chem. Eng.*, 2021, **9**, 11661–11666.
326 Y. Jing, Y. Wang, S. Furukawa, J. Xia, C. Sun, M. J. Hülsey, H. Wang, Y. Guo, X. Liu and N. Yan, *Angew. Chem., Int. Ed.*, 2021, **60**, 5527–5535.

327 L. Chen, Y. Zhu, L. C. Meyer, L. V. Hale, T. T. Le, A. Karkamkar, J. A. Lercher, O. Y. Gutiérrez and J. Szanyi, *React. Chem. Eng.*, 2022, **7**, 844–854.

328 S. D. Jaydev, A. J. Martín and J. Pérez-Ramírez, *ChemSusChem*, 2021, **14**, 5179–5185.

329 J. Z. Tan, C. W. Hullfish, Y. Zheng, B. E. Koel and M. L. Sarazen, *Appl. Catal., B*, 2023, **338**, 123028.

330 B. C. Vance, S. Najmi, P. A. Kots, C. Wang, S. Jeon, E. A. Stach, D. N. Zakharov, N. Marinkovic, S. N. Ehrlich, L. Ma and D. G. Vlachos, *JACS Au*, 2023, **3**, 2156–2165.

331 A. Tennakoon, X. Wu, A. L. Paterson, S. Patnaik, Y. Pei, A. M. LaPointe, S. C. Ammal, R. A. Hackler, A. Heyden, I. I. Slowing, G. W. Coates, M. Delferro, B. Peters, W. Huang, A. D. Sadow and F. A. Perras, *Nat. Catal.*, 2020, **3**, 893–901.

332 D. W. Flaherty and E. Iglesia, *J. Am. Chem. Soc.*, 2013, **135**, 18586–18599.

333 D. W. Flaherty, D. D. Hibbitts and E. Iglesia, *J. Am. Chem. Soc.*, 2014, **136**, 9664–9676.

334 W. Hu, G. Noh and E. Iglesia, *J. Catal.*, 2023, **425**, 125–142.

335 B. C. Vance, P. A. Kots, C. Wang, J. E. Granite and D. G. Vlachos, *Appl. Catal., B*, 2023, **322**, 122138.

336 I. Vollmer, M. J. F. Jenks, R. Mayorga González, F. Meirer and B. M. Weckhuysen, *Angew. Chem., Int. Ed.*, 2021, **60**, 16101–16108.

337 B. C. Vance, P. A. Kots, C. Wang, Z. R. Hinton, C. M. Quinn, T. H. Epps, L. T. J. Korley and D. G. Vlachos, *Appl. Catal., B*, 2021, **299**, 120483.

338 B. Du, X. Chen, Y. Ling, T. Niu, W. Guan, J. Meng, H. Hu, C.-W. Tsang and C. Liang, *ChemSusChem*, 2023, **16**, e202202035.

339 H. Ran, S. Zhang, W. Ni and Y. Jing, *Chem. Sci.*, 2024, **15**, 795–831.

340 A. S. Goldman, A. H. Roy, Z. Huang, R. Ahuja, W. Schinski and M. Brookhart, *Science*, 2006, **312**, 257–261.

341 V. Vidal, A. Théolier, J. Thivolle-Cazat and J.-M. Basset, *Science*, 1997, **276**, 99–102.

342 X. Jia, C. Qin, T. Friedberger, Z. Guan and Z. Huang, *Sci. Adv.*, 2016, **2**, e1501591.

343 M. C. Haibach, S. Kundu, M. Brookhart and A. S. Goldman, *Acc. Chem. Res.*, 2012, **45**, 947–958.

344 M. Zeng, Y.-H. Lee, G. Strong, A. M. LaPointe, A. L. Kocen, Z. Qu, G. W. Coates, S. L. Scott and M. M. Abu-Omar, *ACS Sustainable Chem. Eng.*, 2021, **9**, 13926–13936.

345 N. M. Wang, G. Strong, V. Dasilva, L. Gao, R. Huacuja, I. A. Konstantinov, M. S. Rosen, A. J. Nett, S. Ewart, R. Geyer, S. L. Scott and D. Guironnet, *J. Am. Chem. Soc.*, 2022, **144**, 18526–18531.

346 D. Guironnet and B. Peters, *J. Phys. Chem. A*, 2020, **124**, 3935–3942.

347 L. D. Ellis, S. V. Orski, G. A. Kenlaw, A. G. Norman, K. L. Beers, Y. Román-Leshkov and G. T. Beckham, *ACS Sustainable Chem. Eng.*, 2021, **9**, 623–628.

348 D. Kim, Z. R. Hinton, P. Bai, L. T. J. Korley, T. H. Epps and R. F. Lobo, *Appl. Catal., B*, 2022, **318**, 121873.

349 A. Arroyave, S. Cui, J. C. Lopez, A. L. Kocen, A. M. LaPointe, M. Delferro and G. W. Coates, *J. Am. Chem. Soc.*, 2022, **144**, 23280–23285.

350 M. W. Guzik, T. Nitkiewicz, M. Wojnarowska, M. Sołtysik, S. T. Kenny, R. P. Babu, M. Best and K. E. O'Connor, *Waste Manage.*, 2021, **135**, 60–69.

351 W. Partenheimer, *Catal. Today*, 2003, **81**, 117–135.

352 W. Partenheimer, *J. Mol. Catal.*, 1991, **67**, 35–46.

353 H. Moon, J. S. DesVeaux, E. C. Van Roijen, C. A. Singer, H. M. Alt, M. O. Konev, C. Lincoln, Y.-S. C. Avina, N. R. Meyer, S. J. Haugen, H. Lee, K. An, J. Miscall, K. J. Ramirez, C. W. Johnson, D. Salvachúa, B. C. Klein, T. Uekert, A. Z. Werner, S. S. Stahl and G. T. Beckham, *Nat. Commun.*, 2025, **16**, 9543.

354 C. Rabot, Y. Chen, S. Bijlani, Y.-M. Chiang, C. E. Oakley, B. R. Oakley, T. J. Williams and C. C. C. Wang, *Angew. Chem., Int. Ed.*, 2023, **62**, e202214609.

355 C. Rabot, Y. Chen, S.-Y. Lin, B. Miller, Y.-M. Chiang, C. E. Oakley, B. R. Oakley, C. C. C. Wang and T. J. Williams, *J. Am. Chem. Soc.*, 2023, **145**, 5222–5230.

356 S. Gazi, M. Đokić, K. F. Chin, P. R. Ng and H. S. Soo, *Adv. Sci.*, 2019, **6**, 1902020.

357 V. Conte, A. Coletti, B. Floris, G. Licini and C. Zonta, *Coord. Chem. Rev.*, 2011, **255**, 2165–2177.

358 T. Li, A. Vijeta, C. Casadevall, A. S. Gentleman, T. Euser and E. Reisner, *ACS Catal.*, 2022, **12**, 8155–8163.

359 O. G. Mountanea, E. Skolia and C. G. Kokotos, *Chem. – Eur. J.*, 2024, **30**, e202401588.

360 A. Chamas, H. Moon, J. Zheng, Y. Qiu, T. Tabassum, J. H. Jang, M. Abu-Omar, S. L. Scott and S. Suh, *ACS Sustainable Chem. Eng.*, 2020, **8**, 3494–3511.

361 A. Bunescu, S. Lee, Q. Li and J. F. Hartwig, *ACS Cent. Sci.*, 2017, **3**, 895–903.

362 D. Kong, L. Wang, X. Chen, W. Xia, L. Su, F. Zuo, Z. Yan, S. Chen and J. Wu, *Green Chem.*, 2022, **24**, 2203–2211.

363 C. Shen, Q. Zhang, X. Wei, P. Ye, X. Liu, S. Xu and Y.-Z. Wang, *Polymer*, 2024, **313**, 127689.

364 Y. Nakagawa, S. Oya, D. Kanno, Y. Nakaji, M. Tamura and K. Tomishige, *ChemSusChem*, 2017, **10**, 189–198.

365 Y. Nakaji, Y. Nakagawa, M. Tamura and K. Tomishige, *Fuel Process. Technol.*, 2018, **176**, 249–257.

366 S. Oya, D. Kanno, H. Watanabe, M. Tamura, Y. Nakagawa and K. Tomishige, *ChemSusChem*, 2015, **8**, 2472–2475.

367 S. Lu, Y. Jing, S. Jia, M. Shakouri, Y. Hu, X. Liu, Y. Guo and Y. Wang, *ChemCatChem*, 2023, **15**, e202201375.

368 A. Corma and A. V. Orchillés, *Microporous Mesoporous Mater.*, 2000, **35–36**, 21–30.

369 E. Subbotina, L. R. Souza, J. Zimmerman and P. Anastas, *Nat. Commun.*, 2024, **15**, 5892.

370 J. A. Jennings, S. Parkin, E. Munson, S. P. Delaney, J. L. Calahan, M. Isaacs, K. Hong and M. Crocker, *RSC Adv.*, 2017, **7**, 25987–25997.

371 N. D. Patil, S. G. Yao, M. S. Meier, J. K. Mobley and M. Crocker, *Org. Biomol. Chem.*, 2015, **13**, 3243–3254.

372 W. Partenheimer, *Appl. Catal., A*, 2011, **409–410**, 48–54.

373 Z.-H. Liu, B.-Z. Li, J. S. Yuan and Y.-J. Yuan, *Trends Biotechnol.*, 2022, **40**, 1550–1566.

374 G. Atiwesh, C. C. Parrish, J. Banoub and T.-A. T. Le, *Biotechnol. Prog.*, 2022, **38**, e3226.

375 A. K. Deepa and P. L. Dhepe, *ACS Catal.*, 2015, **5**, 365–379.
376 Z. Wu, Y. Jiang, X. Wang, J. Xu and L. Hu, *Biomass Convers. Biorefin.*, 2023, **13**, 16667–16683.
377 H. Choi, M. Alherech, J. Hee Jang, S. P. Woodworth, K. J. Ramirez, E. M. Karp and G. T. Beckham, *Green Chem.*, 2024, **26**, 5900–5913.
378 M. Lucarini and G. F. Pedulli, *Chem. Soc. Rev.*, 2010, **39**, 2106–2119.
379 B. Gutmann, D. Cantillo and C. O. Kappe, *Angew. Chem., Int. Ed.*, 2015, **54**, 6688–6728.
380 M.-Q. Zhang, Y. Zhou, R. Cao, S. Tian, Y. Jiao, Z. Guo, M. Wang, H. Peng, B. Sun, B. Xu, M. Wang, S. Xu and D. Ma, *Nature*, 2025, **643**, 395–403.
381 M. Lee, Y. Liang, A. A. Cuthbertson, S. Y. Mohamed, A. Puente-Urbina, W. E. Michener, J. Miscall, C. Lincoln, C. W. Lahive, J. S. DesVeaux, E. J. Fastow, K. I. Winey, H. Choi, B. C. Knott, N. Banakis, R. D. Allen, G. T. Beckham and K. M. Knauer, *Nat. Sustain.*, 2025, 1–12.
382 H. Li, B. W. Tipton, H. Aboukeila, E. A. Mendoza, A. Alzailaie, T. Yan, C. R. Landis, J. S. Weston, B. P. Grady and G. W. Huber, *Angew. Chem., Int. Ed.*, 2025, e202517471.
383 P. A. Wender, V. A. Verma, T. J. Paxton and T. H. Pillow, *Acc. Chem. Res.*, 2008, **41**, 40–49.
384 D. Rigo, D. Polidoro, L. Marcuzzo, A. Perosa and M. Selva, *ACS Sustainable Chem. Eng.*, 2023, **11**, 12602–12613.
385 J.-C. Wasilke, S. J. Obrey, R. T. Baker and G. C. Bazan, *Chem. Rev.*, 2005, **105**, 1001–1020.
386 F. Gomollón-Bel and J. García-Martínez, *Angew. Chem.*, 2023, **135**, e202218975.
387 D. G. Brandner, J. Gracia Vitoria, J. K. Kenny, J. R. Bussard, J. H. Jang, S. P. Woodworth, K. Vanbroekhoven, Y. Román-Leshkov and G. T. Beckham, *ACS Sustainable Chem. Eng.*, 2025, **13**, 12573–12582.
388 I. Kumaniaev, E. Subbotina, J. Sävmarker, M. Larhed, M. V. Galkin and J. S. M. Samec, *Green Chem.*, 2017, **19**, 5767–5771.
389 E. M. Anderson, M. L. Stone, R. Katahira, M. Reed, G. T. Beckham and Y. Román-Leshkov, *Joule*, 2017, **1**, 613–622.
390 H. Zhou, J. Y. Xu, Y. Fu, H. Zhang, Z. Yuan, M. Qin and Z. Wang, *Green Chem.*, 2019, **21**, 4625–4632.
391 S. R. Nicholson, J. E. Rorrer, A. Singh, M. O. Konev, N. A. Rorrer, A. C. Carpenter, A. J. Jacobsen, Y. Román-Leshkov and G. T. Beckham, *Annu. Rev. Chem. Biomol. Eng.*, 2022, **13**, 301–324.
392 S. D. Jaydev, M.-E. Usteri, A. J. Martín and J. Pérez-Ramírez, *Chem Catal.*, 2023, **3**, 100564.
393 A. A. Cuthbertson, C. Lincoln, J. Miscall, L. M. Stanley, A. K. Maurya, A. S. Asundi, C. J. Tassone, N. A. Rorrer and G. T. Beckham, *Green Chem.*, 2024, **26**, 7067–7090.
394 D. Di Francesco, C. Dahlstrand, J. Löfstedt, A. Orebom, J. Verendel, C. Carrick, Å. Håkansson, S. Eriksson, H. Rådberg, H. Wallmo, M. Wimby, F. Huber, C. Federsel, M. Backmark and J. S. M. Samec, *ChemSusChem*, 2021, **14**, 2414–2425.